

UNIVERSITY OF MISKOLC  
FACULTY OF MECHANICAL ENGINEERING AND INFORMATICS



**INTEGRITY OF TRANSPORTING PIPELINE GIRTH WELDS BASED  
ON FULL-SCALE TESTS UNDER COMPLEX LOADING  
CONDITIONS**

PHD THESES

Prepared by

**Ahmad Yasser Dakhel**

Mechanical Engineering (BSc),  
Mechanical Engineering (MSc)

**ISTVÁN SÁLYI DOCTORAL SCHOOL OF MECHANICAL ENGINEERING SCIENCES  
ENGINEERING MATERIAL SCIENCE, PRODUCTION SYSTEMS AND PROCESSES  
STRUCTURAL INTEGRITY**

Head of Doctoral School

**Prof. Dr. Gabriella Bognár**  
DSc, Full Professor

Head of Topic Group

**Prof. Dr. János Lukács**  
CSc, PhD, Full Professor

Scientific Supervisor

**Prof. Dr. János Lukács**  
CSc, PhD, Full Professor

Scientific Co-supervisor

**Dr. Zsuzsanna Simon-Koncsik**  
PhD, Integrity Assessment and Data Reporting Engineer

**Miskolc  
2025**



## CONTENTS

CONTENTS.....	I
LIST OF FIGURES.....	III
LIST OF TABLES .....	VII
SUPERVISOR’S RECOMMENDATIONS .....	VIII
LIST OF SYMBOLS AND ABBREVIATIONS.....	X
1. INTRODUCTION, GLOBAL AIMS OF THE RESEARCH.....	12
2. STEELS FOR PIPELINE APPLICATIONS .....	14
2.1. Steel Materials and Manufacturing Innovations .....	14
2.2. Welding Processes and Defect Management .....	17
2.3. Microstructural Evolution and HAZ Performance.....	18
3. FAILURE STATISTICS FOR TRANSPORTING PIPELINES .....	26
3.1. Failure statistics for transporting pipelines .....	26
3.2. Examples of failures.....	26
3.3. Analyzing and contrasting the pipeline’s failures .....	28
3.4. Failure Frequency.....	28
3.5. Failure Causes .....	30
3.6. Failure Consequences.....	30
4. GIRTH WELD DAMAGES .....	32
4.1. Preventing damage possibilities on the girth weld.....	32
4.2. Influencing factors on damages of girth welds .....	34
4.3. The answers to how to prevent damages from transporting pipeline girth welds.....	38
5. FULL-SCALE TEST .....	40
5.1. Overview of full-scale testing .....	40
5.2. The importance of high-quality full-scale testing data.....	43
5.3. Project work vs. Model building.....	44
5.4. Design and preparation of specimen .....	44
6. SUMMARY, SPECIFIC AIMS OF THE RESEARCH WORK .....	53
7. CIRCUMSTANCES OF THE INVESTIGATIONS .....	54

7.1.	Manufacturing of the pipeline sections .....	54
7.2.	Design the fixing device.....	57
7.3.	Calculations for testing experimental pipe sections with complex loads.....	59
7.4.	Testing equipment and their characteristics .....	61
8.	FULL-SCALE INVESTIGATIONS PROCESS .....	68
8.1.	Visual, liquid penetrant, and radiographic investigations .....	68
8.2.	Radiographic investigations before and after the fatigue test .....	68
8.3.	Fatigue test .....	68
8.4.	Pressure test.....	71
8.5.	Burst test.....	74
9.	TESTING RESULTS.....	75
10.	THESES .....	96
11.	SUMMARY AND FURTHER PLANS.....	97
12.	APPLICATION POSSIBILITIES OF THE RESULTS .....	99
	ACKNOWLEDGEMENTS .....	100
	REFERENCES.....	101
	LIST OF PUBLICATIONS RELATED TO THE TOPIC OF THE RESEARCH FIELD .....	109
	Appendix 1 .....	111
	Appendix 2 .....	113
	Appendix 3 .....	115
	Appendix 4.....	117



## LIST OF FIGURES

Figure 1 high-pressure natural gas transmission pipelines of FGSZ Ltd. [15]	13
Figure 2 The amount of niobium in offshore structural steel has changed [24]	16
Figure 3 Microstructure of the heat-affected zone in two-pass and multiple pass welds based on [33]	19
Figure 4 Effects of titanium, niobium, and nitrogen on the grain size of previous austenite [24].	20
Figure 5 TMCP stands for Thermo-Mechanical Controlled Processing, and it shows the effect of niobium and titanium on ferrite particle size [34].	20
Figure 6 HAZ microstructure as a function of cooling rate and hardenability [35]	21
Figure 7 HAZ microstructure of ESW welds in ship steels as a function of transformation temperature [36]	21
Figure 8 Effects of grain size and microstructure on toughness [37]	23
Figure 9 Correlation between FATT and cooling time for coarse-grained HAZ microstructures of pipeline steel [38].	24
Figure 10 Influence of carbon content and microstructure on HAZ microstructure and toughness of structural steels [39].	24
Figure 11 Toughness variations in simulated multipass weld HAZ microstructures(left), Dependence of intercritically reheated HAZ toughness on volume fraction of martensite islands (right) [40].	25
Figure 12 Pipeline Accident in California [44]	26
Figure 13 Pipeline Accident in West Virginia [45]	27
Figure 14 Pipeline Accident in New Mexico[46]	27
Figure 15 Failure frequencies of different causes by EGIG[47]	28
Figure 16 Relationship primary failure frequency, cause, and size of leak (1970-2016)[47]	29
Figure 17 Relationship primary failure frequency, cause and size of leak [47]	29
Figure 18 Failure causes by EGIG [47]	30
Figure 19 Percentages of ruptures that ignited subdivided in diameter and pressure (1970-2016) [47]	31
Figure 20 Percentage of accidents of groups involved in pipeline incidents (1970-2016) [47]	31
Figure 21 Incident distribution by cause [49]	32
Figure 22 Distribution of root causes of failure events in the Hungarian high-pressure natural gas transmission pipeline system [50]	33
Figure 23 Girth weld integrity puzzle [51], [52]	33
Figure 24 Pipelines and nodes in an installation [53]	34
Figure 25 Unacceptable treatment of an axial misalignment [54], [55]	34
Figure 26 Pipeline laying [54]	35
Figure 27 Girth weld crack caused by different pipe and ditch profiles [56]	35
Figure 28 Connection of different pipeline section with different shape and wall thickness [54]	35

Figure 29 Changing of the internal pressure on a Hungarian gas transporting pipeline section[57]	36
Figure 30 Corrosion defects near and on pipeline welded joints [59], [60]	36
Figure 31 Hydrogen embrittlement, cracking and blistering processes [61]	37
Figure 32 EAC modes as a function of pH and electrochemical potential for carbon steel [64]	37
Figure 33 Examples of stress corrosion cracking [65]	38
Figure 34 Pipeline sections after fatigue and burst test with reinforced girth weld; left: system developed at University of Miskolc; right: Clock Spring repair system [66]	38
Figure 35 Full-Scale Test Specimen Schematic [69], [70]	41
Figure 36 Preparation strategy for Full Scale Test specimens and associated materials [69], [70]	41
Figure 37 Instrumentation for Full-Scale Testing (unrolled pipe view) [69], [70]	42
Figure 38 Test setup for an experimental pipe section subjected to or capable of complex loading conditions [79]	43
Figure 39 Four-point bending (4PB) in a testing laboratory with the possibility of applying internal pressure: sketch and construction of the testing apparatus [82]	45
Figure 40 Winding test in a testing laboratory: the design and implementation of the test equipment [82]	45
Figure 41 All-weld tensile sample in small diameter pipe [70]	47
Figure 42 Catastrophic failure of a pipe arch section during a pressure test [102]	48
Figure 43 When MA is present, possible HAZ notch locations [69]	49
Figure 44 When MA is present, the location of the weld centerline notch necessitates further considerations [69]	49
Figure 45 Pipeline XFEM model components assembled, displaying geometry and reference points.[75]	50
Figure 46 The CMOD failure[75]	50
Figure 47 An overview of the bending test for large diameter pipelines [78]	50
Figure 48 Bending test of a pipe section embedded in soil: test layout (left); deformed pipe section (right) [96]	51
Figure 49 Sketch of the four points bending test set-up (left) and test set-up after formation of a local buckle (right) [103]	51
Figure 50 Preparation phase (a) and layer structure (b)[105]	55
Figure 51 The investigated pipeline sections	56
Figure 52 The investigated samples	57
Figure 53 3BP or 4BP	57
Figure 54 The structure of the load transfer	58
Figure 55 The support method	58
Figure 56 The Position of the external load transition device	58
Figure 57 Calculation of the bending force on the experimental pipe section Y4	59
Figure 58 Force-deflection functions of pipe sections with external load	61
Figure 59 The laboratory area with hydraulic cylinders and control units of the testing systems.	62
Figure 60 Block diagram of the pressure boosting system up to 100 bar internal pressure	62
Figure 61 Block diagram of the pressure boosting system up to 700 bar internal pressure	63
Figure 62 The pit area of our developed system with a pipeline section.	63
Figure 63 Setting the deflection by load cell and its verification by extensometer with an extended arm.	64
Figure 64 The positioning plate with scales and holes, and the measurement of the deflection by extensometer with extended arm.	64

Figure 65 The artificial notch configurations	65
Figure 66 Artificial notch in the girth weld HAZ of the Y10 pipeline section (left), artificial notch through the girth weld of the Y8 pipeline section (right)	65
Figure 67 The preparation for the RT test (left), The device that used to do the RT (right)	68
Figure 68 Load cell and deflection meter for the external bending(left), Transfer of external load for the external bending (right)	69
Figure 69 Internal pressure vs. time functions recorded during the fatigue test of pipeline section with minimum superposed external bending load (Y4)	69
Figure 70 Internal pressure vs. time functions recorded during the fatigue test of pipeline section with maximum superposed external bending load (Y12)	70
Figure 71 Deflection vs. time functions recorded during the fatigue test of pipeline section with minimum ( $2 \sigma_a$ ) superposed external bending load (Y4)	70
Figure 72 Deflection vs. time functions recorded during the fatigue test of pipeline section with maximum ( $8 \sigma_a$ ) superposed external bending load (Y12)	71
Figure 73 The samples Y1 and Y2 during the pressure test	71
Figure 74 Y1 pipeline section at the moment of its failures	74
Figure 75 The pressure value during the burst test (example)	74
Figure 76 Average deformation (deflection) values and their variation during fatigue tests under minimal external bending load (Y4 and Y5 pipe sections, $2\sigma_a$ )	75
Figure 77 Average deformation (deflection) values and their variation during fatigue tests under intermediate external bending loads (Y6-Y11, $4\sigma_a$ and $6\sigma_a$ )	77
Figure 78 Average deformation (deflection) values and their variation during fatigue tests under maximal external bending load (Y12 pipe section, $8\sigma_a$ )	77
Figure 79 Average deflection values and their changes during the fatigue tests: all pipeline sections	78
Figure 80 Internal pressure vs. burst test time diagrams of the investigated Y1-Y5 pipeline sections	79
Figure 81 Internal pressure vs. burst test time diagrams of the investigated Y6-Y12 pipeline sections	79
Figure 82 Moment of failure of the pipeline section Y3 during the burst test: side view (top), longitudinal view (middle), the Y3 pipeline section after the burst test: the damaged section and the tested girth weld (bottom)	82
Figure 83 Moment of failure of the pipeline section Y1 during the burst test: side view (top), longitudinal view (middle), the Y1 pipeline section after the burst test: the damaged section and the tested girth weld (bottom)	83
Figure 84 Moment of failure of the pipeline section Y2 during the burst test: side view (top), longitudinal view (middle), the pipeline section Y2 after the burst test: the pipeline section with the damaged section (and the damaged coupling fitting highlighted with red circle) partially ejected from the test pit (bottom)	84
Figure 85 Moment of failure of the pipeline section Y4 during the burst test: side view (top), longitudinal view (middle), the pipeline section Y4 after the burst test: the damaged section (bottom)	85
Figure 86 Moment of failure of the pipeline section Y5 during the burst test: side view (top), longitudinal view (bottom)	86
Figure 87 Pipeline section Y5 after the burst test: pipe section displaced on the support beam in the test pit (top), damaged section (second), moment of failure of the pipeline section Y6 during the burst test: side view (third), longitudinal view (bottom)	87
Figure 88 Pipeline section Y6 after burst test: section of pipe (with the burst support beam and the damaged external load transfer device) in the test pit (top), damaged section (bottom)	88

Figure 89 Moment of failure of the pipeline section Y7 during the burst test: side view (top), longitudinal view (second), the pipeline section Y7 after failure: the pipeline section displaced on the supporting beam (and the damaged external load transfer structure) in the test pit (third), the damaged section (bottom)	89
Figure 90 Moment of failure of the pipeline section Y8 during the burst test: side view (top), longitudinal view (middle), the pipeline section Y8 after failure: the damaged area with axial notch perpendicular to the girth weld (bottom)	90
Figure 91 Moment of failure of the pipeline section Y9 during the burst test: side view (top), longitudinal view (middle), the pipeline section Y9 after the burst test: the damaged section (bottom)	91
Figure 92 Moment of failure of the pipeline section Y10 during the burst test: side view (top), longitudinal view (middle), the pipeline section Y10 after the burst test: the damaged section (bottom)	92
Figure 93 Moment of failure of the Y11 pipeline section during the burst test: side camera image (top), longitudinal camera image (middle), the pipeline section Y11 after the burst test: the damaged section (bottom)	93
Figure 94 Moment of failure of the Y12 pipeline section during the burst test: side camera image (top), longitudinal camera image (middle), tested pipe section Y12 after the burst test: the damaged section (bottom)	94
Figure 95 The damage section	95

## LIST OF TABLES

Table 1 Main characteristics of the Hungarian hydro-carbon transporting pipelines systems[15], [16]	13
Table 2 Tensile Properties – Pipe Body of SMLS and Welded Pipes PSL 2[23]	15
Table 3 Primary failure frequencies of different causes by EGIG[47]	29
Table 4 Failure frequency, cause and size of leak (2007-2016) [47]	30
Table 5 Chemical composition of the pipe material based on inspection certificate and the applied filler metals based on company specifications, weight%	54
Table 6 The basic mechanical properties of the pipe material based on the inspection certificate	54
Table 7 Key mechanical properties of welding filler metals	55
Table 8 Main characteristics of the welding process for the tested girth welds	55
Table 9 The length measurements and wall thicknesses	56
Table 10 Main characteristics of the RT carried out on the full size test pipe sections after preparing the weld	66
Table 11 The main characteristics of the full-scale tests	67
Table 12 The temperature and the pressure values for the investigated pipeline sections (except Y3) during the 6-hour pressure test	72
Table 13 Results of radiographic testing (RT) performed on the test girth welds by Albera'97 Kft., before and after the fatigue test	76
Table 14 The main characteristics and the burst pressure (BP) and the safety factor (SF) values of the investigations	81
Table 15 The damage section measurements	95

## SUPERVISOR'S RECOMMENDATIONS

Ahmad Yasser Dakhel was born in Aleppo (Syria) on 11th May 1992; his nationality is Syrian. He was a bachelor student between 2011 and 2016, studied at the University of Aleppo (Syria) and got his BSc degree in Mechanical Engineering – Production Engineering. The title of his BSc thesis was *Modeling and Control of a Three-dimensional Overhead Crane (Gantry Crane) via MATLAB Software*. During his BSc studies he was a teacher in a middle school (2012-2014, Aleppo), volunteer at World Health Organization (2014-2015, Aleppo), assembler of electronic circuits (2016 / 6 months, Aleppo), and maintenance supervisor (2017 / 4 months, Khartoum, Sudan). After all, he was a master student between 2017 and 2019, studied at the Faculty of Engineering / University of Debrecen (Hungary) and got his MSc degree in Mechanical Engineering – Production Engineering. The title of his MSc thesis was *Design Clamping Device*. Between his MSc and PhD studies (Jun 2019 – July 2019), he was an intern at Audi Hungaria Zrt. He started his PhD studies in September 2019 at István Sályi Doctoral School of Mechanical Engineering Sciences / University of Miskolc (Hungary); his affiliated organisation is the Institute of Materials Science and Technology / Faculty of Mechanical Engineering and Informatics. During his PhD studies, he was a part-time R&D engineer at Research Institute of Electronics and Information Technology / University of Miskolc (September 2022 – September 2024), furthermore, part-time mechanical design engineer at Schneider Electric in Gyöngyös, Hungary (March 2024 – October 2024). Since December 2023, he is a remote advisor at the Syrian Professional Network (Budapest, Hungary), and since October 2024, he has been an assistant research fellow at the University of Miskolc (Hungary).

During both his MSc and PhD studies, he was a full-time student in the framework of the *Stipendium Hungaricum Scholarship Programme*.

Through his previous studies and industrial practice, he has had a wide knowledge in different specializations, but he had not adequate and sufficient knowledge in the field of structural integrity, and high pressure hydro-carbon transporting pipelines. Therefore, in the first period, he started to study the relevant literature focusing on his research topic. He has selected systematically the subjects, hold presentations at research seminars, and taken part in institutional research work.

We have planned his research work collectively, and built-up a research and investigation plan. He has been actively and proactively involved in the design and implementation of the testing system, in collaboration with academic and administrative staff of the Institute of Mechanical Science and technology. His perseverance throughout the long period of the investigations under cyclic loading conditions has a great importance for the feasibility of the experimental work. Unfortunately, the pandemic period slowed down the practical work, but the lost time was made up for by the extension of the fellowship.

After the successful complex exam and reaching the first investigation results, his publication activity has increased. The results of the research work have been presented in doctoral seminars, doctoral forums, and different conferences; scientific papers have been prepared for both journals and conference proceedings. His self-dependence has developed in this field continuously and spectacularly.

During his PhD studies, his knowledge, his affinity to research work, his ability and suitability for the holding of presentations have developed significantly. He has acquired new knowledge and competences, which can be utilised and individually developed his future work, his future academic and scientific life, or an industrial environment.

Ahmad Yasser Dakhel has become an excellent member of the institute's collective and has also become involved in university life through his activities. He was a member of organization team of Process Control Systems (PCS) Meetings (2022-2024), mentor at the National Union of Students in Hungary (HÖÖK), and member of promotion and advertisement team of University of Miskolc.

It was a great pleasure for me to be the supervisor of his PhD research work. I rely on that he will be able to continue his professional and academic work at the University of Miskolc as a valued citizen of the University.

Based on his previous persistent scientific activity, he is highly recommended for obtaining the PhD degree.

17th April 2025

Prof. Dr. János Lukács  
Supervisor

## LIST OF SYMBOLS AND ABBREVIATIONS

3PB	Three-Point Bending	N/A
4PB	Four-Point Bending	N/A
A, A <sub>f</sub> , A <sub>65</sub>	Elongation at Failure	%
BP	Burst Pressure	bar
CMOD	Crack Mouth Opening Displacement	mm
C-SCC	Circumferentially Oriented Stress Corrosion Cracking	N/A
CTOD	Crack Tip Opening Displacement	mm
D&C	Deviations & Classification	N/A
DN	Nominal diameter	mm
EAC	Environmentally Assisted Cracking	N/A
ECA	Engineering Critical Assessment	N/A
FCAW	Flux Core Arc Welding	N/A
FEA	Finite Element Analysis	N/A
FfP	Fitness For Purpose	N/A
FfS	Fitness For Service	N/A
FL	Fusion Line	N/A
FST	Full-Scale Test	N/A
GCHAZ	Grain Coarsened Haz Cycle	N/A
GCT	Grain Coarsening Temperature	N/A
GRHAZ	Grain Refined Haz Cycle	N/A
GTN	Gurson-Tvergaard-Needleman	N/A
GWS	Girth Weld Symbol	N/A
HAZ	Heat Affected Zone	N/A
HSLA	High Strength Low Alloy	N/A
ICGCHAZ	Intercritically Reheated GCHAZ	N/A
ICHAZ	Intercritical Haz Cycle	N/A
ID	Inside Diameter	mm
IIW	International Institute of Welding	N/A
JIP	Joint Industry Project	N/A
KV	Charpy-V Impact Energy	J
L	Length of the Tested Pipeline Section	mm
LVDT	Linear Variable Displacement Transducers	N/A
MA	Misalignment	N/A
MAOP	Maximum Allowable Operating Pressure	bar
MMAW	Manual Metal Arc Welding	N/A
N/A	Not Applicable or Not Available	N/A
NDE	Non-Destructive Examination	N/A
NS	Not Suitable	N/A
OD	Outside Diameter	mm



## LIST OF SYMBOLS AND ABBREVIATIONS

---

PGMAW	Pulsed Gas Metal Arc Welding	N/A
PSL	Product Specification Level	N/A
PT	Liquid Penetrant Test	N/A
R <sub>eH</sub>	Upper Yield Strength	MPa
R <sub>m</sub>	Tensile Strength	MPa
R <sub>p0.2</sub>	Proof Strength	MPa
RT	Radiographic Test	N/A
R <sub>t0.5</sub>	Specific Yield Strength	MPa
R <sub>y</sub>	Yield Strength	MPa
s	Wall Thickness	mm
S	Suitable	N/A
SBD	Strain Based Design	N/A
SBD	Strain-Based Design	N/A
SCC	Stress Corrosion Cracking	N/A
SCGHAZ	Subcritically Reheated GHAZ	N/A
SCHAZ	Subcritical Haz Cycle	N/A
SF	Safety Factor	–
SMLS	Seamless	N/A
t	Wall thickness	mm
T/E	Time of Examination	N/A
TMCP	Thermo-Mechanical Controlled Processing	N/A
TSC	Tensile Strain Capacity	N/A
UEL	Uniform Elongation	%
UTS	Ultimate Tensile Strength	MPa
VT	Visual Test	N/A
WM	Weld Metal	N/A
WPS	Welding Procedure Specification	N/A
XFEM	Extended Finite Element Method	N/A
Y/T	Yield-To-Tensile Ratio	–
σ <sub>a</sub>	Axial Stress	N/mm <sup>2</sup>
σ <sub>t</sub>	Tangential Stress	N/mm <sup>2</sup>

## 1. INTRODUCTION, GLOBAL AIMS OF THE RESEARCH

Pipelines for the transportation of hydrocarbons are strategically important not only within a single country but also between countries and, more recently, even between bigger geographical groupings. Regardless of the origin, these pipeline failures typically result in longer or shorter disruptions to a geographic unit's energy balance. This has the direct effect of applying various tiers of regulations and standards with differing purview to every phase of the pipelines' life cycle [1], [2].

Usually consisting of 12–18 m long pipe strands, transporting pipes are joined by welding, either longitudinally or seamlessly. There will consequently be thousands of these girth welds, usually created by welding on location, along a pipeline that is several hundred kilometers long. This logically means that various standards also apply to the welding jobs and the evaluation of the finished circumferential welds [3].

Assessing the integrity of an operating structure or structural element is a complex task [4]. The content of the term already indicates this complexity: the suitability for operation at any moment of its lifetime. Understanding the practical problems and tasks requires or presupposes theoretical knowledge, structure-specific knowledge and relevant experimental work [5], [6]. Structure-specific knowledge includes design, technological and operational elements.

Pipelines used to transport crude oil or natural gas over long distances and at high pressures need a mix of high strength and toughness, as well as good weldability, to save transportation costs. The use of higher-grade steel pipes with improved weldability is being advocated to improve pipeline transport efficiency [6], [7], [8]. As a result, a major aspect in the pipeline sector is the exploration and development of enhanced and creative welding procedures to meet new technical problems. The ability of steel to be welded, and hence its good weldability, allows for the adoption of welding technology in general and the manufacturing of welded pipes [10], [11], [12], [13]. Weldability, as a technological quality, thus dictates the application of welding production technology, which has been increasingly popular in recent years across all industries. Steel is one of the most common materials used in the manufacture of welded structures in general, and welded pipes, due to its welding ability and good weldability. It's worth noting that weldability is a complicated concept that is influenced by a variety of factors, ranging from the chemical composition of steel to its processing history, welding technology applied to the interaction with the environment, temperature, air humidity, wind intensity in an open ground, and so on.

Girth welds play an important role during both the construction and the operation of the transporting pipelines[14]. Only high-quality girth welds reassure the operators of reliable function of the pipeline systems during their lifetime. Numerous girth welds can be found in different transporting systems, Table 1, Figure 1 summarizes the main characteristics (type, length and number of girth welds) of the Hungarian hydro-carbon transporting systems[15].

The loads on the girth welds are not only due to internal pressure, but also the location and the path as well as the construction of the pipeline, and the modifications during the operation can cause additional loads superposed on the internal pressure. Both base and superposed loads can be quasi-static and cyclical in nature.

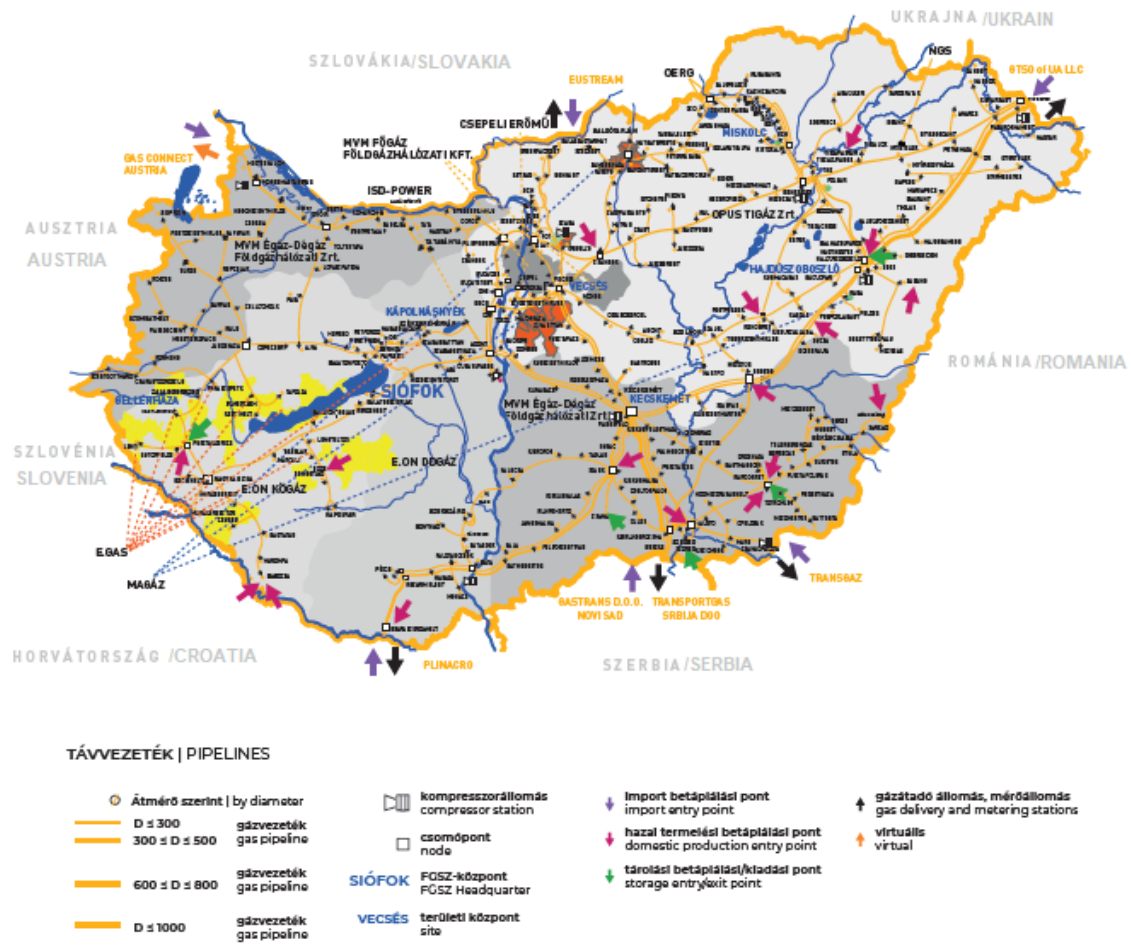


Figure 1 high-pressure natural gas transmission pipelines of FGSZ Ltd. [15]

Table 1 Main characteristics of the Hungarian hydro-carbon transporting pipelines systems[15], [16]

Characteristic	Value	Unit
Natural gas system	~ 6000	km
Crude oil system	~ 850	km
Other systems transporting liquid media	~ 1200	km
Total length	~ 8050	km
Average length of individual pipe sections	~ 11	m
Girth welds	~ 732.000	item

Because of the huge number of the girth welds the global aims of the research are as follows:

- Investigation and analysis of the development of a measurement possibility for girth welds subjected to complex loads.
- Assessment of the integrity of girth welds subjected to complex loads.
- Exploration of operational reserves in girth welds through assessment of the hazardousness of different types of failures.

## 2. STEELS FOR PIPELINE APPLICATIONS

### 2.1. Steel Materials and Manufacturing Innovations

#### **High Strength Low Alloy (HSLA) steels for structural applications in pipelines**

The requirement for greater combinations of strength, toughness, and weldability in bulk amounts at accessible prices has spurred the development of HSLA structural steels during the last four decades. Whether the applications were for energy pipelines, offshore steel structures, or ships, the goals were largely the same, however, the balance of requirements varied depending on the design or operational needs [17], [18], [19].

All sectors of the industry have been involved in achieving this goal: steelmakers and product producers, constructors, operators, and safety regulators. Many of the significant steps were because of these interactions, building the broad industry-based confidence necessary for making the often-significant investments in capital plant and industry practice; Many of the important steps were taken as a result of these exchanges, which helped to create the broad industry confidence needed to make the often-large expenditures in capital equipment and industry practice [19], [20], [21], [22].

Niobium can rightfully be considered the enabler of current, controlled processed HSLA steels due to the thermodynamic and kinetic properties of its carbide and nitride precipitates in steel. In a range of applications, these steels have undoubtedly enabled efficient and cost-effective design and construction technologies. For example, in the field of transportation pipelines, increases in the available strength level of line pipe over the last forty years (from X52 to X80, with X100 on the horizon) have resulted in cumulative benefits worth billions of dollars, largely because they were achieved without compromising industry-standard construction methods. Table 2 showing the tensile properties – pipe body of SMLS and welded pipes, PSL.

The parallels and contrasts in pipeline and structural steels' steelmaking, metal forming, and welding processes illustrate the vast range of influences on the weld heat affected zone (HAZ). They also explain why so much effort has gone into gaining a better understanding of the relationship between microstructure and mechanical properties inside the HAZ's various zones.

In HSLA steel weldments, similar issues apply to the weld metal. Because, in addition to all the issues mentioned above, the weld metal composition is a function of both the parent and consumable chemistries, as well as the welding process variables, the relationship between weld metal composition, microstructure, and mechanical properties is even more complicated than it is for the HAZ.

Several articles have been written over the last 40 years to investigate the effects of various parameters on the characteristics and microstructure of both the HAZ and the weld metal. The goal of this paper is not to attempt yet another review; rather, it is to concentrate on the parent metal HAZ and identify some of the key trends and influencing factors that provide an overall understanding of first, how metallurgical and thermal conditions influence the formation of the HAZ microstructure, and second, how the HAZ microstructure affects critical qualities including weldability and toughness.

Table 2 Tensile Properties – Pipe Body of SMLS and Welded Pipes PSL 2[23]

Pipe Grade	Tensile Properties – Pipe Body of SMLS and Welded Pipes PSL 2					Seam of Welded Pipe	
	Yield Strength <sup>a</sup>		Tensile Strength <sup>a</sup>		Ratio <sup>a, c</sup>	Elongation (on 50 mm)	Tensile Strength <sup>d</sup>
	R <sub>t0.5</sub> (MPa)		R <sub>m</sub> (MPa)		R <sub>t0.5</sub> /R <sub>m</sub> (–)	A <sub>f</sub> (%)	R <sub>m</sub> (MPa)
	Min	Max	Min	Max	Max	Min	Min
BR, BN, BQ, BM	245	450 <sup>e</sup>	415	655	0.93	f	415
X42R, X42N, X42Q, X42M	290	495	415	655	0.93	f	415
X46N, X46Q, X46M	320	525	435	655	0.93	f	435
X52N, X52Q, X52M	360	530	460	760	0.93	f	460
X56N, X56Q, X56M	390	545	490	760	0.93	f	490
X60N, X60Q, S60M	415	565	520	760	0.93	f	520
X65Q, X65M	450	600	535	760	0.93	f	535
X70Q, X65M	485	635	570	760	0.93	f	570
X80Q, X80M	555	705	625	825	0.93	f	625
X90M	625	775	695	915	0.95	f	695
X90Q	625	775	695	915	0.97 <sup>g</sup>	f	695
X100M, X100Q	690 <sup>b</sup>	840 <sup>b</sup>	760	990	0.97 <sup>h</sup>	f	760
X120M	830 <sup>b</sup>	1050 <sup>b</sup>	915	1145	0.99 <sup>h</sup>	f	915

a. For intermediate grades, use the yield and tensile strength differences from the next higher grade.

- Up to Grade X46: tensile strength ≤ 655 MPa
- Between X46 and X80: tensile strength ≤ 760 MPa
- Above X80: max tensile strength by interpolation (round to nearest 5 MPa)

b. For grades above X90, R<sub>p0.2</sub> applies.

c. Yield strength limit applies to pipes with D > 323.9 mm.

d. For intermediate grades, weld seam tensile strength = pipe body value (per a).

e. For longitudinal testing, max yield strength ≤ 495 MPa.

f. Minimum elongation A<sub>f</sub> is calculated using:

$$A_f = C \frac{A_{xc}^{0.2}}{U^{0.9}} \text{ where:}$$

- C = 1940 (IS units),
- A<sub>xc</sub> depends on test piece type and size (e.g., 130 mm<sup>2</sup> for 12.7 mm dia., max 485 mm<sup>2</sup> for others),
- U = min tensile strength (MPa) Lower R<sub>t0.5</sub> / R<sub>m</sub> may be agreed upon.

g. Lower R<sub>t0.5</sub> / R<sub>m</sub> values can be specified by agreement.

h. For grades > X90, R<sub>p0.2</sub> / R<sub>m</sub> applies, with lower ratios by agreement

### Steelmaking and Plate Forming Trends:

Understanding the physical and chemical metallurgy of the steel product, and how it is influenced, Steelmaking and plate-forming advancements have been driven first by steelmaking and metal forming techniques, and then by welding methods. These steps, when combined, determine the final installation's integrity and reliability, ensuring that it meets the initial design requirements. Steelmakers around the world have invested in new production and infrastructure to meet the demand for low-cost, high-quality steel, resulting in substantial advancements in steelmaking technology. Major developments include the introduction of basic oxygen steelmaking, increases in process control accuracy, and reductions in Sulphur and phosphorus content through procedures such as ladle steelmaking and ladle refining. In addition to decreases in residual elements, overall composition and homogeneity control have vastly improved.

Changes in casting technology from ingot to continuous slab, as well as further refining, have considerably improved product homogeneity, minimizing the consequences and quantity of centerline segregation.

A second important trend is the development and refining of controlled rolling and thermo-mechanical processing. Approximately forty years ago, pipeline plate steels were rolled under regulated circumstances. Controlled rolling and heat treatment were utilized in the early years to lower the carbon equivalent of the normalized product. The later introduction of thermo-mechanical processing allowed for even more carbon equivalent and microalloying content reductions, as well as increased parent metal strength without reducing weldability.

During the last 20 years, the development and refining of rapid cooling has increased the possibility to obtain strength without adding extra carbon or microalloying.

Controlled rolling and thermo-mechanical processing were first limited to thinner products, such as pipeline plates, with a thickness of less than 25 mm (1 in). Because increased strength was not very beneficial for many offshore structural applications where plastic collapse and fatigue were more critical, the benefits were mostly focused on improving weldability and weld zone toughness. Normalizing remained an important manufacturing method only for the thickest plates, which were used for offshore and shipbuilding applications.

Carbon-manganese-niobium steel was and is the original basic material. However, advancements in steelmaking and processing technologies have resulted in a gradual reduction in the quantity of niobium added; for example, between 1972 and 1981, the niobium level in offshore structural steels fell from around 0.05 percent to below 0.03 percent (Figure 2).

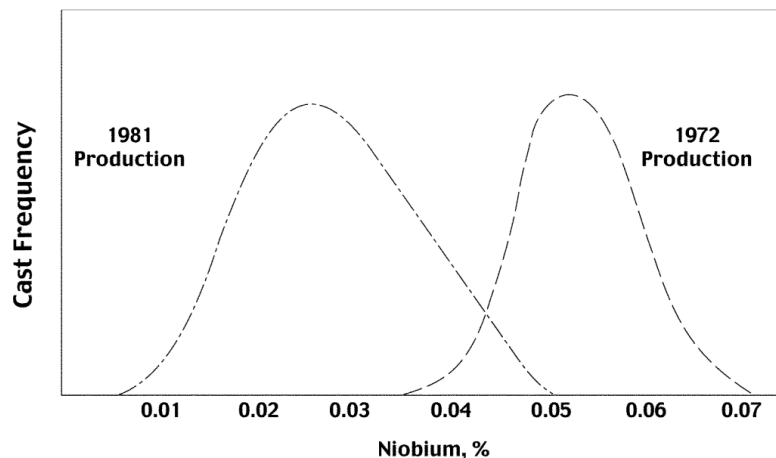


Figure 2 The amount of niobium in offshore structural steel has changed [24]

This was largely due to the more effective use of niobium, combined with better usage and control of rolling operations, resulting in the same grain size control effect with less alloying. It should

also be emphasized that at the same time span, carbon content decreased practically proportionally, resulting in a significantly less influence on the niobium-carbon balance.

## **2.2. Welding Processes and Defect Management**

### **Welding Processes:**

The welding procedure has a significant impact on the finished installation's integrity. Much of the early attention on large-diameter pipelines was on achieving appropriate toughness in the submerged arc seam weld to give the same assurance against fracture initiation as the source metal. With inputs of heat 2 to 4 kJ/mm, such seam welds are normally accomplished in two passes. Once the significance of axial stresses coming from geomechanically produced and operational loads was realized, the focus shifted to manual girth weld toughness [25].

The development of semi-automated and mechanized welding methods, as well as the shift toward assessing weld flaws on a fitness-for-service basis, has raised awareness of the girth weld's toughness, both in terms of the weld zone and the heat affected zone (HAZ). For manual procedures, such welds are typically performed at heat inputs of 0.7-2 kJ/mm and 0.5-1 kJ/mm for automated processes [26], [27], [28].

Manual and semi-automatic welding procedures are commonly utilized for offshore structural steels, however with greater plate thickness comes more weld passes and asymmetric weld preparation. The desire to shorten construction times has resulted in a slightly higher range of heat inputs (typically 3–5 kJ/mm) than for pipeline girth welds. However, this is constrained by the necessity to minimize hydrogen cracking while fabrication on the one hand, and the need for adequate hardness in the HAZ on the other.

The accomplishment of high weld deposition rates through high heat input welding is a primary requirement for shipbuilding applications. The weld zone's toughness is less essential.

Submerged arc welds can have heat inputs of 2 – 10 kJ/mm, while electroslag welds can have heat inputs of 25 – 50 kJ/mm. As will be explained later, such significant heat inputs might result in extensive HAZs and coarse microstructures.

### **The Weld Metal:**

The goal of this paper is not to go into great depth about the microstructure and characteristics of the weld metal. It's worth noting, however, that the interactions between weld metal microstructure, composition, and welding circumstances are more complicated than they are in the HAZ.

This is because, while all the foregoing elements play a role, the chemical composition of the weld metal and its macro distribution in the solidified weld pool are determined by the parent and consumable compositions, flux activity, and welding process variables.

Many of the same fundamental microstructural concepts that apply to the HAZ also apply to the weld metal. However, acicular ferrite, which consists of thin interconnecting grains with a basket-weave look, is another essential microstructure. Its development is dependent not only on the presence of an acceptable distribution of fine non-metallic inclusions, but also on a correct combination of chemical composition and cooling rate. The flux or shielding gas composition has a big impact on the inclusion distribution. Following the discovery of acicular ferrite microstructures in weld metals in the 1970s and their associated high toughness, titanium-containing oxide-dispersion compositions for structural steels were developed, with similar improved HAZ capabilities.

**Weldability - Resistance to Hydrogen-assisted Cold Cracking Approaches to Cold Cracking Control Have Changed Over Time**

A study and summary of the history of approaches to cold cracking in structural and pipeline steels, as well as some of the accompanying testing methodologies, has been provided. These advancements, to a considerable part, reflect the advancements in materials that have occurred over the same time. The steels used for line pipe and other structural applications in the 1950s and early 1960s were mostly simple carbon-manganese formulations; if micro-alloying elements were used at all, it was only to aid in grain-size control during heat treatment of materials that could not achieve the specified toughness in the as-rolled condition.

Hydrogen cracking was already known to occur within a narrow temperature range and to be dependent on a crucial combination of hydrogen concentration, tensile stress, and sensitive microstructure. However, the transformation properties of these steels, as well as the vulnerability of the transformed microstructures to cracking, allowed for the successful application of a crack prevention strategy based primarily on HAZ hardness. Hardened microstructures, for the most part, were so prone to cracking that their creation could only be permitted if extremely low hydrogen concentrations and stress levels could be ensured. In these steels, however, the variation in hardness (an approximate measure of crack susceptibility) with cooling rate was steep throughout the transformation range. Controlling the cooling rate by limiting heat input and thermal severity (basically, the whole thickness of the weldment accessible to transmit heat away from the weld) could therefore be utilized to prevent cracking.[29], [30], [31].

Critical hardness levels might be determined based on the hydrogen potential of the welding electrodes and linked to welding circumstances that would prevent cracking. The old ("IIW") carbon equivalent was a good technique to express the impact of chemical composition on hardenability. For basic joint configurations like pipeline girth welds, methods like the Controlled Thermal Severity (CTS) test and under-bead cracking tests were useful techniques of determining weldability.

### **Cracking the Root Pass As a result of lifting or restraint**

The first approaches to cold cracking management were developed primarily for structural and shipbuilding purposes, thus it's only logical that they focused on thermal contraction against constraint as the primary source of stress. In reality extremely thorough engineering methodologies to calculating restraint stress have been devised and used in cracking models.

The condition thus far has the potential for cracking within minutes of the root pass being deposited, and it can be controlled by paying attention to the root-bead completion, the gap between the root and hot passes, and preheating as needed. True delayed cracking, on the other hand, can occur in specific circumstances, particularly in the presence of wind and a low ambient temperature [32].

Glover and Graville provided study findings on the subject, evaluating the influence of procedural and meteorological variables on cracking risk. In such instances, the local stress to consider is the final residual stress in the completed weld, while the local hydrogen concentration must be monitored throughout the consecutive weld passes and subsequent cooling.

## **2.3. Microstructural Evolution and HAZ Performance**

### **Microstructure Development in the Weld Zone:**

The HAZ is made up of a variety of microstructures, each of which is impacted by the heating rate, peak degree, and cooling rate utilized during the solidification and cooling of surrounding weld metal (Figure 3).

The peak degree of weld heat inputs delivered to structural HSLA steels may be sufficient to cause significant coarsening of the austenite grains nearest to the fusion line. Cooling periods from 800 C to 500 C (1470 – 930 F) can range from 15 seconds or fewer at 1 kJ/mm (25 kJ/in) to 30 seconds



at 5 kJ/mm (125 kJ/in) and over 200 seconds at 40 kJ/m (1000 kJ/in). The intra-granular microstructure can range from auto tempered martensite to ferrite-pearlite, and the equivalent preceding austenite grain diameters can range from 50 m to over 250 m.

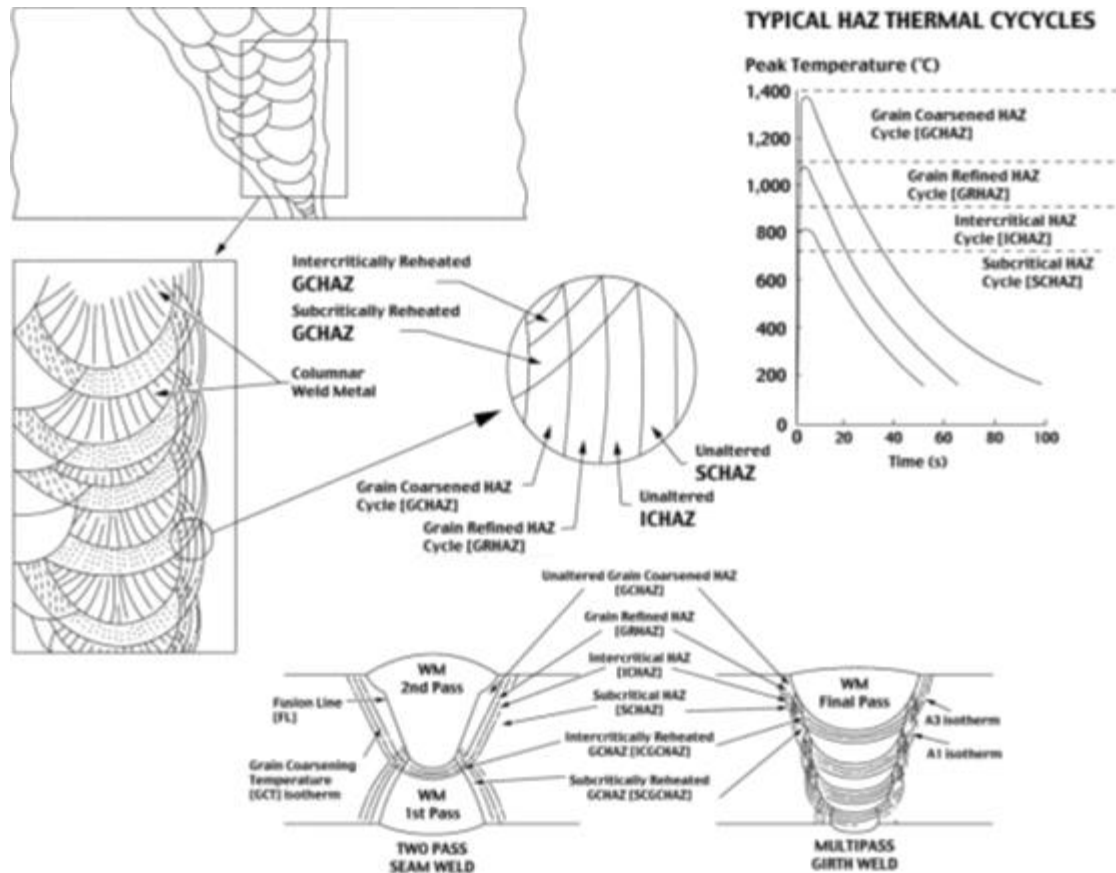


Figure 3 Microstructure of the heat-affected zone in two-pass and multiple pass welds based on [33]

A multi-pass weld results in a variety of partially and totally reheated zones as the HAZ from the second round overlaps the HAZ from the first round (Figure 3). The most crucial zones are the sub-critical or intercritically reheated coarse-grained HAZ areas, where the preceding microstructure would either be tempered or partially retransformed and re-cooled.

### Heat Affected Zone with Coarse Grains:

The interaction of the weld thermal cycle and steel composition on the microstructure of the coarse-grained heat affected zone has been studied extensively.

It's hardly unexpected that the claimed effects are perplexing and often contradictory, given the complicated and interacting impacts of multiple alloy constituents. The following are the most important microstructural parameters in terms of subsequent properties: (see also Figure 3).

### Austenite Grain Size:

Unless small particles such as micro-alloy carbides or nitrides constrain austenite grain formation, it grows fast at temperatures beyond 1000°C (1830°F). Niobium has long been used for this (Figure 4), but the amount utilized must be carefully monitored to ensure that the particle dispersion is neither too coarse nor too fine. Titanium (Figure 5), which forms a stable nitride even

at extreme temperatures, has recently been employed for grain growth in a variety of pipeline, structural, and shipbuilding steels.

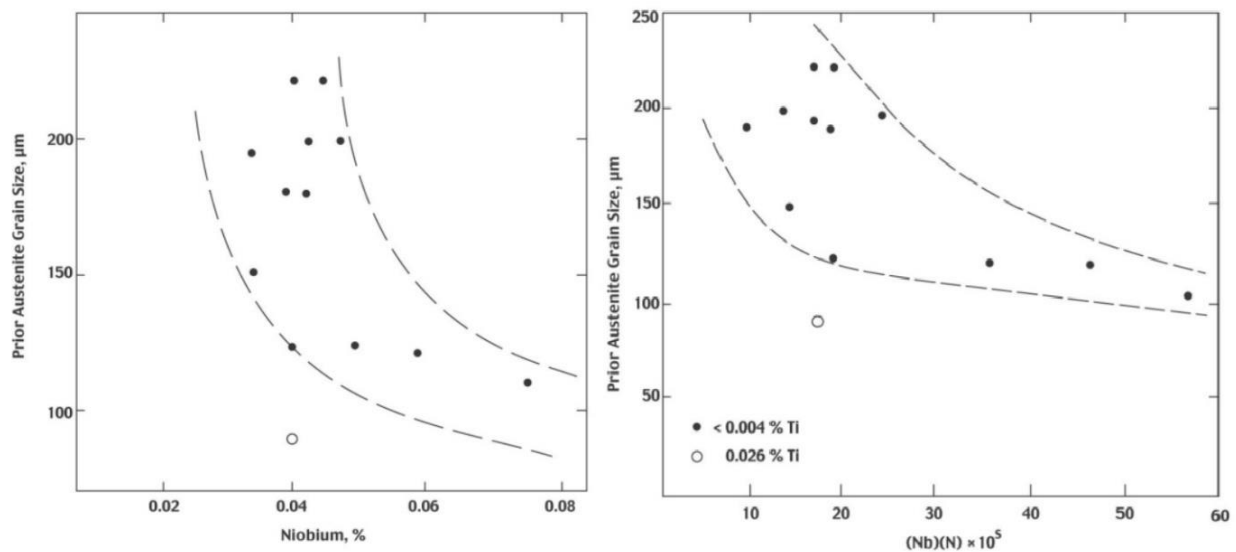


Figure 4 Effects of titanium, niobium, and nitrogen on the grain size of previous austenite [24].

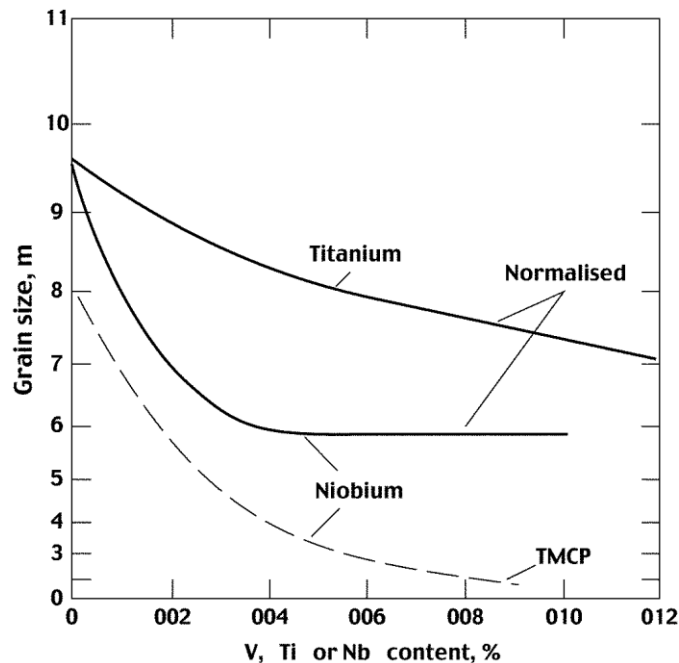


Figure 5 TMCP stands for Thermo-Mechanical Controlled Processing, and it shows the effect of niobium and titanium on ferrite particle size [34].

### Intragranular Microstructure:

The microstructure that forms because of cooling is determined by the material's hardenability and, as a result, the temperature range across which the transfer from austenite to ferrite and carbides occurs. Manganese, chromium, molybdenum, vanadium, copper, and nickel are alloying elements that have an influence on this. It is also controlled by the extent to which elements like boron can reduce ferrite grain border nucleation, as well as the extent to which tiny particles like titanium oxide can enhance intra-granular ferrite nucleation. Finally, and most importantly, the

microstructure is determined by the carbon concentration, which affects the final microstructure's balance of ferrite and carbide phases.

Figure 6 and Figure 7 show the correlations between transformation temperature and microstructure. At the highest transformation temperatures, ferrite tends to develop as equiaxed grains at the previous austenite borders and as randomly orientated grains in the core. Carbon-rich areas become carbide aggregates, which are relatively coarse. Grain boundary ferrite is gradually replaced by interior colonies of laths in parallel orientation or Widmanstätten ferrite as the transformation temperature decreases; discrete carbide particles form at the lath boundaries at higher transformation temperatures and are gradually replaced by islands of high-carbon martensite-austenite as the transformation temperature decreases.

There is insufficient time for long-range carbon partitioning at the lowest transformation temperatures, resulting in transformation to bainite or martensite; if martensite forms, additional cooling may result in some auto tempering.

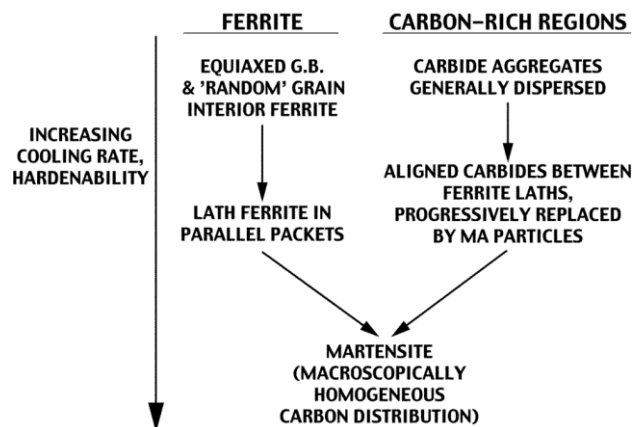


Figure 6 HAZ microstructure as a function of cooling rate and hardenability [35]

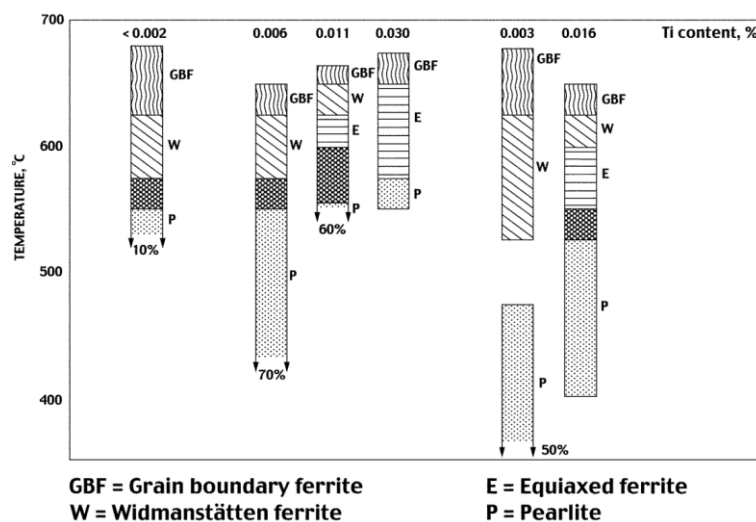


Figure 7 HAZ microstructure of ESW welds in ship steels as a function of transformation temperature [36]

Microalloying elements can have a variety of effects on the coarse-grained microstructure of HAZ:

- Elements that produce stable fine precipitate dispersions at high temperatures (e.g., Ti) can limit grain development, enhance intragranular ferrite nucleation, and expand the temperature range of transformation.

- Solid-solution elements (e.g., Mn, Ni) might reduce the transformation temperature range and contribute to the transformed product's solid solution hardening.
- Elements that are largely absorbed at the peak of the weld thermal cycle and form fine carbides or nitrides on cooling could either promote ferrite formation (e.g., V), increase overall transformation temperature range, and decrease intra-lath carbide formation, or delay ferrite formation (e.g., Mo, Cr), lower the transformation temperature range, and start encouraging martensite-austenite formation.

The solubility qualities of niobium's carbonitride, which are more soluble than titanium but less soluble than vanadium and molybdenum, play a unique function in determining HAZ microstructures. As a result, Niobium, alone among the micro-alloying elements, could act in several of the above ways determined by the amount present, the carbon value, the 'competitive' interaction with the other microalloying elements, the available nitrogen content, the prior manufacturing history, and the weld thermal cycle.

Only at temperatures exceeding 1000 °C (1830 °F) does niobium carbonitride dissolve in austenite. Because there is insufficient time above this temperature for considerable dissolution in rapid weld heat cycles, the constraining effect of niobium on austenite grain development is linked to the previous dispersion. Dissolution occurs during the slowest weld heat cycles, followed by reprecipitation in austenite or ferrite. Precipitation in austenite can limit grain development and encourage early ferrite nucleation at grain borders. During the change to bainite, precipitation as ultra-fine particles can occur, limiting the breadth of bainite laths and boosting carbide aggregate development at the interstices. The precipitation of ultrafine particles may be reduced at moderate cooling rates, favoring martensite-austenite islands in the interstices.

When the impacts of alloy composition and weld heat cycle are combined, it is evident that there are numerous competing and interacting influences. As a result, developing a general quantitative explanation of how all these microstructural influences interact to define HAZ features is a challenging task. Nonetheless, the fundamental impacting elements discussed above can be used to forecast the likely outcome of specific changes in compositional or processing characteristics.

### **The Intercritically Reheated Coarse-grained Heat Affected Zone:**

The overlaid HAZ from the second bead causes a range of partially and totally retransformed zones within the original coarse-grained HAZ in multi-pass welds. The coarse-grained HAZ that has been intercritically reheated, in which the preceding microstructure is largely changed to austenite, is the most important zone in terms of HAZ characteristics. Localized regions of carbon-rich austenite result from the partial transformation, which are enriched further by dissolution of more carbon from the surrounding area and then retransformed to high-carbon twinned martensite on cooling. As will be seen later, these brittle 'islands,' which can be up to 5 µm in size and make up to 5% of the microstructure, can have a considerable impact on toughness qualities.

Detailed studies of martensite islands in inter-critically reheated zones have revealed that, as expected, Individual beads' chemical composition, heat input, and relative location in the multi-pass weld all have an impact on their production and dispersion. Increased alloy element concentration (for a given carbon content) increases the volume fraction of martensite islands and reduces the possibility that the martensite will be dissolved by following weld heat cycles in terms of compositional effects.

### **Toughness of HAZ Performance**

**HAZ is a coarse-grained material:** The relative strengths and microstructures of the individual regions in the weld zone, as well as their spatial relationship to one another, determine the overall toughness of the HAZ. The various implications of HAZ microstructure discussed previously are

readily visible in a multi-pass weld. Toughness is frequently controlled by the coarse-grained HAZ.

There have been several investigations of HAZ toughness during the last 40 years, and it would be impossible to examine them all in one study. Studies have employed multiple-pass welds, single beads, and weld thermal simulations, with test setups ranging from tensile and Charpy specimens to CTOD and broad plate combinations. Several of this research has focused on the austenite grain size and intra-granular microstructure to investigate the link between microstructure and toughness, particularly for coarse-grained HAZ.

Many studies have shown that the size of austenite grains has a substantial impact on toughness. The benefits of lowering grain size for thermomechanical treated steels with a variety of basis microstructures are shown in Figure 8. In most cases, grain size has an indirect influence; the size of the 'covariant packet' or sub-grain that governs fracture initiation is proportional to the austenite grain size.

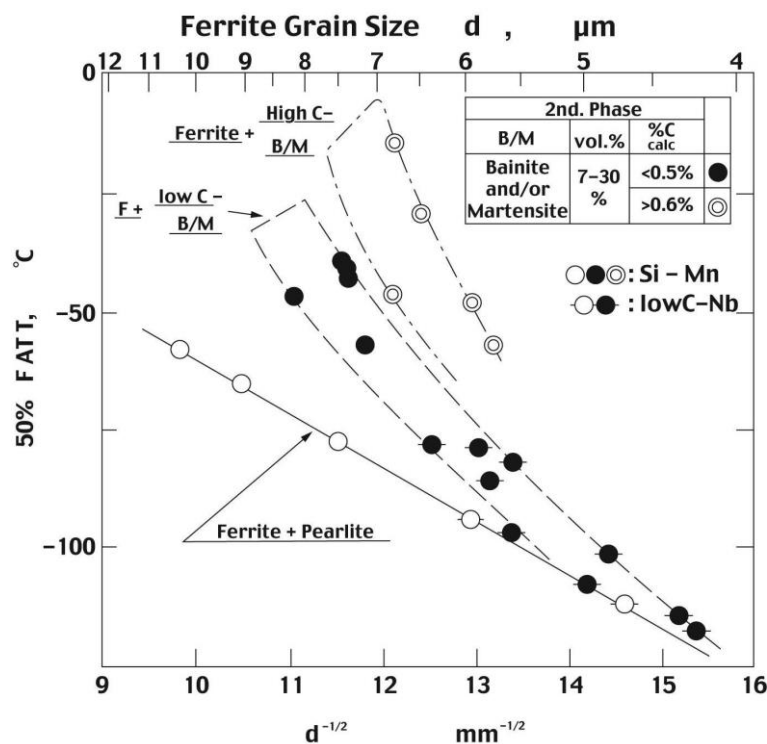


Figure 8 Effects of grain size and microstructure on toughness [37]

The impact of intragranular microstructure on toughness is more difficult to determine, however it can be illustrated by looking at the correlations between cooling rate, transformation temperature, carbon content, and microstructure that were established before. Figure 10a depicts the impact of carbon content and transformation temperature on microstructure, while Figure 10b depicts the impact on toughness. Although they were heavily based on test data, the pair of diagrams should be considered schematic rather than quantitative. Figure 10a depicts the zones in which various HAZ microstructural types can be found. Figure 10b illustrates the link between transformation temperature and hardness by showing sections of Figure 10a at three carbon contents:

- Good toughness can be achieved only rarely at high carbon levels (0.21 percent), Because even lower bainite has low toughness, and martensite generated at low temperatures is twinned and fundamentally fragile in its untempered condition, very minimal auto-tempering may occur.

- At low carbon levels (0.07 percent), In the 460-400 °C temperature range, the poor microstructure found above 530 °C is slowly replaced by low bainite and auto-tempered martensite. As a result, good toughness can be achieved over a large range of transformation temperatures, and hence a wide range of weld heat inputs.
- A similar pattern holds true for intermediate carbon levels (0.14 percent), with the exception that the range in which good toughness can be achieved is limited.

The correlations shown in Figure 10 were calculated for basic C-Mn-Nb steels with no substantial alloy additions. The core concepts, however, have been proved to apply to a wide range of current steels with microalloying additions, as well as HSLA pipeline (Figure 9), structural, and shipbuilding steels. The degree to which the microalloying additions contribute to solid solution strengthening, grain size refinement, or carbonitride precipitation, there is a general 'shift' of the toughness values for these steels.

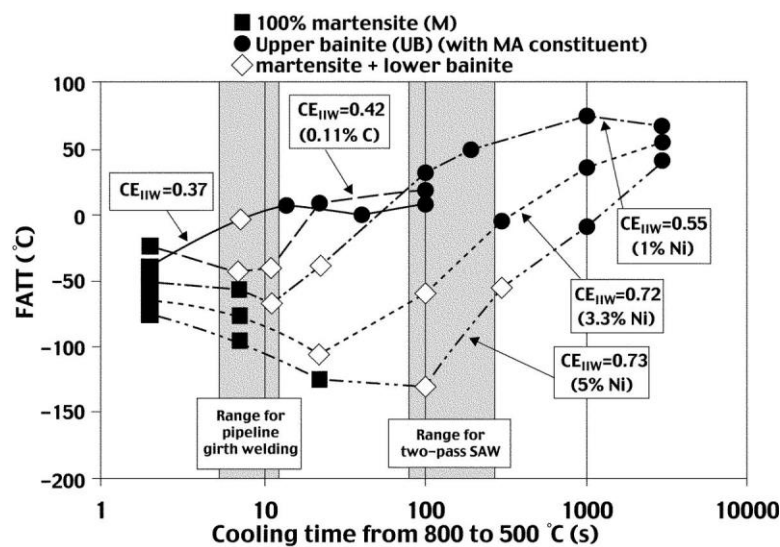


Figure 9 Correlation between FATT and cooling time for coarse-grained HAZ microstructures of pipeline steel [38].

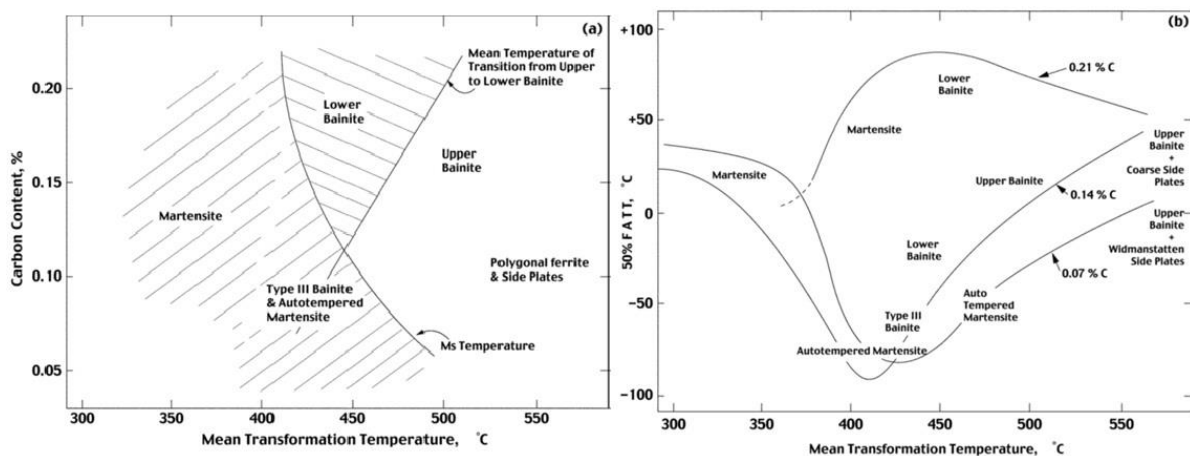


Figure 10 Influence of carbon content and microstructure on HAZ microstructure and toughness of structural steels [39].

## The Inter-critically Reheated Zone



As the chemical composition and thermomechanical techniques have enhanced the toughness of the coarse grained HAZ, the problem of the intercritically reheated coarse-grained area has attracted increasing attention. As previously stated, the intercritically reheated region is known to have low toughness, especially if islands of martensite-austenite are present.

In some steels, detailed studies of the occurrence and structural significance of martensite-austenite islands have shown that the intercritically reheated region can have toughness that is at least as low as the coarse-grained region (Figure 11), and that the reduction in toughness is dependent on the volume fraction of martensite islands present.

While the adverse effect of martensite islands in multi-pass welds can be mitigated to some extent by the influence of subsequent weld passes, the only effective remedy is to choose a chemical composition that minimizes the extent to which martensite islands can develop, a balance of carbon contents and microalloying additions. Empirical formulas connecting the volume fraction of martensite islands to alloy element concentrations have been developed in recent investigations.

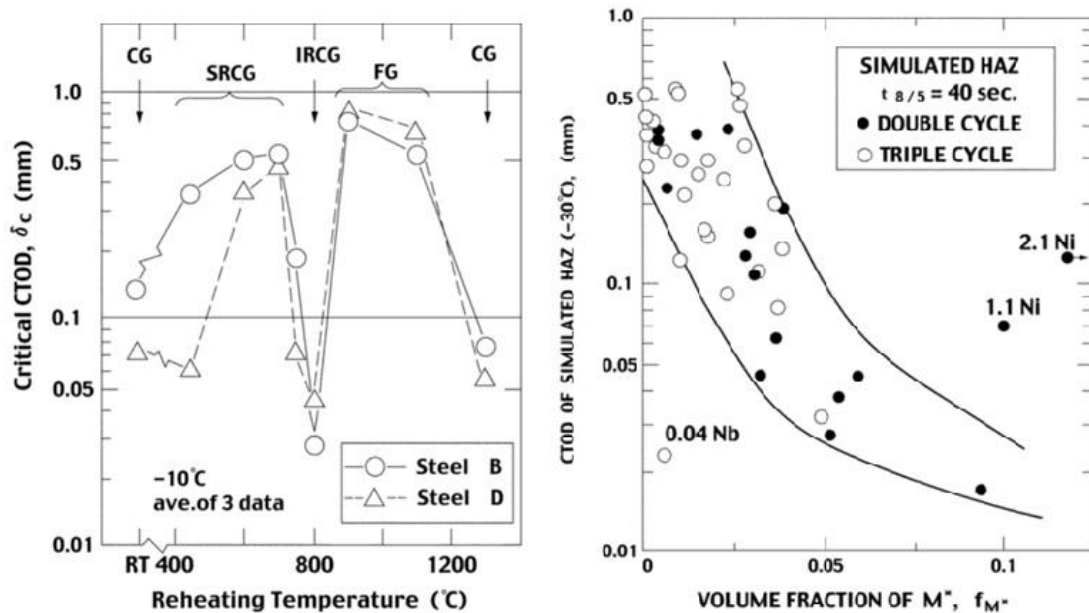


Figure 11 Toughness variations in simulated multipass weld HAZ microstructures(left), Dependence of intercritically reheated HAZ toughness on volume fraction of martensite islands (right) [40].

### 3. FAILURE STATISTICS FOR TRANSPORTING PIPELINES

#### 3.1. Failure statistics for transporting pipelines

When we talk about the transporting pipelines, it is essential to maintain high-pressure oil and gas pipeline systems safety because the products are dangerous. Perhaps, it will cause fire, explosion or poisoning and lead to substantial economic losses, casualties and environmental pollution, Pipeline operators collect and review the failure data and recognize the critical detection of pipeline risk, integrity evaluation, risk reduction and accident avoidance[41], [42], [43]. The statistical results of European pipeline failures, causes, and consequences will be analysed. The similarity and the differences of pipeline managements will be studied, too.

#### 3.2. Examples of failures

##### **Pipeline Accident in California [44]**

A pipeline owned and run by the Pacific Gas and Electric Company (PG&E) broke down in a residential area in California on September 9, 2010 (Figure 12). The ruptured section was installed with a 0.762 m diameter. A crater about 21.95 m long by 7.92 m wide was formed by the rupture. The ruptured pipe part, about 8.53 m long and weighing about 1,360.78 kg, was located 30.48 m to the south of the crate.

PG&E has projected the release of 1,348,312 cubic meters of natural gas. The natural gas released ignited, leading to a fire that destroyed 38 homes and damaged 70. Eight people died, and dozens were wounded.



*Figure 12 Pipeline Accident in California [44]*



**Pipeline Accident in West Virginia [45]**

The 11th of December, 2012. A buried 0.508 m diameter interstate pipeline, owned and operated by Columbia Gas Transmission Corporation (Columbia Gas), ruptured in West Virginia, a sparsely populated region (Figure 13). Just before the rupture, the pipeline was running at around 6.41 MPa. The pipe was expelled from the underground pipeline by about 6.10 m and landed more than 12.19 m away.



*Figure 13 Pipeline Accident in West Virginia [45]*

**Pipeline Accident in New Mexico[46]**

A 0.762 m diameter natural gas transmission pipeline owned by the El Paso Natural Gas Corporation broke down in New Mexico on Saturday, August 19, 2000 (Figure 14). It released the inflamed gas and burned it for 55 minutes. Twelve people who were camping under a concrete-decked steel bridge supporting the river pipeline were killed, and their three vehicles were burned.



*Figure 14 Pipeline Accident in New Mexico[46]*

### 3.3. Analyzing and contrasting the pipeline's failures

Failure statistical results of European Gas pipeline Incident data Group (EGIG) in Europe on long-distance pipeline failure frequencies, causes, and consequences are comparatively analysed. the pipeline types that the analysis involves in our case Natural Gas[47].

The overall length of the EGIG gas pipeline will be 144,000 km until 2016. In order to show the safety performance of the European gas transmission network to the general public and authorities, the goal of EGIG is to collect and present data on gas loss incidents.

The conditions required to be reported in the EGIG database for an incident are the following:

- An event could result in accidental release of gas.
- The pipeline must meet the conditions set out below:
  - = to be built of steel;
  - = being onshore;
  - = have an operating maximum pressure greater than 15 bar;
  - = to be placed outside the fences of the gas stations.

### 3.4. Failure Frequency

Figure 15 illustrates the decreasing failure frequencies per cause over the years, between 1974 and 2016. The decrease may be explained by technological developments, such as welding, inspection, condition monitoring using in-line inspection and improved procedures for damage prevention and detection. Improvements in the prevention of external interference incidents may be explained by more stringent enforcement of land use planning and the application of one-call systems for the digging activities of external parties. (Figure 15) In several countries, there is now a legal requirement to report digging activities. Companies have adopted appropriate actions, like supervision or marking of the pipeline in the direct neighborhood of the digging activities.[47]

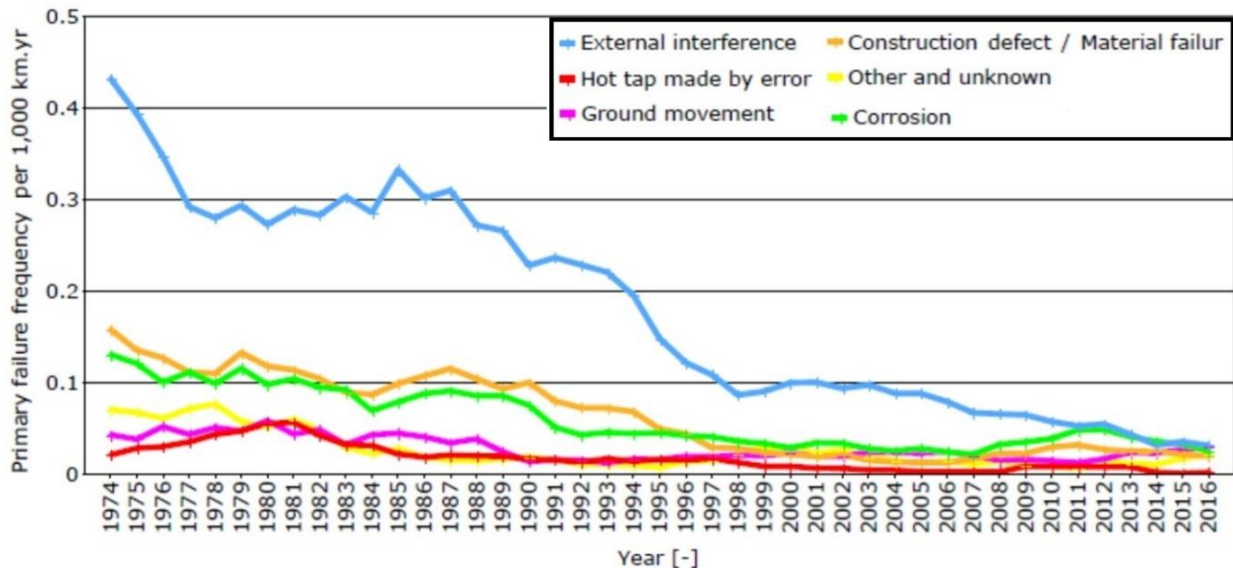


Figure 15 Failure frequencies of different causes by EGIG[47]

To demonstrate failure frequencies over a more recent period (Table 3) in addition to the frequencies for the whole period, frequencies over a time span of the last 5, 10 and 20 years. As far as the cause external interference is concerned, its associated primary failure frequency over the five-year moving average has levelled off at around 0.03 per 1,000 km\*yr.[47]

Table 3 Primary failure frequencies of different causes by EGIG[47]

Cause	Primary failure frequency			
	1970-2016	1997-2016r	2007-2016	2012-2016
	per 1,000 km·year			
External interference	0.144	0.064	0.043	0.032
Corrosion	0.052	0.034	0.037	0.027
Construction defect / Material failure	0.051	0.022	0.027	0.021
Hot tap made by error	0.014	0.006	0.006	0.003
Ground movement	0.026	0.023	0.022	0.031

Figure 16 and Figure 17 show the failure frequency per leak size and per-incident cause for 1970-2016 and 2007-2016, respectively.

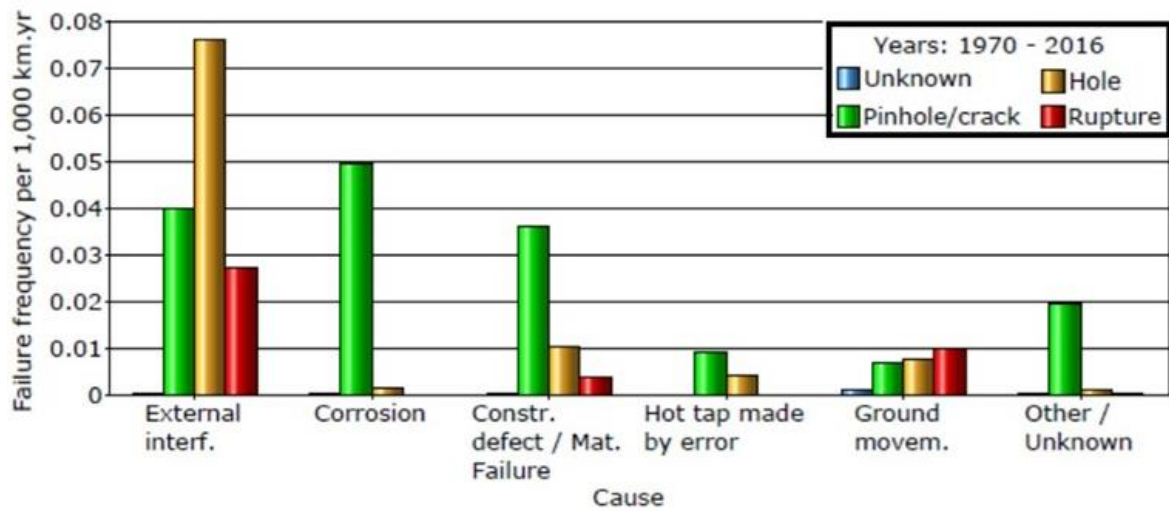


Figure 16 Relationship primary failure frequency, cause, and size of leak (1970-2016)[47]

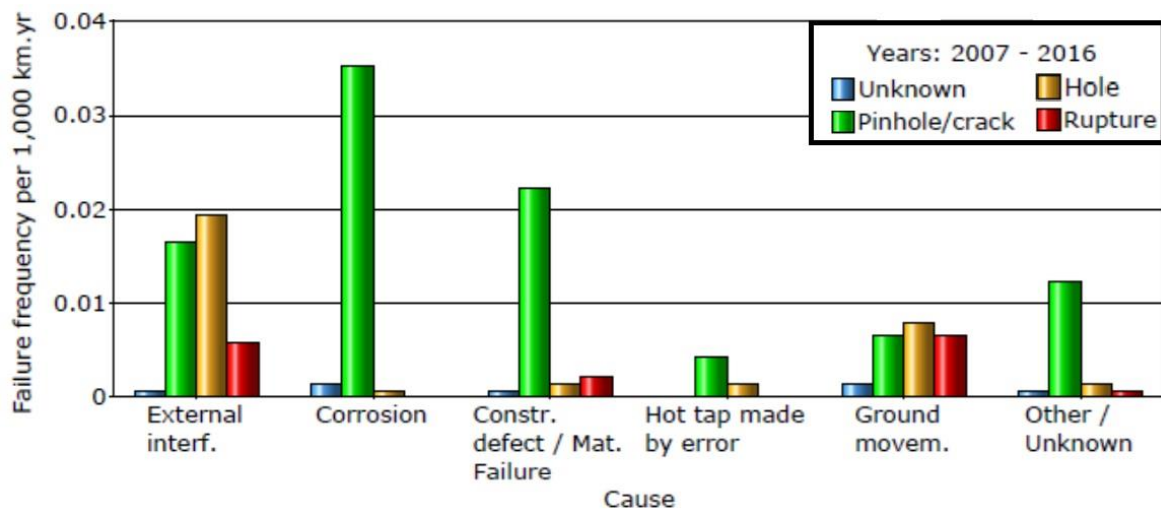


Figure 17 Relationship primary failure frequency, cause and size of leak [47]

The data for the period 2007-2016 were summarized in Table 4. Although the failure frequency decreased over the years, the general trend in the distribution of the leak sizes remain the same: holes and ruptures were mainly caused by external interference. For pinhole/crack leak sizes, corrosion remains the main cause.

Table 4 Failure frequency, cause and size of leak (2007-2016) [47]

Leak size	Failure frequency per 1,000 km·year					
	External interference	Corrosion	Construction defect / Material failure	Hot tap made by error	Ground movement	Other and unknown
<b>Rupture</b>	0.0058	0.0000	0.0022	0.0000	0.0065	0.0007
<b>Hole</b>	0.0195	0.0007	0.0014	0.0014	0.0079	0.0014
<b>Pinhole / crack</b>	0.0166	0.0353	0.0224	0.0043	0.0065	0.0123
<b>Unknown</b>	0.0007	0.0014	0.0007	0.0000	0.0014	0.0007

### 3.5. Failure Causes

External interference, corrosion, and design defects/material failure are the leading three causes of gas pipeline failures in EGIG.

In Figure 18 the incident distribution per cause over the last 10 years is given. Corrosion and external interference incidents occurred at about the same rate. However, corrosion incidents tend to have smaller leak sizes.

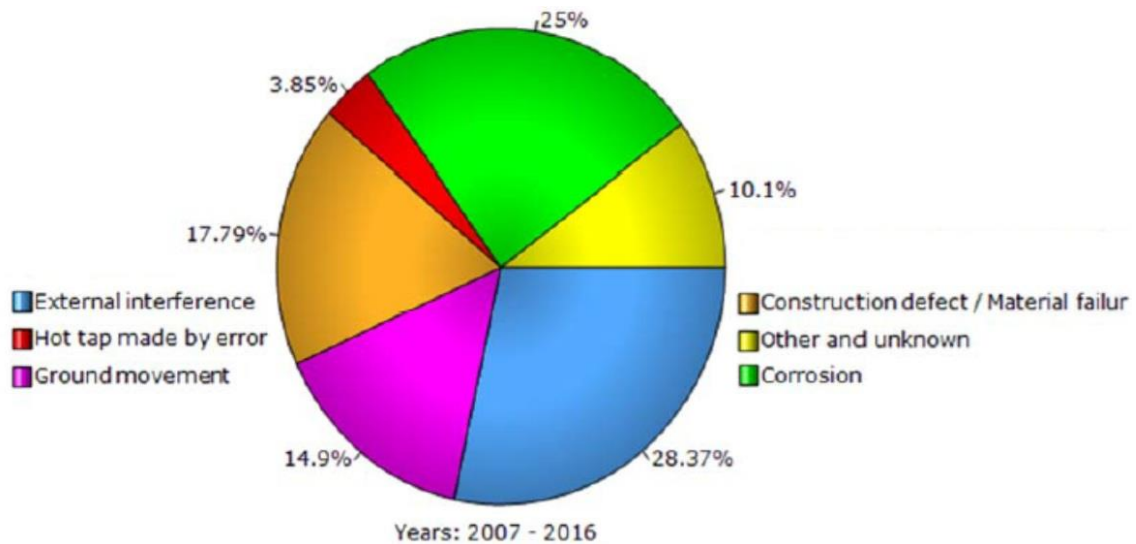


Figure 18 Failure causes by EGIG [47]

### 3.6. Failure Consequences

Figure 19 shows that gas releases from large diameter pipeline ruptures at high pressure have ignited more frequently than smaller diameter pipeline ruptures at lower pressure. This data is based on only a few ruptures. Care should be taken when using it as an ignition probability, as the uncertainty is high.

In the paper [48] an analysis is made of ignition probabilities. This paper shows that even ruptures of large diameter pipelines and high pressure not always ignite.



EGIG database also registers qualitative information about the consequences of incidents, amongst other injuries and fatalities that, unfortunately, occurred in some of them (Figure 20).

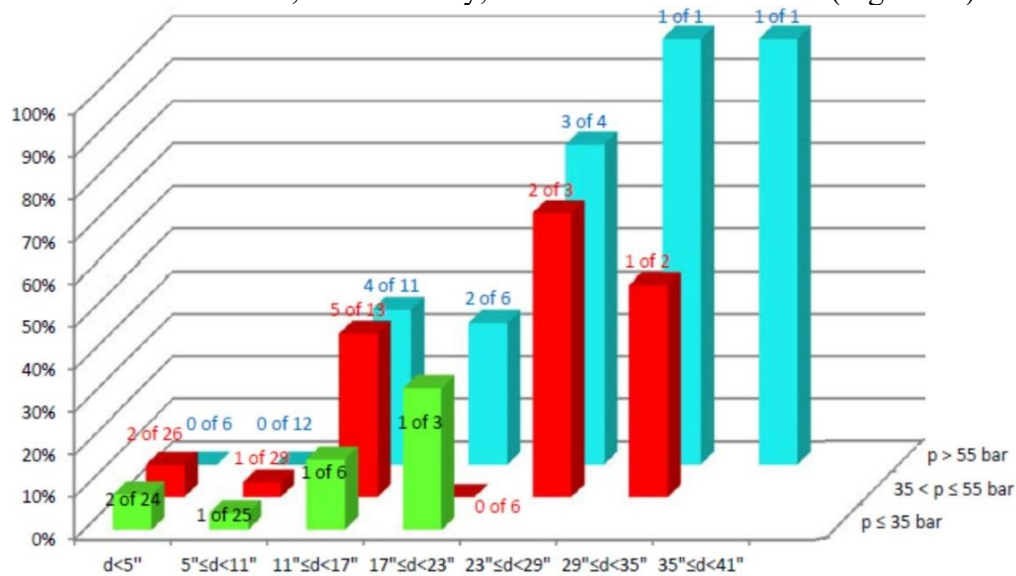


Figure 19 Percentages of ruptures that ignited subdivided in diameter and pressure (1970-2016) [47]

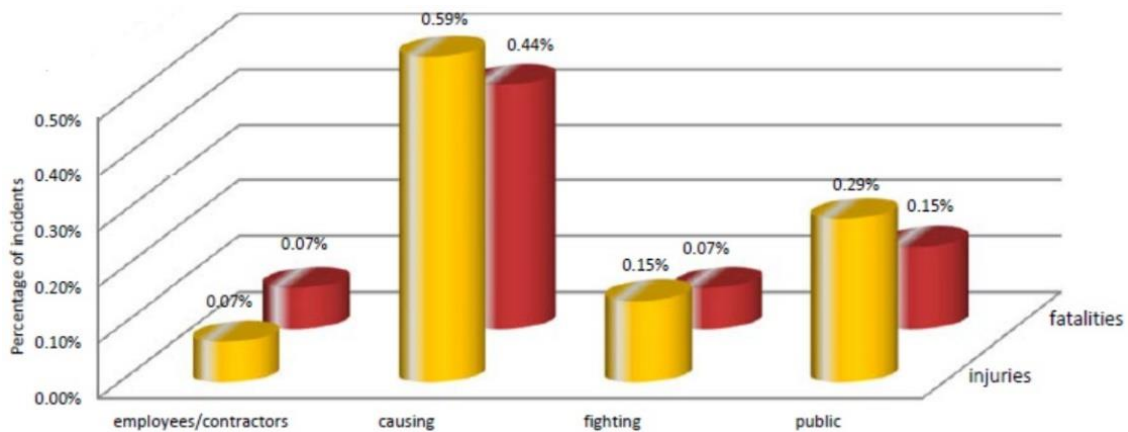


Figure 20 Percentage of accidents of groups involved in pipeline incidents (1970-2016) [47]

EGIG studied the injuries and fatalities among different groups involved in pipeline incidents. These groups are:

- employees or contractors of the transmission system operator;
- third party directly involved in causing the incidents (for example digger drivers in the case of external interference incidents);
- emergency services (firefighters, medical assistance);
- the general public.

In the EGIG database, 1,366 pipeline incidents were recorded in the period from 1970 to 2016. Reliable failure frequencies are provided by the history of incidents collected in the database. The average level of failures over the period 1970-2016 is equivalent to 0.31 accidents per 1,000 km per year. External interference, corrosion, construction defects and ground movement have accounted for 28%, 25%, 18% and 15% of the pipeline incidents reported over the past ten years, respectively. Failure data analysis is an important step for the failure prevention, and the improving of the pipeline integrity is a complex task [47].

## 4. GIRTH WELD DAMAGES

### 4.1. Preventing damage possibilities on the girth weld

A study [49] summarizes the obligated-to-reports incidents of a 6.5 year re-search process. Figure 21 shows the cause distribution for all incidents (621 items) and for weld defects (50 items). Based on Figure 21, it can be stated, that welds are more damageable, as we have no reason to suppose that welds have more favourable position from the point of view of corrosion and external force than the other parts of the pipeline. At the same time, the construction defects and material discontinuities occurs in much higher ratio in welds than in the other parts of the pipelines.

Figure 22 illustrates failure data from the Hungarian high-pressure natural gas transmission pipeline system [50], grouped similarly to Figure 21, with the overall time period divided into two sub-periods. Comparing the two periods, a slight rearrangement can be observed among corrosion, third-party damage, and weld defects as primary failure causes[3]. However, over the whole time period, weld defects represent the highest proportion. It is also important to note that weld defects typically occur in the early years (or decade) of operation, while the probability and share of corrosion-related failures increase with time. The high number and proportion of weld defects highlight the need for special attention to this category. According to Hungarian failure statistics significant part of failures were retraceable for weld defects, basically in girth welds. The comparison of the international data and the Hungarian statistics show, both in the past and present, that the ratio of the weld defects in Hungarian transporting pipelines is higher than the above-mentioned one and weld defects typically occur in girth welds.

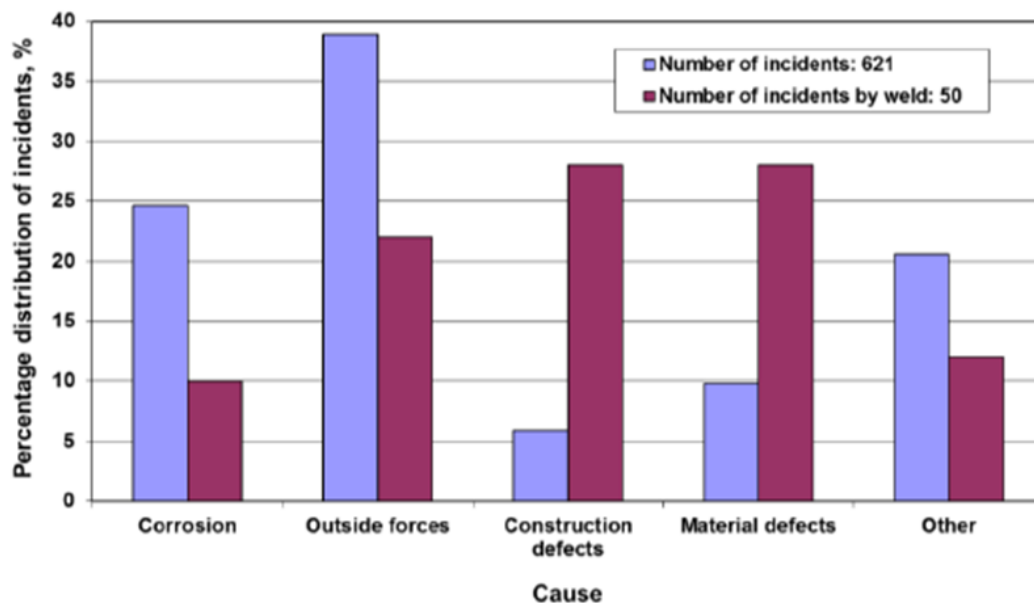


Figure 21 Incident distribution by cause [49]

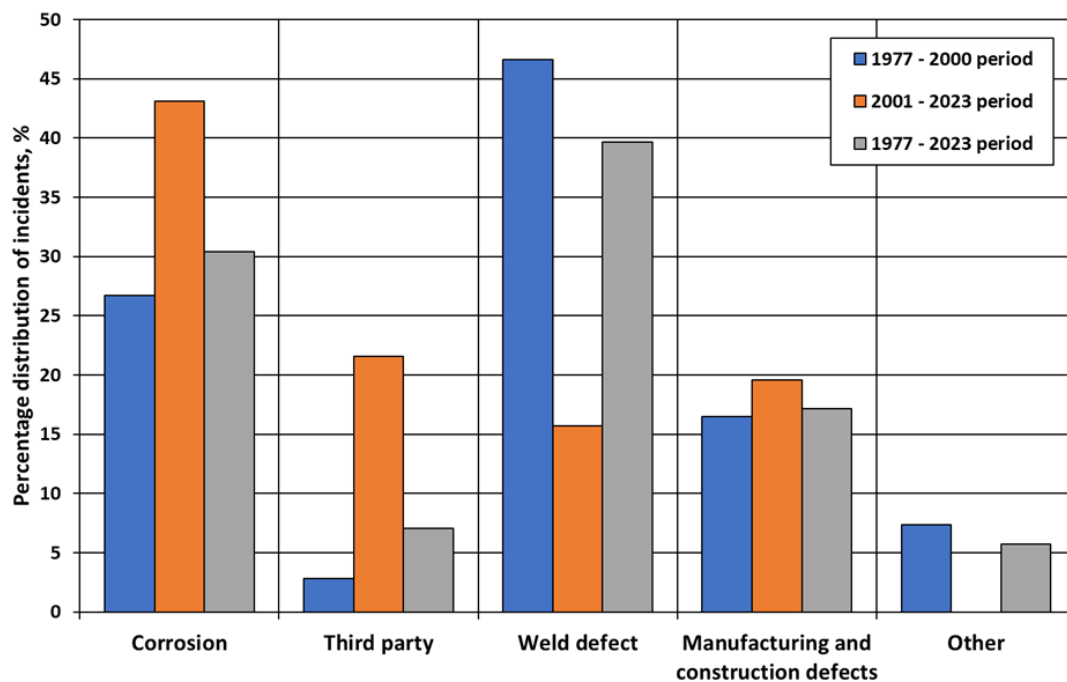


Figure 22 Distribution of root causes of failure events in the Hungarian high-pressure natural gas transmission pipeline system [50]

The different defects of welded joints occurring in the welded structures with high importance can be classified into three groups of acceptability:

- defects acceptable by the assessment rules (workmanship criteria) of welded joints;
- defects unacceptable by the assessment rules of welded joints, but having no influence on the Fitness for Purpose (FfP) or Fitness for Service (FfS) of the welded joint;
- defects influencing the Fitness for Purpose or Fitness for Service of the welded joint.

The three groups require different approaches with special emphasis of girth welds particularities. These characteristics are summarized in Figure 23, whereon the girth weld integrity puzzle demonstrates that the girth weld integrity depends on many factors interacting with each other [51], [52].

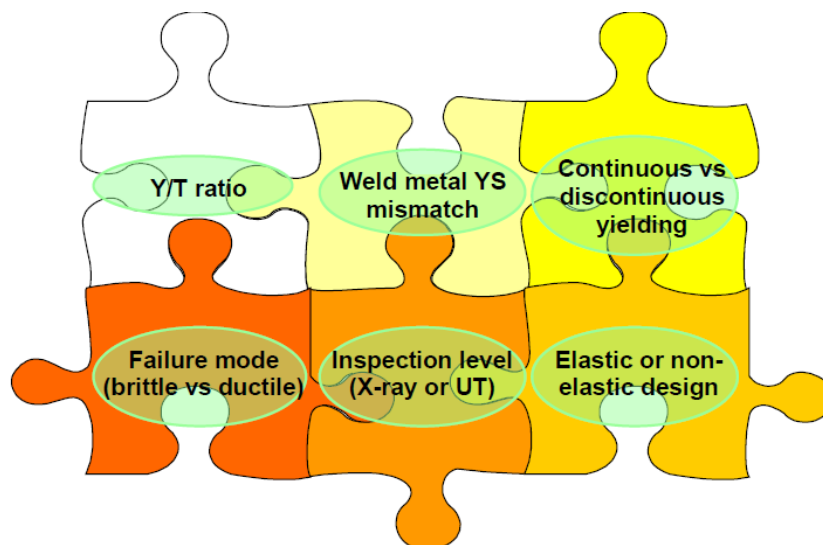


Figure 23 Girth weld integrity puzzle [51], [52]

#### 4.2. Influencing factors on damages of girth welds

The influencing factors on damages of girth welds can be divided into three main groups, as follows:

- Design of the pipeline;
- Construction of the pipeline;
- Operation of the pipeline including integrity management.

Either part of the design is the design and designation of the pipeline path and tracing. Especially, the crossings and the different installations have an important role. Figure 24 demonstrates the difficulty and the hazardousness of the problem [53]. (How do make up the sculptures of the modern age?)



*Figure 24 Pipelines and nodes in an installation [53]*

Another part of the design is the specification of the welding technology, including the welding of the pipeline and the related facilities. Extraordinary attention should be appropriated for the specification of possible axial misalignment, changing of wall thicknesses etc.

Figure 25, Figure 26, and Figure 27 illustrate three determining parts of the pipeline construction, the treatment of the axial misalignment [54], [55], the realisation of the laying the pipeline [54], [56] and the connection of different sections with different characteristics (Lee), respectively. The selected unfavourable examples point out the complexity of the tasks and the problems.



*Figure 25 Unacceptable treatment of an axial misalignment [54], [55]*

Regarding that welded joints of buried steel transporting pipelines may contain such defects, which have not been detected during the construction or are discovered only during the operation, we



must declare about their permissibility and correction. Since failure detection and especially defect correction represents extremely expensive procedures (Figure 28), it is reasonable to complete critical analysis (Engineering Critical Assessment) of the effects of flaws. This provides the possibility for minimizing the necessary corrections, so that the risk of further operation should not exceed the acceptable level.



*Figure 26 Pipeline laying [54]*



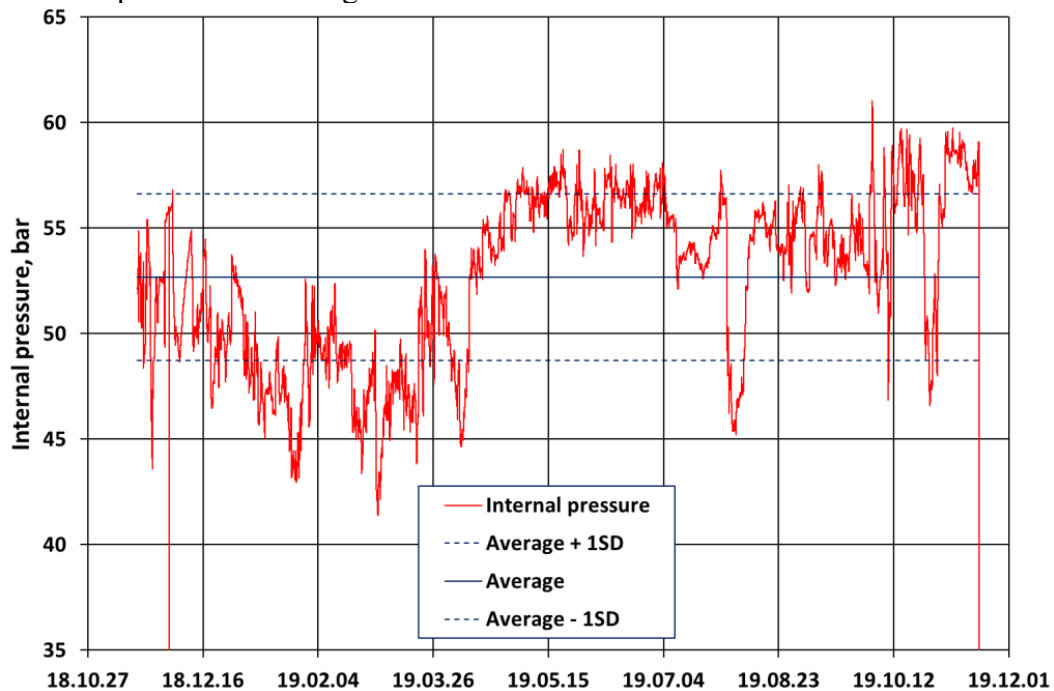
*Figure 27 Girth weld crack caused by different pipe and ditch profiles [56]*



*Figure 28 Connection of different pipeline section with different shape and wall thickness [54]*

The operation and/or integrity management part includes the analysis of the values and the variations of the internal pressure. Figure 29 shows an example using 1.039.753 registered data

from a Hungarian pipeline section, where data clearly demonstrates the cyclic loads on the section designed under quasi-static loading conditions.



*Figure 29 Changing of the internal pressure on a Hungarian gas transporting pipeline section[57]*

Important parts of the operating transporting pipeline are the periodic (state) inspection and the continuous (state) control. Since the corrosion defects are the most common metal loss defects and their forms are various, differentiated consideration should be attended to their location, sizes, growth rate etc[58]. Figure 30 shows corrosion defects near and on pipeline (girth and spiral) welds [59], [60].



*Figure 30 Corrosion defects near and on pipeline welded joints [59], [60]*

Another corrosion category is the Stress Corrosion Cracking (SCC), with classical terminology, or Environmentally Assisted Cracking (EAC), with more general terminology. Hydrogen play important role in this field and hydrogen damage is a term that covers a range of different types of failure modes, including embrittlement (HE), cracking (HIC, HAC etc.) and blistering. Figure 31 shows schematically.

The main hydrogen problems which can occur in steel at normal temperatures, although it must be stressed that not all types can occur simultaneously, or in the same type of steel. The probability

of all such forms of hydrogen damages usually increases with increasing strength, although blistering can occur in almost any steels[61], [62], [63]. Concurrently, Figure 32 illustrates the electrochemical potential and pH regions where SSC can occur for carbon (e.g. pipeline) steels in typical production environments [64].

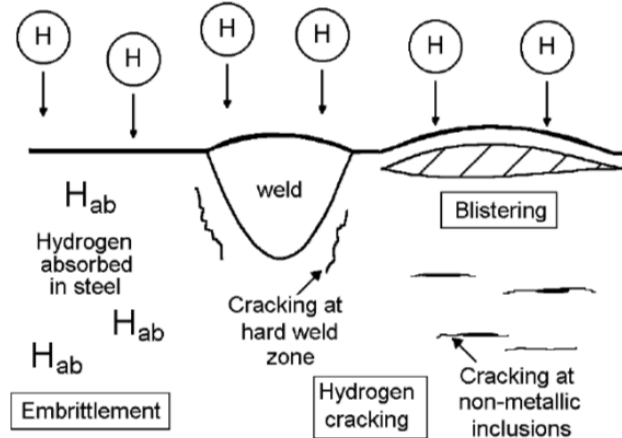


Figure 31 Hydrogen embrittlement, cracking and blistering processes [61]

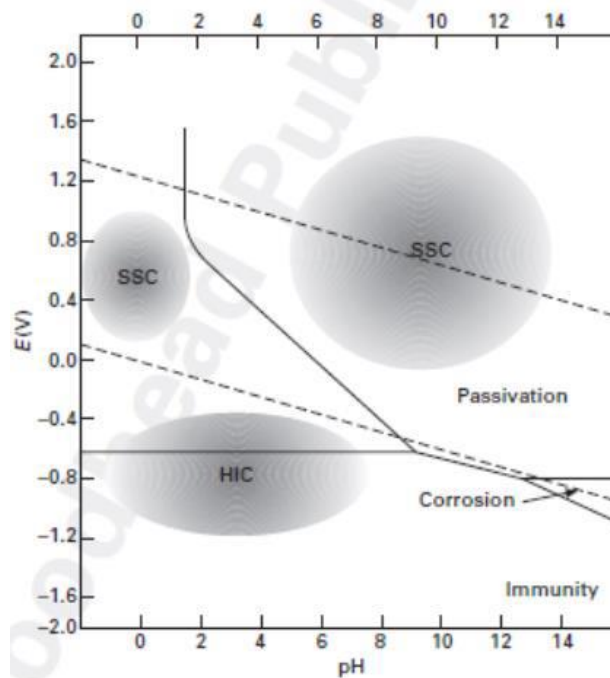


Figure 32 EAC modes as a function of pH and electrochemical potential for carbon steel [64]

Figure 33 shows two circumferentially oriented stress corrosion cracking (C-SCC) either in a pipe body and another in a girth weld [65].





*Figure 33 Examples of stress corrosion cracking [65]*

The sustainment and reconstruction of the girth weld integrity are continuous tasks of the pipeline operators. Besides the replacing of girth welds, which means making two new girth welds, the reinforcing is an effective way for the improving of the girth weld integrity. Figure 34 shows the results of two full scale fatigue and burst tests of our practice, where the reinforced girth welds with not passed quality have tolerated the loads, the pipe body has been damaged in both cases [66].



*Figure 34 Pipeline sections after fatigue and burst test with reinforced girth weld; left: system developed at University of Miskolc; right: Clock Spring repair system [66]*

#### **4.3. The answers to how to prevent damages from transporting pipeline girth welds**

Since there are several influencing factors on the damages of pipeline girth welds, there are different possibilities for prevention of the damages, too. These possibilities are as follows:

- observance of the technological discipline and prescriptions
  - = during the construction,
  - = during the operation and the maintenance;
- applying Engineering Critical Assessment (ECA) methods, for which
  - = reflect the operational experiences,
  - = demonstrate and endorse the compromise of rational risk and striving for safety ensuring pipeline integrity,
  - = use the results of the non-destructive examinations, and
  - = validated by the results of full-scale investigations on different pipeline sections;
- reinforcing of the girth welds using non-welded methods (e.g. composite wraps).

Girth welds of hydro-carbon transporting pipelines play important role of the life and the lifetime, during both the construction and the operation. Several factors have influence on the behaviour of the girth welds and they can be divided into three main groups, as follows: design of the pipeline;

construction of the pipeline; operation of the pipeline including integrity management. In line with these influencing factors, there are different possibilities for the prevention of damages which can be divided into three groups, too, as follows: observance of the technological discipline and prescriptions; applying Engineering Critical Assessment (ECA) methods; reinforcing of the girth welds using non-welded methods.

It should be noted that efficient and cost-effective solutions on whole transporting pipeline systems can only be reached with complex approaches and based on the common works of different expert groups.

## 5. FULL-SCALE TEST

A lot of efforts have been made to estimate the mechanical performance of pipes subjected to longitudinal plastic stresses as a result of the progress of strain-based design (SBD) for pipelines. Ductile ripping from a girth weld flaw is a common failure condition that defines tensile strain capacity (TSC). Because of factors like welding bevel angles and high-low misalignment, this condition is difficult to predict (MA) [67], [68].

Material property changes, as well as defect location/geometry. The real failure mechanics, which involves localized plastic deformation and material shredding, is equally difficult to model. Stationary crack modeling and the damage mechanics technique are two typical finite element analysis (FEA) techniques. Both strategies have drawbacks. It has been noted that stationary crack modeling can underestimate TSC because it is unable to account for all of the plasticity that happens in the area of a tearing fracture and does not explicitly simulate tearing [69], [70].

When it comes to the damage mechanics technique for modeling the tearing process, there is a lot of discussion on how to tune/calibrate the micro-mechanical parameters that the model relies on. So, what should an engineer do when the failure scenario is complex and modeling approaches are limited? There are often two solutions to this conundrum, one of which is significantly more important. The first step is to execute a large number of modeling runs and sensitivity analyses that cover all of the variable ranges in depth [71].

This entails hundreds of modeling runs for models with a half-dozen or so variables (as is the case for TSC prediction). While such exercises can help with recognizing patterns (for example, as MA grows, TSC decreases), they are insufficient to build a credible model on their own [72].

The second, and far more important, solution is that model results must be compared to full-scale experiments (FSTs).

In applied mechanics, this has always been the authoritative answer. It is also the answer for TSC prediction.

### 5.1. Overview of full-scale testing

Full-scale pipe strain tests involve stretching and bending a section of pipe to failure. The fundamental metric is strain capacity, which refers to how much longitudinal strain the specimen can withstand before failing, which is commonly referred to as maximum load. It's possible that the specimen is parent pipe or that it has one or even more girth welds. Manmade flaws (notches) are common in girth welds, thus including different degrees of welding joint MA might be beneficial. To replicate service conditions, the specimens might be compressed.

When there are girth weld faults, the failure scenario frequently involves ductile ripping from the defect till the remaining ligament fails. To replicate service conditions, the specimens might be compressed [73].

When there are girth weld faults, the failure scenario frequently involves ductile ripping from the defect till the remaining ligament fails. A schematic of a typical full-scale test (FST) specimen with girth welds is shown in Figure 35. The cost of specimen design and manufacture, followed

by testing and analysis, may go into the tens of thousands of dollars each test. A single test might take weeks or months to complete.

The preparation of a specimen with known qualities is the most significant component of test specimen design and production.

The true qualities of the specimen cannot be determined since it was damaged during testing. To create data indicative of the specimen, small scale experiments on additional material are required. Companion tests are crucial inputs for TSC model predictions and are referred to as companion tests. Successful ways of preparing companion materials can be found elsewhere. The design in Figure 35 is created by the layout in Figure 36. The test pups' rings are first cut to generate tensile data for overmatch calculations. At the spots where the rings were removed, the FST girth welds unite the three puppies. Companion welds are produced at the FST specimen's ends, or they might be put on one end of the specimen.

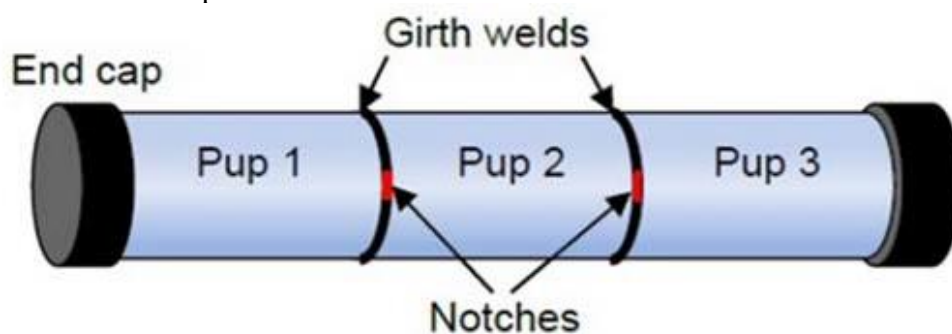


Figure 35 Full-Scale Test Specimen Schematic [69], [70]

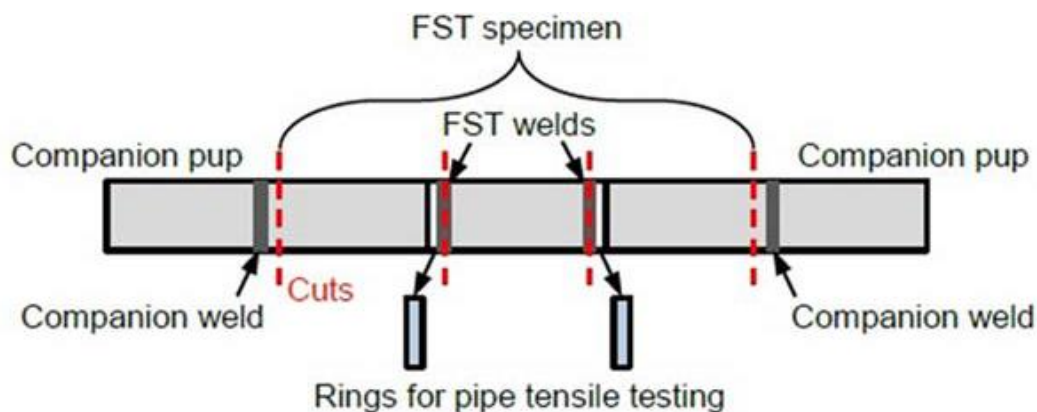


Figure 36 Preparation strategy for Full Scale Test specimens and associated materials [69], [70]

The most difficult part of preparing companion material is girth welding so that representative data can be generated. The companion girth welds have shown to be more effective when extra pups are welded directly to the ends of the FST specimen (subsequently cut off). The companion girth welds should be done as soon as feasible after the FST welds, and they should be made with the same welder, welding tools, and welding processes as the FST welds.

Full-scale testing also necessitates the use of specimen instrumentation. Longitudinal strain and notch opening are monitored using instrumentation. Linear variable displacement transducers (LVDTs) are commonly employed to monitor strain, while clip gages are utilized to measure crack mouth opening displacement (CMOD). Figure 37 is an example of an effective instrumentation layout. A possible unrolling of the pipe specimen is depicted in the diagram. To detect global strain

over the specimen length, three massive LVDTs are employed. The anchor points are as near to the end cap confluence with the pipe specimen as practicable. The FST's strain capacity is defined as the average of these LVDTs at maximum load.[74]

Additional, shorter LVDTs are placed on each pup, and these LVDTs are used to detect possible non-uniform straining. The employment of scribe lines is the least technical (but most beneficial) of all strain monitoring methods (Figure 37).

Regular (100-150 mm) cross hairs on scribe lines can be placed along the same linear routes as the LVDTs. To quantify strain, the distance between the marks and the thickness of the wall at the markings are measured before and after the test. Data from scribe lines may be utilized to double-check LVDTs and track non-uniform strains.

The process of assessing the data post-test to gain a complete picture of specimen performance is just as vital as test preparation. This necessitates a cross-validation of LVDT and scribe line data. Non-uniform straining should be looked for during the activity. If this is suspected, further ultrasonic wall thickness measurements may be beneficial.

The CMOD data should be compared to the results of the other notch assessment methods (fractography, sectioning). One of the main objectives is to see if any notches were "active" throughout the test, indicating that ductile tearing has started.

The CMOD data is typically easy if the specimen does not fracture. If the specimen cracks, the first step is to pinpoint the location of the fracture, which is usually the notch with the highest CMOD at the conclusion of the test. It should be highlighted that brittle fractures have been recorded farther from the notch with the biggest CMOD. Fractured specimens might be difficult to interpret. Fractography is a useful tool for gaining a better understanding of the failure event and, in many cases, assessing the importance of the FST.

Fractography is used to detect the location of quick fracture initiation, whether crack propagation was ductile, brittle, or mixed, and the crack propagation direction. The plethora of subtleties that might accompany fractography is beyond the scope of this work. To summarize, the texture, geometry, and varied shades of grey revealed on the fracture surface frequently allow the failure event to be recreated.

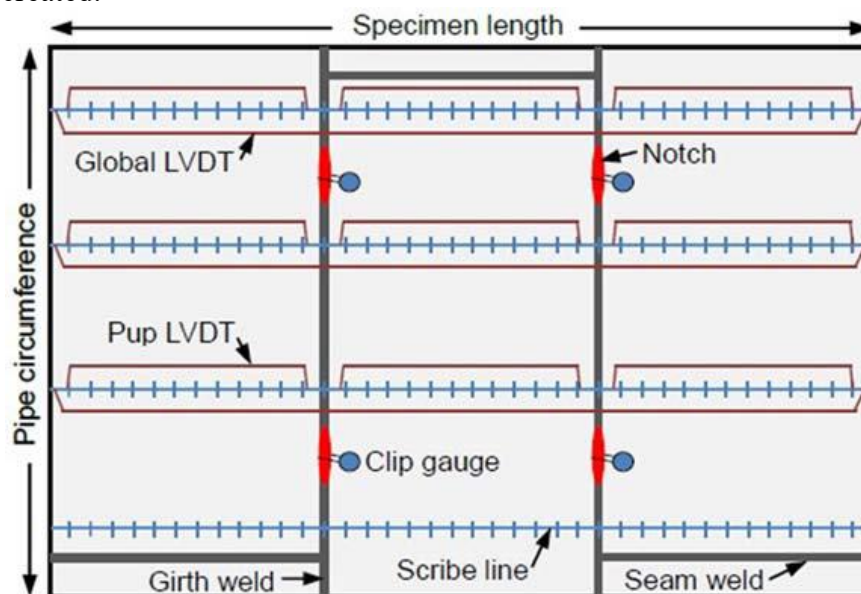


Figure 37 Instrumentation for Full-Scale Testing (unrolled pipe view) [69], [70]



## 5.2. The importance of high-quality full-scale testing data

Full-scale testing is a large-scale representation of experimental fracture mechanics. FST specimen preparation is more difficult than, instance, Charpy or crack tip opening displacement (CTOD) tests due to a number of variables. The amount of material is substantial, and specimen manufacturing necessitates extensive welding. As a result, the likelihood of material property variation and the occurrence of unintentional flaws is enhanced. Furthermore, notch insertion in the heat affected zone (HAZ), which must be done "blind" into the specimen surface, is extremely challenging [75], [76], [77], [78].

One overarching concept and two instances may be used to demonstrate the necessity for high-quality FST data. The guiding assumption is that developing predictive TSC models is a difficult applied mechanics task, and that rigorous model validation using FSTs is essential because present models are relatively new and broad SBD pipeline service experience is lacking (figure 38). Two hypothetical examples are instructive in relation to the typical reasons for doing FSTs (model verification and project work). Consider the following scenario: a forecast from a relatively recent TSC model does not match the result of an FST, and no evident testing abnormalities are discovered.

Is the model incorrect, or is there an issue with the test? If the model is defective, the next step is to upgrade. If the test fails, a failure analysis is necessary to uncover the root reason. The defect geometry may not have been as expected, or brittle fracture may have happened, in which case the test should be disregarded. In view of the time/cost required to conduct these tests, there will certainly be opposition to abandoning an FST, but it is occasionally essential, as will be detailed below.

Consider a second scenario in which an FST is performed as a final proof test of project materials and the model forecast differs from the outcome. A similar dilemma arises: is it better to solve a model problem or a test problem? If the pipeline project is on a tight schedule, this scenario might be extremely difficult, especially if the test falls short of the goal TSC. Concluding that project materials do not fulfill design goals is a risk that may be avoided by paying close attention to all FST aspects. Late project adjustments are limited, and they frequently include more stringent defect acceptance standards, which can be expensive.

Unless addressed through failure analysis, problematic FSTs (those that do not match forecasts) constitute roadblocks to advancement because they raise unresolved issues about whether bad predictions were generated by an erroneous model, a flawed FST, or a mix of both.



*Figure 38 Test setup for an experimental pipe section subjected to or capable of complex loading conditions [79]*

### 5.3. Project work vs. Model building

There will be references to these motives throughout this work since they often drive decisions about how to design and build the specimens.

The aim to isolate the influence of particular factors on strain capacity is a fundamental difference between FSTs for model development and FSTs for project work. A sequence of FSTs for model building, for example, might be developed with steadily rising defect sizes while keeping all other factors constant. The aim will be jeopardized if variables other than defect size alter accidentally. It can be difficult to maintain consistency in crucial factors such as weld strength, which affects overmatch, given the volume of test specimen manufacture.

As a result, because 1G-rolled, automated welding techniques are exceedingly consistent, they are excellent for FSTs connected to model making.

Because of the size of the specimens, the importance of test variable control cannot be overstated. FSTs are large-scale experiments in fracture mechanics.

Engineers have been battling welding-induced fracture differences in specimens (Charpy, CTOD) orders of magnitude less than full-scale pipe strain tests for decades.

Because of the amount of girth weld material in an FST and the possibility for fluctuation along the circumference, all elements of specimen fabrication, especially those impacting strength or toughness, must be closely monitored.

When the FST is employed for project work, however, the welding technology will be determined by the pipeline fabrication processes. The 5G position is usual for field welding; however semi-automatic or manual methods may also be employed. With project processes, a larger degree of girth welding variation is unavoidable; nonetheless, this variation is allowed because the purpose of project work is to proof test any variances that may occur within the authorized techniques [80], [81], [82].

### 5.4. Design and preparation of specimen

#### **Bending vs. Tensile Loading:**

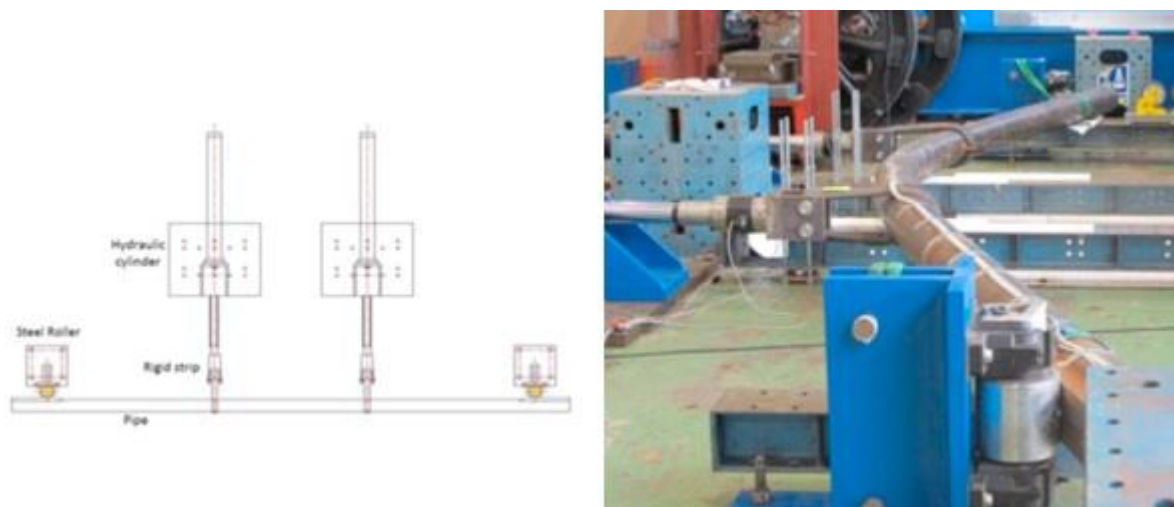
For actual pipes, strain-based loading will nearly always result in bending (Figure 39 and Figure 40); nonetheless, tensile loading is recommended for full-scale testing for various reasons (perhaps reeling is an exception, but this application is not the focus of this study). If the goal of the test is to develop a model, sample statistics are critical, and it is best to include as many notches as feasible without jeopardizing other objectives. In bending FSTs, stresses are spread non-uniformly throughout the circle, and it is typical to notch at the greatest strain site, which is the outer fibers on the tensile side [83], [84], [85].

Only one notch may be put at this position due to the limited size of the outer fiber region.

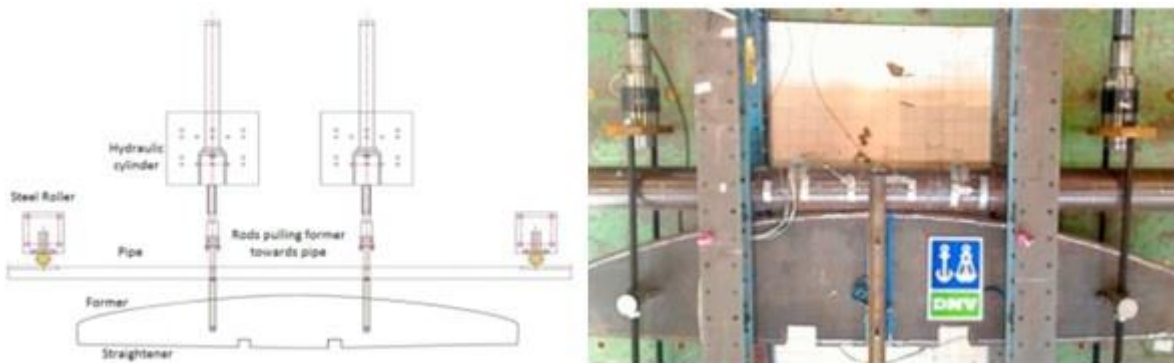
Bending tests are limited to one or two notches since there are normally only one or two welds per specimen with just one notch per weld. Tension testing, on the other hand, may readily tolerate several welds and many notches per weld, as detailed below.

For project-related FSTs, sampling statistics might also be a source of worry. The advantage of many notches is significant insurance against the obstacles of full-scale testing, given the difficulty of notch placement, equipment dependability, and material variability.

The potential of buckling is another reason why bending tests might be troublesome. The strain capacity of the notched region cannot be evaluated if a buckle (wrinkle) arises on the compression side of the specimen (a rather typical occurrence). When the specimen wrinkles, consistent straining is no longer possible. Wrinkling can jeopardize FST goals if the goal is to evaluate the whole strain capacity of the materials involved (Figure 42).



*Figure 39 Four-point bending (4PB) in a testing laboratory with the possibility of applying internal pressure: sketch and construction of the testing apparatus [82]*



*Figure 40 Winding test in a testing laboratory: the design and implementation of the test equipment [82]*

### **Pup Selection and Basic Design**

Preparation is much simpler if the FST is on base pipe. Tests using girth welds are more difficult. Figure 35 shows a schematic of an FST specimen. This design consists of two girth welds that connect three pipe segments known as pups. Welding tests are usually performed outside of the test lab by a different welding contractor. To develop dependable techniques to accomplish the intended weld joint misalignment, weld strength overmatch, fault size, and flaw locations, design considerations and quality controls are required [84], [86], [87].

In FSTs with girth welds, the number of girth welds (and hence pups) to include must be decided. The writers have worked with a variety of welds ranging from one to four (two to five pups). More girth welds provide the benefit of improving testing statistics. It permits additional artificial faults (notches) to be included, thereby turning a single FST into as many fracture tests as there are notches. More welds and notches have the disadvantage of increasing specimen complexity, preparation time, and the chance for mistakes, not to mention limiting the capacity of test machines. The authors prefer the configuration depicted in Figure 35 (two welds, three pups) based on their experience, since it appears to maximize the conflicting elements.

Another factor to consider is the length of the pup. Pups must be long enough to avoid interfering with neighboring welds and/or end caps. The authors recommend a minimum pup length of 1.5 to 2 diameters since this provides a total specimen length (many diameters) that more closely

resembles an actual strain event in a pipeline. Strain demand and pipe-soil interactions are beyond the scope of this work; suffice it to state that the length of a real pipeline exposed to the whole target demand is expected to be no less than a few diameters. As a result, FST specimens of at least a few diameters appear to be acceptable.[88], [89], [90], [91]

It's possible that a decision on the pups' origins will be required. If there is just one pipe available from which to construct the specimen, the choice is clear. If numerous pipelines are present, however, the upstream source may change. If the goal of the test is to make a model, the pups for each specimen should be cut immediately adjacent to each other and then welded back together in their original arrangement.

This reduces variance in strain capacity (i.e., UEL) across pups while maintaining the purpose of evaluating only one variable. If the FST is tied to a project, the original source is less important.

The goal can be achieved as long as the puppy reflects project material.

There have been instances where pups from different pipes were utilized, and test interpretation was challenging owing to differences in pipe qualities. In general, if combining puppies from separate pipes serves no benefit, this procedure should be avoided.

### **Prior Material Knowledge**

Materials with which the designers have existing expertise should be used in the design and production of specimens for model building aims. This involves understanding the pipe longitudinal characteristics, weld strength, and weld toughness, at a minimum. Pre-testing can be quite beneficial. FST design and production should be guided by base metal tensile testing, welding trials, and measurement of weld characteristics. It's vital to remember that the FST specimen will have different material than any pre-tests, and there's a chance that there may be unanticipated alterations in the specimen.

For example, if pre-tests reveal that pipe UEL is too near to the strain capacity target (say, within 1 or 2 percent), then the pipe's usage should be examined since the test might be compromised by the pipe's below-average performance.[92], [93], [94], [95]

Obtaining the correct degree of weld strength overmatch is one of the most essential parts of test specimen design and manufacturing. One of the most important factors affecting girth weld strain capacity is overmatch. Unexpected test findings have been linked to unintended overmatch variation, notably lower than desired overmatch. To avoid this, it's best to err on the side of caution when it comes to pre-testing.

Each FST costs tens of thousands of dollars, and the uncertainty posed by inadequate pre-tests puts the overall full-scale testing objectives at risk.

It is preferable to conduct pre-tests on material that closely resembles the final FST. This is true for related tests as well (discussed below). Longitudinal tensile samples can be collected from rings cut right near to the pipe edges that will be beveled for welding to assess pipe tensile qualities. If this isn't possible, samples should at the very least be collected from the pipe that will supply the FST pups.

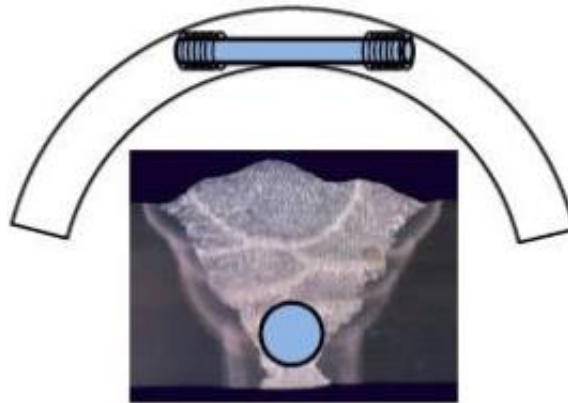
Trial welding and all-weld metal testing are required without prior knowledge of weld metal qualities. Measuring weld tensile characteristics (which are used to calculate overmatch) may be difficult, thus planning ahead of time for pipe/weld geometry and tensile specimen shape is recommended.

The sample region must be weighed against the location of the FST notch. A round bar sample for small diameter pipe will be skewed toward the weld root (Figure 41), which may not reflect overall weld strength or be consistent with an FST notched from the outside diameter (OD).

If the pipe wall thickness approaches 25 mm, two round bar specimen sites in the weld cross section should be considered, one higher and one lower. A rectangular cross section specimen is an alternative to the round bar geometry. This specimen has been recommended for narrow groove

welds, but because the design samples a larger quantity of weld metal than round bars, it has merit regardless of bevel form [96], [97].

To summarize, designers must account for the implications of variable pipe and weld qualities and choose an acceptable method for characterizing strength and calculating overmatch.



*Figure 41 All-weld tensile sample in small diameter pipe [70]*

#### **Internal vs. External Notches:**

Notches on the inside versus outside FST notches can be drilled into the pipe's inside diameter (ID) or outside diameter (OD). This decision is influenced by a variety of factors. Because of access issues, ID notches are impracticable for pipes with a diameter of less than 18-20". It is technically viable to apply ID notches if the FST is large enough for access, but the test will be pressured; nevertheless, the inside environment (water) considerably increases test complexity and restricts the durability of notch instrumentation. The chance of losing ID signals during the test is high, and the authors have had similar concerns in the past.

The authors have shown that real pipeline failures occur more frequently at the root than at the cap, owing to the higher risk of root faults. FSTs from the ID are more likely to be notched because of this reality. However, as previously stated, ID instrumentation is difficult and raises the risk of an erroneous test. The authors have opted to employ OD notches; thus the rest of this work will be devoted to them [98], [99], [100], [101].

#### **Cracks vs. Notches:**

Cracks vs. Notches Large fracture mechanics tests are essentially what FSTs are.

Because of the influence of defect tip acuity and the possibility for brittle fracture in structural steels, fracture tests have traditionally been done with fatigue precracks. Precracks, on the other hand, are extremely difficult to implement in full-scale pipe specimens. FSTs for strain based design (SBD) are currently done with notches. The following is the justification:

SBD circumstances necessitate careful consideration of design elements and material integrity. Both the pipe and the weld materials must be ductile, and this must be shown by a comprehensive materials testing procedure. Other tests (Charpy, CTOD) can be used to confirm ductile behavior in more traditional methods. After that, FSTs can be performed using sharp notches rather than precracks because both will operate similarly in ductile material. The results of SENT testing have corroborated this. The breadth of the notch should be kept to roughly 0.2 mm.

Low temperature testing may be of relevance because of the brittle fracture worry; nevertheless, for model construction FSTs, room temperature testing can be justified. This is due to the fact that SBD models are only applicable to ductile behavior by definition. If the test materials are suspected of not being ductile at room temperature, Charpy and/or CTOD testing should be conducted to guarantee that the test will not be hampered by brittle behavior. If the testing is for a project, the



test temperature may be determined by the application's severity. If the service temperature is expected to be very low (below  $-10^{\circ}\text{C}$ ), it could be prudent to undertake at least some testing at that temperature.

It can be the cracks or the notches the significant reason for failure, a similar situation happened to the pipeline in Figure 42 during the pressure test.



*Figure 42 Catastrophic failure of a pipe arch section during a pressure test [102]*

### **The Quantity of Notches**

Because it enhances test statistics, it is preferable to include as many notches as feasible in an FST. Too many notches, on the other hand, may produce interaction between neighboring notches, jeopardizing the test findings (unless flaw interaction is the goal). To investigate interaction effects and improve notch spacing, FEA can be employed. For pipe diameters smaller than roughly 30", two notches, spaced  $180^{\circ}$  apart, are usually utilized. For pipes ranging from 30" to 42", three evenly spaced notches can be utilized. Four notches might be considered for bigger pipes. The flexibility to adjust notches in the last phases of specimen preparation and/or to obtain the desired level of misalignment must be balanced with an aggressive notch number strategy (MA). After the weld MA and non-destructive examination (NDE) results are known, the notch placements may be finalized. It's possible that the target MA is only found in a few places. To reach the right MA or prevent weld defects, it may be required to shift notches a substantial distance from the initial plan.

### **Misalignment in Weld Joints (MA)**

One of the most important factors influencing strain capacity is weld joint MA. By raising MA from 0 to a few millimeters, strain capacity can be greatly lowered. It has been established that the pipe offset approach may be utilized to construct MA in an FST. Once the weld joint has been constructed, it is recommended that MA be measured at regular intervals around the perimeter and that this information, together with weld NDT data, be utilized to guide final notch placement.

MA makes determining fault depth difficult. A schematic of probable HAZ notch placements in relation to a misaligned weld is shown in Figure 43. Despite the fact that these notches all enter the material to the same depth, the FST notch depth must be defined differently. The notch location should be consistent with the model if the FST's

objective is to construct models. In the case of HAZ notches, the notch is often placed on the "lower" side of the weld, whether for model construction or project work.

When compared to the "higher" HAZ position, this position is more cautious since it generates a smaller cross section between the notch tip and the weld root. One example of how MA may impair strain capacity is this tiny cross section, which is frequently the failure plane.

Calculation changes will be required if the notch position is at the weld centerline and the notch depth is referred to the low side of the weld (Figure 44). The notch penetration depth is derived by multiplying the notch depth by the height of the notch entrance point X. The cap is frequently ground to assist clip gage installation, thus the weld cap in Figure 44 is rather flat to approximate this. The height of the entrance point X in this example is roughly half of the MA. The actual cap height may differ from that depicted in Figure 44, requiring the designers to make the required changes.

These details must be supplied to the notching professional, regardless of cap shape or notch depth. If the FST is constructed with 3 mm of MA, a 3 mm notch depth, and the cap is ground as indicated in Figure 44, the technician must realize that 4.5 mm of notch penetration is required to accomplish the appropriate notch depth. The authors have seen examples of incorrect notching where the test findings were deemed to be out of the ordinary, but after posttest measurements (notch opening), the notch size was determined, and the amended predictions were more in line with the FST results.

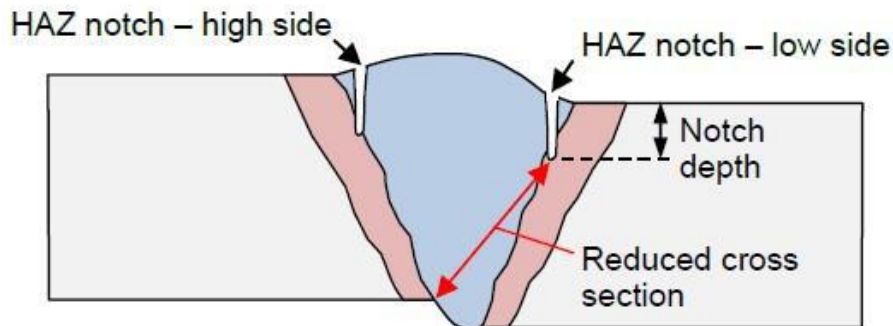


Figure 43 When MA is present, possible HAZ notch locations [69]

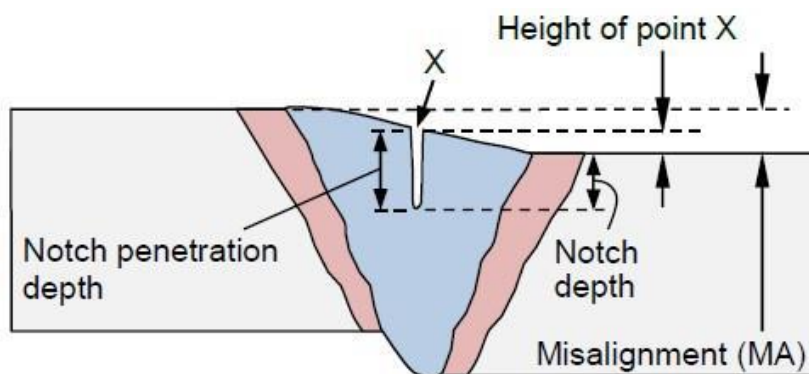


Figure 44 When MA is present, the location of the weld centerline notch necessitates further considerations [69]

### The XFEM Model

Two endplates and two loading tongues are included in the pipe model (Figure 45); each are represented by reference nodes with a 50 mm eccentricity from the pipe's longitudinal axis. To replicate properly welded connections, the tie constraint was employed to link the endplates to the shell pieces. Finally, the experimentally applied eccentric loading was modelled using a tie constraint connecting the loading tongues to the endplates with a 50 mm eccentricity.

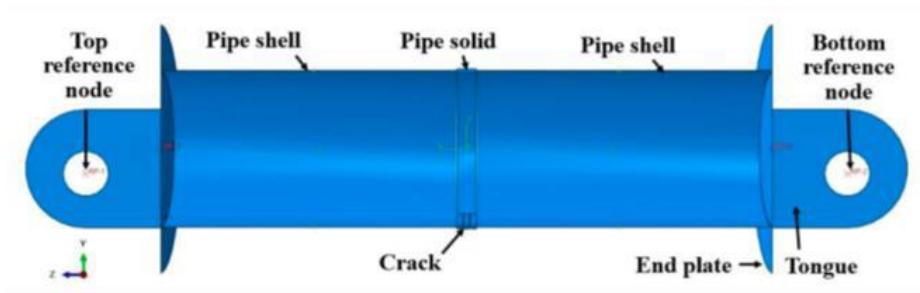


Figure 45 Pipeline XFEM model components assembled, displaying geometry and reference points.[75]

The CMOD critical values for all tests and models are compared with the results of CMOD failure, which is the CMOD value when the failure occurs, as described previously and shown in Figure 46

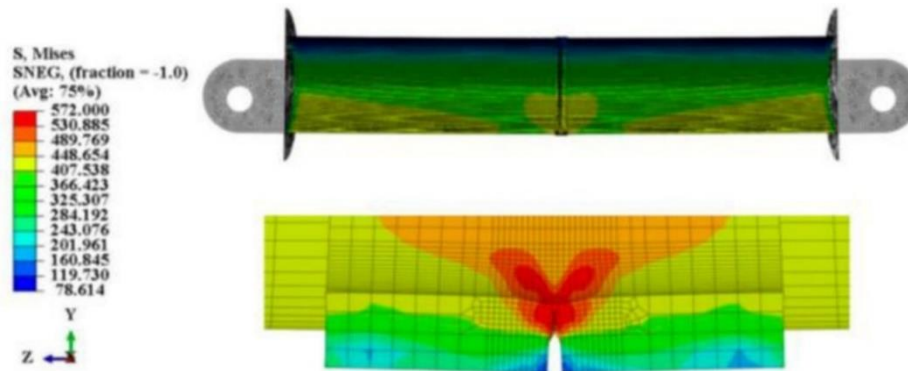


Figure 46 The CMOD failure[75]

### Pipeline Buckling Limit Assessment Using a Large-Scale Bending Test Rig

Figure 47 depicts the test rig, which is made up of two-moment arms, an oil hydraulic jack that drives the moving arm, and a primary frame that holds the whole thing together. The test rig is also constructed such that, during the bending test, internal pressure may be applied to the test pipe using a water hydraulic pump. The test pipe is soldered between the two-moment arms, and the movement of the moment arms' ends generates bending moment in the pipe.

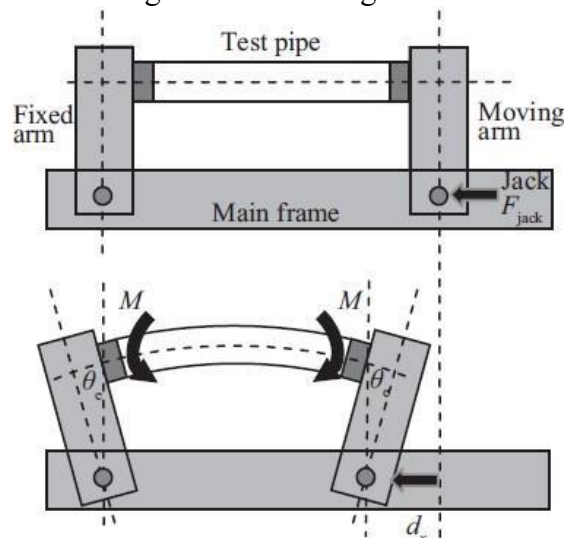


Figure 47 An overview of the bending test for large diameter pipelines [78]



Further examples of global and local buckling are illustrated in Figures 48 and 49, respectively.

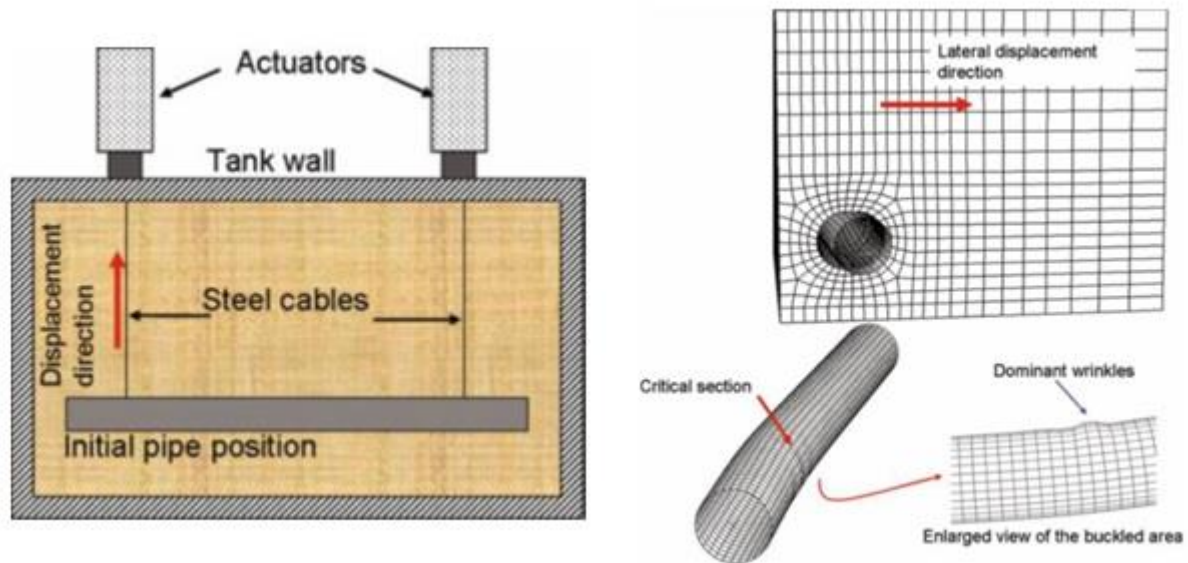


Figure 48 Bending test of a pipe section embedded in soil: test layout (left); deformed pipe section (right) [96]

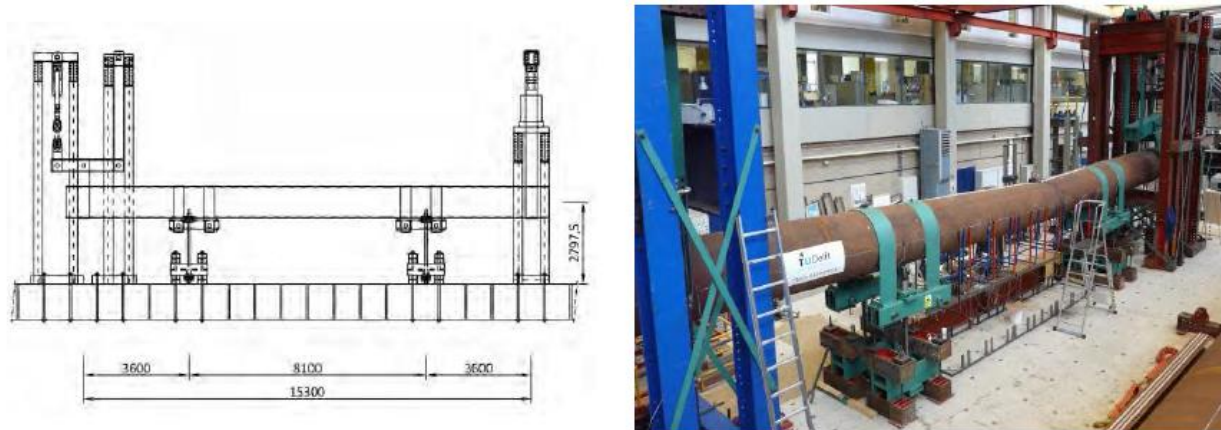


Figure 49 Sketch of the four points bending test set-up (left) and test set-up after formation of a local buckle (right) [103]

Based on the reviewed references, the following conclusions can be drawn for designing and implementing our full-scale testing system and investigations.

- When designing and preparing the full-scale tests, all available information and data on the pipeline sections, the actual operating conditions, as well as the test possibilities and their limitations should be used.
- If necessary, additional mechanical and/or microstructural investigations should be carried out to ensure high reliable and reproducible preparation of the tested pipeline sections.
- The tested pipeline sections should be constructed from the same material quality (same heat number). In cases where this is not possible, special attention should be paid to differences in the properties of the pipes and their effects on the tested pipeline section and girth welds.
- The length of the individual pipes applied for the assembly of the tested pipeline sections should exceed twice their outside diameter.

- The four-point bending (4PB) test is appropriate for three-segment pipeline sections with two tested girth welds. A three-point bending (3PB) test is preferable if only one girth weld is to be tested (Figure 39).
- In order to modelling real operating conditions as exactly as possible, applying an external load (bending) in addition to the internal (cyclic) pressure is desirable. In such cases, positioning the tested girth weld in the middle of the investigated pipeline section is advisable. This will result in the highest bending stress (3PB) and eliminate errors due to possible asymmetry (4PB).
- Before full-scale tests under complex loading, it is also advisable to investigate a pipeline section that has not been subjected to cyclic loading (burst test only), furthermore a pipeline section that has not been subjected to additional loading (fatigue test followed by burst test). These investigations provide bases for comparison with the tests under complex loading conditions.
- Notches should be used to model the real imperfections (defects) of the girth welds. The location of notches along the circumference is indifferent for simple loads, but for complex loads the locations with the highest stress should be prioritized. The circumferential notches should be located in the weld metal (WM) or heat affected zone (HAZ) of the girth weld, and the longitudinal notches should be located parallel to the longitudinal axis of the pipe (perpendicular to and in this case symmetrical with the girth weld).
- The post-weld treatment of girth welds is not used in Hungarian practice; therefore, it is not relevant for full-scale tests of pipeline sections containing girth welds.

## 6. SUMMARY, SPECIFIC AIMS OF THE RESEARCH WORK

The steels used for hydrocarbon transporting pipelines are based on or correlate to [23], worldwide. The increase in strength for this type of steel is also continuous, but the increased strength must also be matched with adequate ductility. As the joining of the pipe segments is done by welding (girth welds), the welding technology must also follow the evolution of the base materials.

Damage statistics for pipelines show well-defined groups of causes. The ratios between each group are different based on international and Hungarian data, with Hungarian data showing less favourable data for damage to girth welds compared to international data.

There can be, and are, many causes of damage to girth welds, and the same is true of the possibilities for preventing damages. In the case of transporting pipelines, especially those in service for a long time, it is no longer possible to speak of clearly quasi-static operation and simple loads, but of cyclic and/or complex loads.

Despite the fact that several modelling options and computational algorithms are known, their limitations are also known, thus the role and importance of full-scale tests has been enhanced.

Based on the previously mentioned facts, the objectives of the research work are as follows:

- to develop a measurement system for full-scale tests of pipeline sections containing girth welds under cyclic internal pressure and superposed external loads;
- to design experimental pipeline sections with the same characteristics for full-scale tests;
- to design and perform full-scale tests on girth welds under complex loading conditions, for girth welds with different discontinuities (defects) and artificial defects;
- to identify the operational reserves in girth welds based on a safety factor;
- to rank the hazard of different discontinuities and defects;
- to propose options and requirements for safer operation of girth welds.

## 7. CIRCUMSTANCES OF THE INVESTIGATIONS

### 7.1. Manufacturing of the pipeline sections

The investigated pipeline sections were made of P355NH seamless steel tubes for pressure purposes [104]. The welding process was made entirely by the industrial partner, The nominal geometrical sizes were as follows: OD = 114.3 mm (DN 100) outside diameter,  $t = 5.6$  mm wall thickness,  $L = 4,000$  mm (4 m) pipeline section length (Figure 51). The tested girth welds located in the middle of the pipeline section were made under industrial conditions using manual metal arc welding (MMAW). The chemical composition of the base material and applied filler metals are summarized in Table 5, furthermore, the basic mechanical properties of the base material can be found in Table 6.

*Table 5 Chemical composition of the pipe material based on inspection certificate and the applied filler metals based on company specifications, weight%*

Material	Element						
	C	Mn	Si	P	S	Cr	Mo
<b>P355NH</b>	0.18	1.24	0.22	0.016	0.009	0.08	0.02
<b>Böhler FOX CEL–E383C21</b>	0.12	0.14	0.5	N/A	N/A	N/A	N/A
<b>Böhler FOX CEL Mo–E423MoC25</b>	0.1	0.14	0.4	N/A	N/A	N/A	0.5
	Ni	Al	Cu	Ti	V	Nb	N
<b>P355NH</b>	0.06	0.027	0.19	0.001	0.004	0.000	0.090

*Table 6 The basic mechanical properties of the pipe material based on the inspection certificate*

Yield strength, $R_{eH}$ (MPa)	Tensile strength, $R_m$ (MPa)	Elongation, $A_{65}$ (%)	Charpy-V impact energy at -20 °C, KV (J)	
			Individual values	average value
406	536	28.4	150, 154, 160	155

The Carbon Equivalent (CE) for the base material and filler metal were calculated, the chemical composition (typically the weight percentage of elements like C, Mn, Cr, Mo, V, Ni, Cu) for both. based on the WPS provided documents (appendix 1).

The CE formula (IIW method) have been used:

$$CE = C + \frac{Mn}{6} + \frac{Cr+Mo+V}{5} + \frac{Ni+Cu}{15} \quad (1)$$

$$CE_{Base} = 0.424 \quad (2)$$

$$CE_{Böhler\ FOX\ CEL-E383C21} = 0.143 \quad (3)$$

$$CE_{Böhler\ FOX\ CEL\ Mo-E423MoC25} = 0.223 \quad (4)$$

In the Table 7, Charpy-V impact energy (KV) data for two filler materials at different temperatures, along with the mechanical properties like yield strength ( $R_y$ ), tensile strength ( $R_m$ ), and elongation (A) can be seen. Comparing the strength properties of the base material and the filler materials,

the welded joints produced can be classified as matching (the strength of the base material and the filler metal are approximately the same).

Table 7 Key mechanical properties of welding filler metals

R <sub>y</sub> (MPa)	R <sub>m</sub> (MPa)	A (%)	Charpy-V impact energy at the following temperatures, KV (J)				
			20 °C	0 °C	-20 °C	-30 °C	-40 °C
Böhler FOX CEL (E383C21)							
450(≥380)	550 (470-600)	26(≥22)	100	90	70	55 (≥ 47)	N/A
Böhler FOX CEL Mo (E423MoC25)							
480(≥420)	550 (500-640)	23(≥20)	100	95	85	50 (≥ 47)	42

The Welding Procedure Specification (WPS) can be seen in appendix 1, in Figure 50, a metal welding process involving two different materials A1 and A2 can be seen and that is the general situation, however in our study A1 and A2 from the same material, the preparation phase (a) and the layers of the welding process (b) can also be seen.

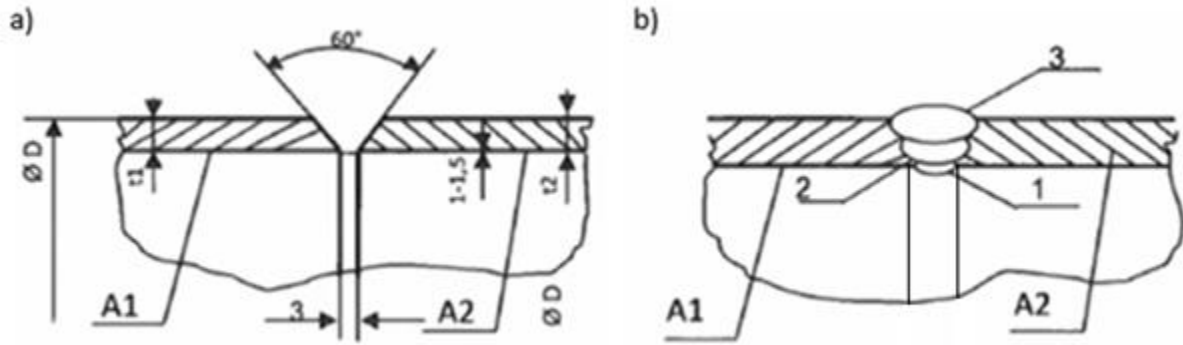


Figure 50 Preparation phase (a) and layer structure (b)[105]

Table 8 shows the main characteristics of the applied welding processes for the tested girth welds.

Table 8 Main characteristics of the welding process for the tested girth welds

Layer	1st (root)	2nd	3rd
Position	PH	PJ	PJ
Filler metal	Böhler FOX CEL	Böhler FOX CEL Mo	Böhler FOX CEL Mo
Electrode diameter (mm)	3.2	3.2	3.2
Current (A)	DC/EN 45-55	DC/EP 55-70	DC/EP 50-65
Voltage (V)	21.8-22.2	22.2-22.8	22.0-22.6
Welding speed (cm/min)	7-12	15-20	10-15

Figure 51 shows the main characteristics of the pipeline sections investigated.

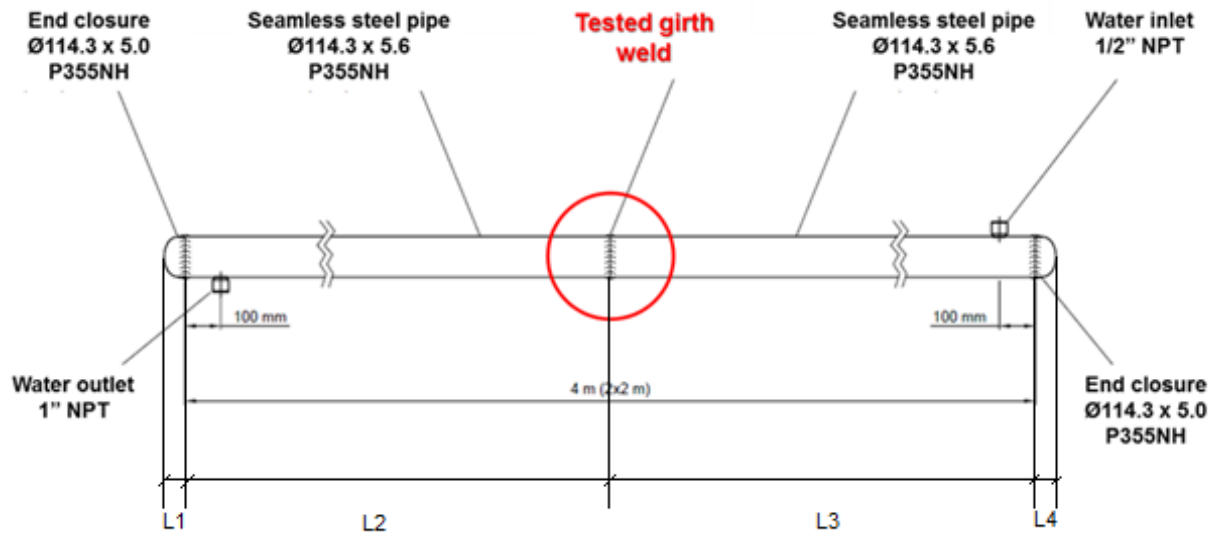


Figure 51 The investigated pipeline sections

The samples were already measured, dividing into four parts, L1, L2, L3, and L4. Also, the wall thickness was measured at four points, the first one at the fitting, the second and the third are before and after our studied girth weld, and the fourth one at the second fitting (Table 9).

Table 9 The length measurements and wall thicknesses

Sample number	Length (mm)				Wall thickness(mm)			
	L1	L2	L3	L4	1 <sup>st</sup>	2 <sup>nd</sup>	3 <sup>rd</sup>	4 <sup>th</sup>
Y1	50	2010	2010	50	5.9	6.3	5.9	5.7
Y2	50	2010	2015	50	5.7	5.5	6	6
Y3	48	2008	2008	48	5.8	5.8	5.6	5.7
Y4	48	2012	2010	50	6	5.7	5.8	5.8
Y5	50	2010	2008	50	5.7	6.1	5.6	5.8
Y6	50	2010	2010	50	5.7	5.8	5.6	5.7
Y7	50	2012	2012	50	5.9	5.6	5.9	5.8
Y8	50	2005	2010	50	5.3	5.3	5.4	5.7
Y9	50	2010	2010	50	6.2	5.9	5.4	6.2
Y10	50	2015	2010	50	5.9	5.9	5.8	6.1
Y11	50	2010	2010	50	5.8	5.7	6	6.1
Y12	50	2010	2010	50	5.7	5.5	5.7	5.8



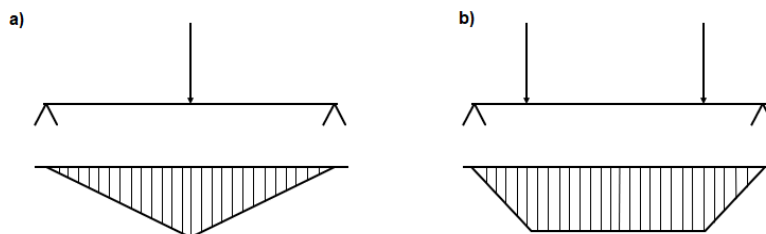
*Figure 52 The investigated samples*

## 7.2. Design the fixing device

Before the next part of the investigations was started, the fixing device had to be designed to hold the samples during the cycle fatigue test and the burst test. The fundamental requirements were as follows:

- ensuring the reproducibility of the tests;
- the use of robust support beams made of steel;
- enabling the interchangeability of smaller components, both in case of potential damage and when changing the diameter of the tested pipe;
- ensuring the safe execution of the tests;
- cost-effectiveness.

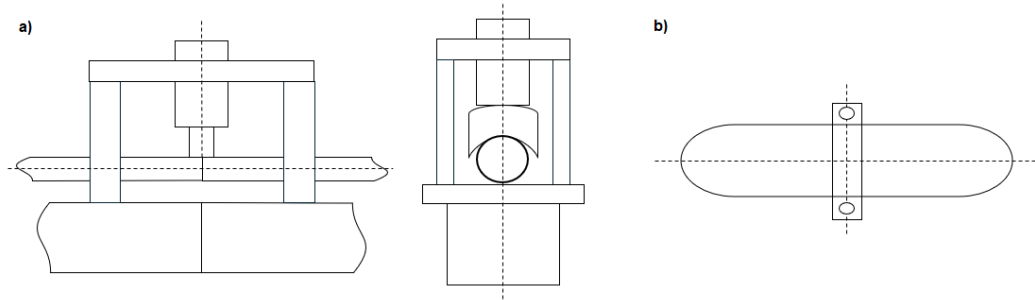
The fixing device should be designed to perform three points bending (Figure 53-a) or four points bending (Figure 53-b); the three points bending was chosen for maximum bending moment.



*Figure 53 3BP or 4BP*

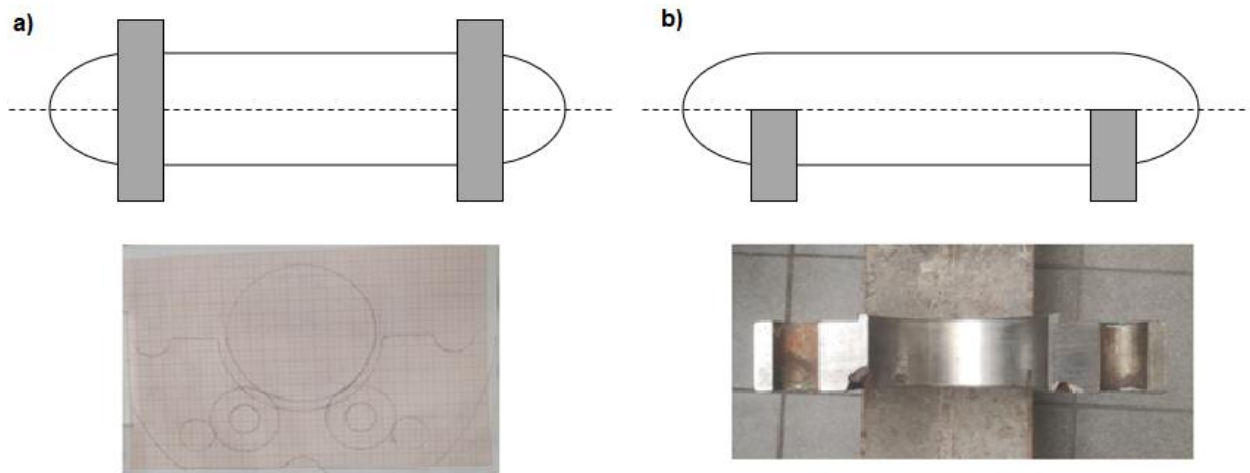


Should the structure of the load transfer be designed as a close frame (Figure 54-a) or a simple load transfer (Figure 54-b)? The simple load transfer was chosen for easier construction.



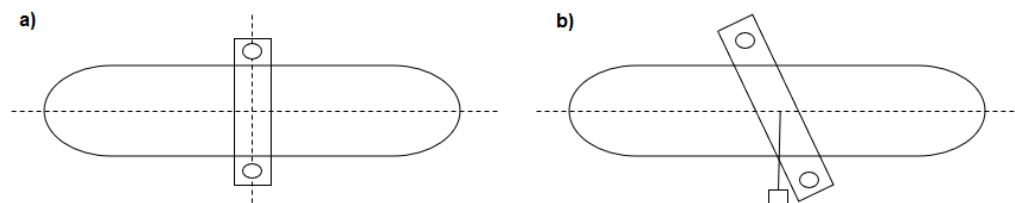
*Figure 54 The structure of the load transfer*

Regarding the support method, should a Closed (rigid) grip be used at the ends (Figure 55-a) or free supports (Figure 55-b), The free support was chosen for a better approximation of real conditions.



*Figure 55 The support method*

Regarding the position of the external load transition device, should it be positioned perpendicular to the longitudinal axis of the pipe (Figure 56-a) or at an angle to the longitudinal axis of the pipe (Figure 56-b), The angled position relative to the longitudinal axis of the pipe was chosen because the deflection can be reliably measured and easier access to the tested section is provided.



*Figure 56 The Position of the external load transition device*



### 7.3. Calculations for testing experimental pipe sections with complex loads

The initial data and their sources for the calculations performed using the relationships from the reference [106] were as follows:

- the pipe material is homogeneous, isotropic and free from material discontinuities;
- the outer diameter of the pipe:  $D_k = 114.3$  mm [expert quality certificate];
- the wall thickness of the pipe:  $s = 5.6$  mm [expert quality certificate];
- the inner diameter of the pipe:  $D_b = D_k - 2*s = 103.1$  mm;
- the maximum internal pressure applied during fatigue:  $p = 63$  bar =  $6.3$  N/mm<sup>2</sup> [operator data];
- second moment of area of the pipe cross-section:

$$I = \frac{(D_k^4 - D_b^4)\pi}{64} \quad (5)$$

resulting in  $I = 2831880$  mm<sup>4</sup>;

- section modulus of the pipe cross-section:

$$K = \frac{I}{D_k/2} \quad (6)$$

resulting in  $K = 49552$  mm<sup>3</sup>;

- distance between supports:  $l = 3600$  mm.
- elastic modulus:  $E = 205000$  N/mm<sup>2</sup> [current value].
- density of steel:  $\rho_{\text{pipe}} = 7850$  kg/m<sup>3</sup> [current value].
- density of water at 25°C:  $\rho_{\text{water}} = 997.04$  kg/m<sup>3</sup> [current value].
- gravitational acceleration:  $g = 9.81$  m/s<sup>2</sup>.
- The tangential stress, since  $s/D_b = 0.054$ , can be calculated from the known

$$\sigma_t = \frac{D_b p}{2s} \quad (7)$$

resulting  $\sigma_t = 57.99$  N/mm<sup>2</sup>. The axial stress is:

$$\sigma_a = \frac{D_b p}{4s} = \frac{\sigma_t}{2} \quad (8)$$

resulting  $\sigma_a = 28$  N/mm<sup>2</sup>.

Calibration of the force from bending on pipe section Y4 can be seen in Figure 57.

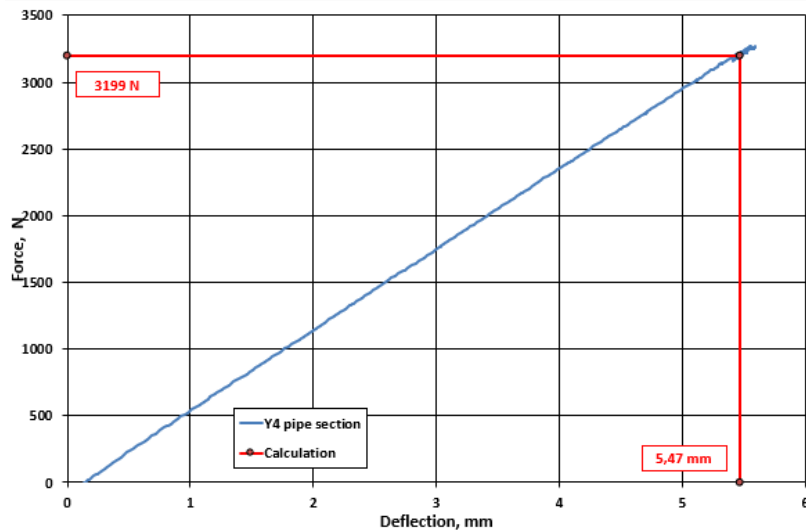


Figure 57 Calculation of the bending force on the experimental pipe section Y4

After this, the deflection values caused by the mass of the pipe section and the water inside it were calculated. The cross-sectional areas of the pipe and the water are:

$$A_{pipe} = \frac{(D_k^2 - D_b^2)\pi}{4} \quad (9)$$

and

$$A_{water} = \frac{D_b^2\pi}{4} \quad (10)$$

from which their masses are calculated as:

$$m_{pipe} = V_{pipe}\rho_{pipe} = A_{pipe}l\rho_{pipe} \quad (11)$$

and

$$m_{water} = V_{water}\rho_{water} = A_{water}l\rho_{water} \quad (12)$$

The calculated values are  $A_{pipe} = 1912.3 \text{ mm}^2$ ,  $A_{water} = 8348.2 \text{ mm}^2$ ,  $m_{pipe} = 54.3 \text{ kg}$ , and  $m_{water} = 29.96 \text{ kg}$ . The uniformly distributed load from these masses is:

$$q_{pipe} = \frac{m_{pipe}g}{l} \quad (13)$$

and

$$q_{water} = \frac{m_{water}g}{l} \quad (14)$$

from which the total force for deflection calculation is:

$$F_q = (q_{pipe} + q_{water})l \quad (15)$$

and the maximum deflection value, using the elastic modulus of the steel;

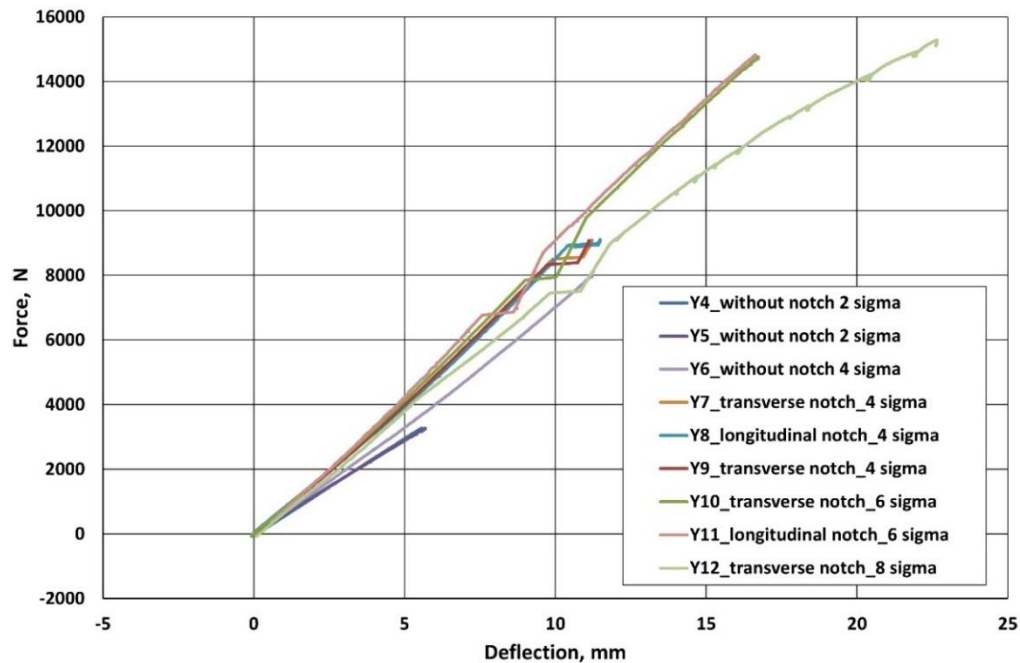
$$f_{max,q} = \frac{5F_q l^3}{384EI} \quad (16)$$

The calculated values are  $q_{pipe} = 0.147 \text{ N/m}$ ,  $q_{water} = 0.229 \text{ N/m}$ , and  $F_q = 824.4 \text{ N}$ , resulting in a maximum deflection at the critical cross-section of  $f_{max,q} = 0.86 \text{ mm}$ .

The results show that the  $f_{max,q}$  value exceeds the difference between the measured deflection and the deflection calculated from the  $F_{2\sigma_a}$  concentrated force ( $5.47 \text{ mm} - 5.35 \text{ mm} = 0.12 \text{ mm}$ ). Possible reasons for this discrepancy include:

- The pipe is not homogeneous or isotropic, partly due to the base material properties and partly due to the tested circumferential weld located at the center of the pipe section.
- Nominal values (dimensions, material constants) were used in calculations.
- Measurement errors (perfect symmetry is impossible, and temperature effects were not accounted for).

Considering these factors, the calibration and adjusted the bending-induced deflection values for complex-loaded pipe sections accordingly were accepted, always prioritizing deflection values as the guiding parameter. The force-deflection functions for overloaded pipe sections are illustrated in Figure 58. In this figure, and all others showing overloads of  $2\sigma_a$ ,  $4\sigma_a$ ,  $6\sigma_a$ , and  $8\sigma_a$ , the terms "2sigma", "4sigma", "6sigma", and "8sigma," or "2S", "4S", "6S", and "8S" are used. When no external bending load was applied, this was either omitted or labelled as "0S".



*Figure 58 Force-deflection functions of pipe sections with external load*

In the context of Figure 58, the following observations were made:

- the minimum negative values (not all force-deflection curves start from positive ranges) are due to the measurement conditions and can be neglected;
- the force-deflection values are consistent with the multiplication of the excess loads;
- the different behaviour of pipe sections without notches (Y4, ..., Y6) and pipe sections with notches (Y7, ..., Y12) is due to the notches themselves.
- the deformations are elastic, except for the Y12 section, with a nominal value of  $8 \cdot \sigma_a$  of  $232 \text{ N/mm}^2$ , which could already cause a small plastic deformation near the notch, and which is reflected in the corresponding force-deflection function.

#### 7.4. Testing equipment and their characteristics

The elements and equipment that make up the test system are located in two areas, one in a laboratory building and the other in a test pit built in front of the building. The tests are controlled from the building, and the experimental pipeline sections are located in the test pit. Two systems are available for testing structures subjected to internal pressure, and a separate system has been developed for external bending loading.

The two pressure increasing systems are essentially identical in design, one for pressures up to 100 bar (called NEW) and the other up to 700 bar (called OLD). The lower capacity system is used for fatigue testing and the higher capacity system for burst testing. The hydraulic cylinders and control units in the laboratory area are shown in Figure 59; the hydraulic power supplies are located in a separate room directly next to the laboratory to reduce operating noise. The block diagrams of the NEW system and the OLD system can be seen in Figures 60 and 61, respectively.

Based on these abilities and capacities a unique testing system has been developed for the complex loading of pipeline sections. Cyclic internal pressure and superimposed external bending loads can be applied for the investigations in the three-point bending (TPB or 3PB) configuration. In this series of experiments the tested girth weld was positioned in the middle of the tested pipeline section. The experimental layout together with the introduction of the key elements in the test pit can be seen in Figure 62.

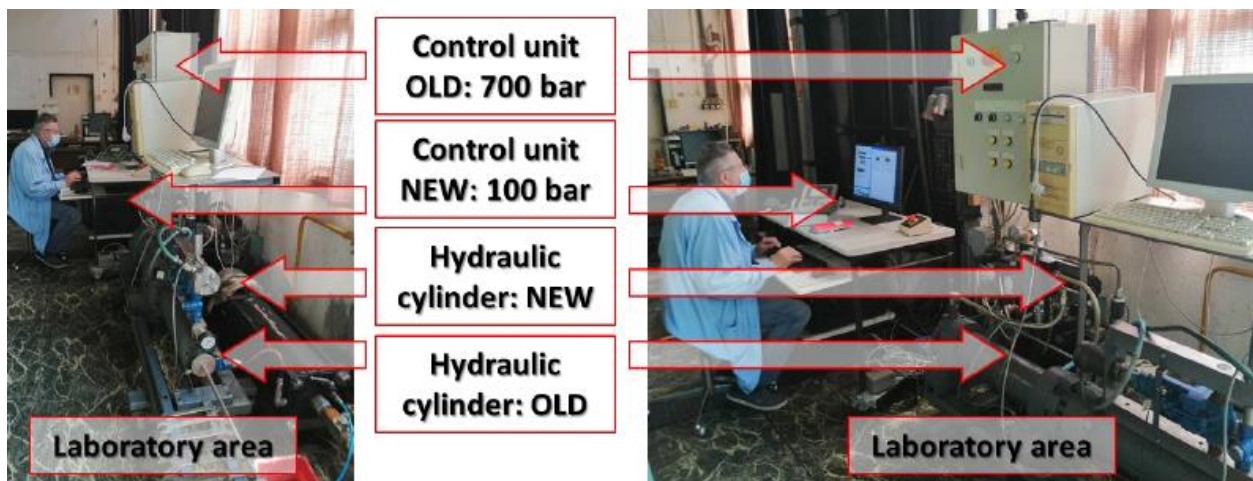


Figure 59 The laboratory area with hydraulic cylinders and control units of the testing systems.

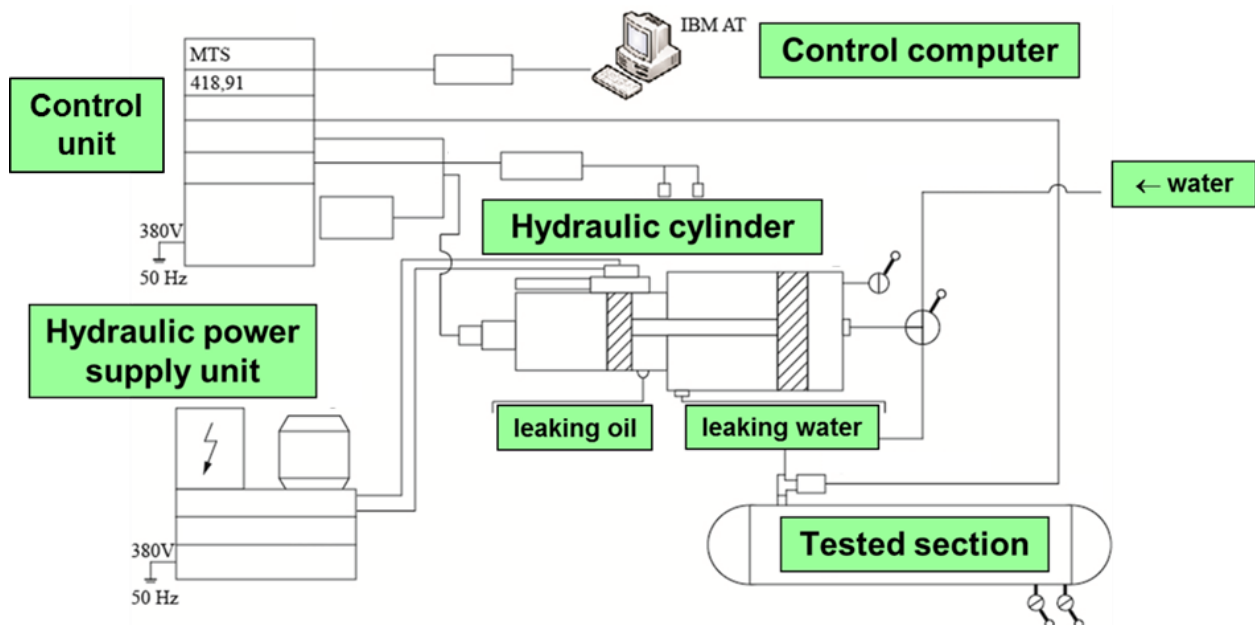


Figure 60 Block diagram of the pressure boosting system up to 100 bar internal pressure

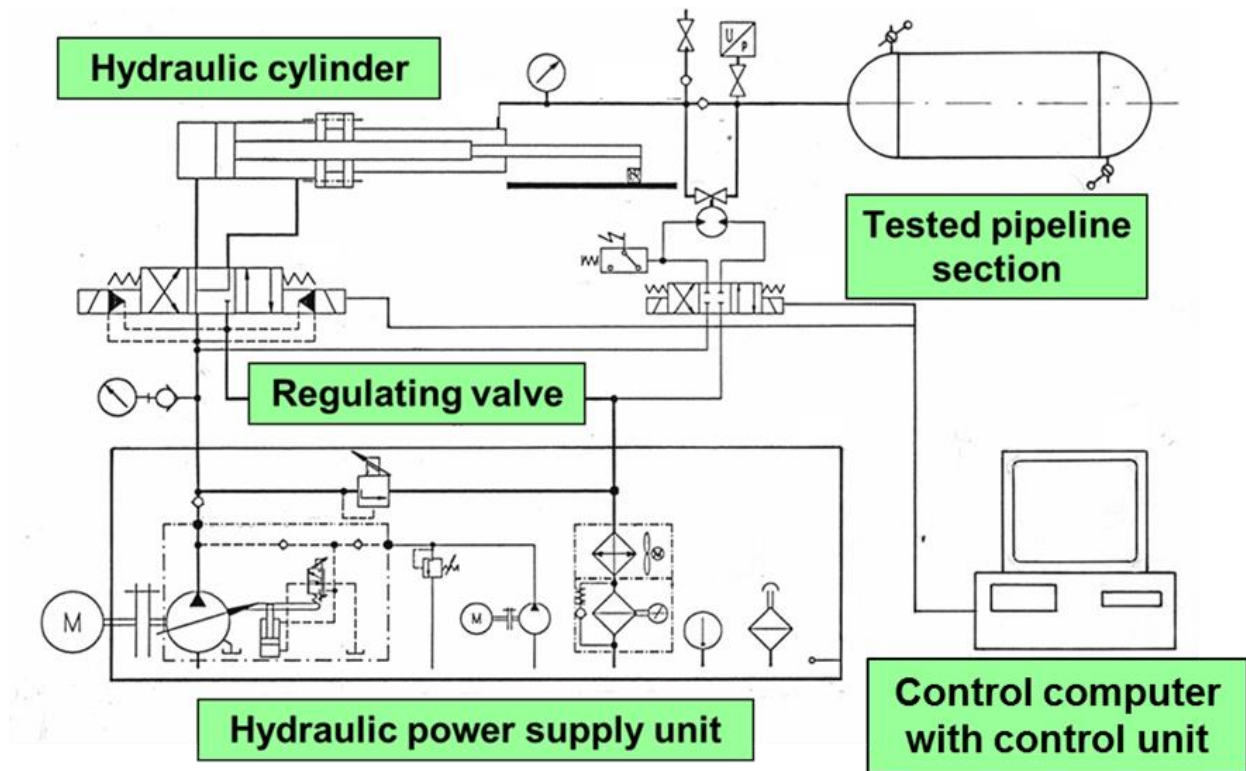


Figure 61 Block diagram of the pressure boosting system up to 700 bar internal pressure

As can be seen in Figures 60 and 61, the two systems are very similar in structure.

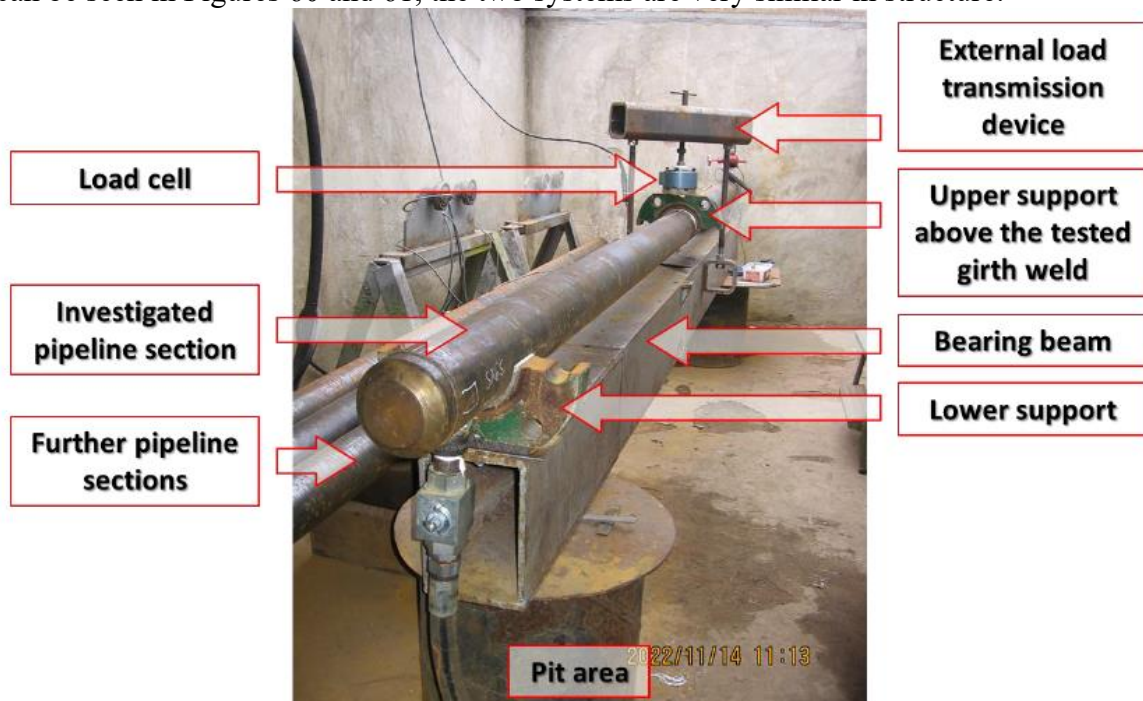


Figure 62 The pit area of our developed system with a pipeline section.

The superimposed bending moment was set using a certified load cell and verified using a certified extensometer with an extended arm. Positioning of the tested girth welds was performed using a scaled plate with drilled holes (see Figure 63 and Figure 64).



The burst process was recorded with two video cameras, both positioned at the edge of the pit area, following the burst process from above. One camera was positioned in the direction of the longitudinal axis of the tested pipeline section and the other perpendicular to it.

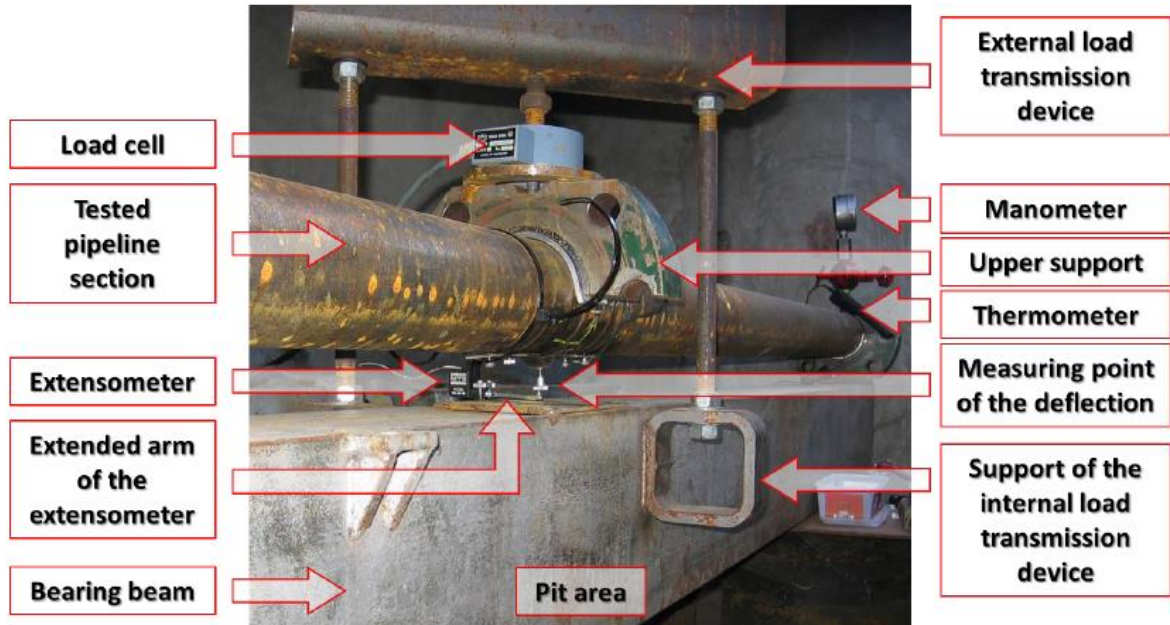


Figure 63 Setting the deflection by load cell and its verification by extensometer with an extended arm.

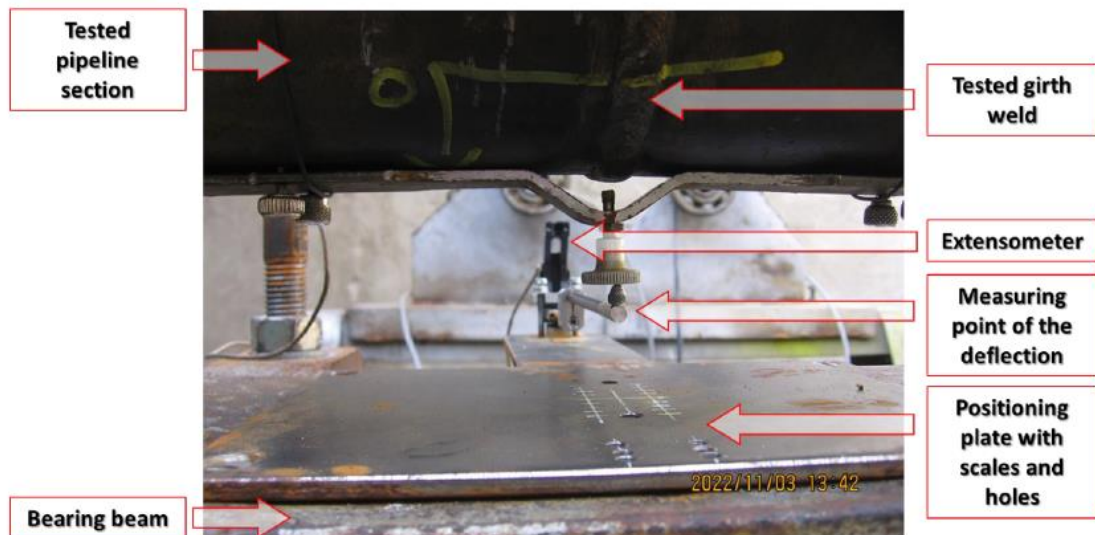


Figure 64 The positioning plate with scales and holes, and the measurement of the deflection by extensometer with extended arm.

Twelve pipeline sections were tested with different characteristics. The experiences of the Hungarian transporting pipeline operator (FGSZ Ltd.) have pointed to that external undercuts and lack of fusions (between the base materials and weld metals) can be found in inadequate girth welds. Other experiences of the Hungarian transporting pipeline operator have shown that third-party (near) longitudinal damages are also common and significantly increase the operational risk, especially when interacting with both girth and spiral welds. These were the reasons why we also

tested girth welds with artificial notches. The notches were cut using a hand grinding machine and located either in the heat-affected zone (HAZ) of the girth weld (circumferential direction) or through the girth weld (axial direction). The external undercuts and lack of fusions were modelled using circumferential notches, the third-party (near) longitudinal damages interacting with girth welds were modelled by longitudinal notches. Since the artificial notches were made by the same person using the same hand grinder, their maximum nominal width was 2 mm. The shape of the artificial notches followed the shape of both the pipe and the grinding wheel (Figure 65), with their width decreasing slightly in the direction of the pipe wall thickness. Figure 66 demonstrates the two types of notch configurations.



*Figure 65 The artificial notch configurations*



*Figure 66 Artificial notch in the girth weld HAZ of the Y10 pipeline section (left), artificial notch through the girth weld of the Y8 pipeline section (right)*

All pipeline sections, except Y3, were subjected to 100,000 cycles of fatigue loading. The cyclic internal pressure was adjusted to the real operating pressure and was changed between 60% and 100% of the maximum allowable operating pressure (MAOP, 64 bar). The applied axial stress

from bending was two, four, six and eight times (in relevant figures 2 sigma, 4 sigma, 6 sigma and 8 sigma, respectively) of the axial stress ( $\sigma_a$ ) from the maximum internal pressure. During the fatigue tests 0.2 Hz testing frequency was applied, moreover during the fatigue and the burst tests water was used as testing media. During the long test period, the ambient temperature varied between 15 °C and 30 °C, but this variation had no significant effect on the implementation of the tests or the mode of the fracture behaviour of the pipeline sections. The main characteristics of the full-scale tests can be found in Table 11.

After the girth welds were made, they were radiographed by Gamma-Control Ltd. The results of the investigations are summarised in Table 10, which shows that the girth welds contained only tolerable or suitable (S) discontinuities. Therefore, the condition that the quality of the girth welds should not influence the results of the mechanical tests was fulfilled.

*Table 10 Main characteristics of the RT carried out on the full size test pipe sections after preparing the weld*

Pipeline section ID	Weld No.		Gamma-Controll Kft.	
	Girth welds	GWS	T/E	D&C[107]
<b>Y3</b>	F3, F15, F27	F15	2022.04.12	Nothing
<b>Y1</b>	F1, F13*, F25	F13	2022.04.12	2011 – S; 3012 – S; 514 – S
<b>Y2</b>	F2, F14, F26	F14	2022.04.12	504 – S; 507 – S
<b>Y4</b>	F4, F16, F28	F16	2022.04.12	504 – S; 514 – S
<b>Y5</b>	F5, F17, F29	F17	2022.04.12	2011 – S; 514 – S
<b>Y6</b>	F6, F18, F30	F18	2022.04.12	504 – S; 5013 – S
<b>Y7</b>	F7, F19, F31	F19	2022.04.12	5013 – S; 515 – S
<b>Y8</b>	F8, F20, F32	F20	2022.04.12	2011 – S; 504 – S
<b>Y9</b>	F9, F21, F33	F21	2022.04.12	2011 – S; 504 – S
<b>Y10</b>	F10, F22*, F34	F22	2022.04.12	3012 – S
<b>Y11</b>	F11, F23, F35	F23	2022.04.12	504 – S; 507 – S; 514 – S
<b>Y12</b>	F12, F24, F36	F24	2022.04.12	3012 – S; 504 – S

\* The RT test report can be seen in appendix 2



*Table 11 The main characteristics of the full-scale tests*

<b>Pipeline section ID</b>	<b>Fatigue*</b>	<b>External bending</b>	<b>Notch location</b>	<b>Notch direction</b>	<b>Nominal notch depth</b>	<b>Nominal notch length (mm)</b>
<b>Y3</b>	N/A	N/A	N/A	N/A	N/A	N/A
<b>Y1</b>	performed	N/A	N/A	N/A	N/A	N/A
<b>Y2</b>	performed	N/A	N/A	N/A	N/A	N/A
<b>Y4</b>	performed	$2\sigma_a$	N/A	N/A	N/A	N/A
<b>Y5</b>	performed	$2\sigma_a$	N/A	N/A	N/A	N/A
<b>Y6</b>	performed	$4\sigma_a$	N/A	N/A	N/A	N/A
<b>Y7</b>	performed	$4\sigma_a$	girth weld HAZ	circumferential	0.37 t	29
<b>Y8</b>	performed	$4\sigma_a$	through girth weld	axial	0.50 t	41
<b>Y9</b>	performed	$4\sigma_a$	girth weld HAZ	circumferential	0.67 t	40
<b>Y10</b>	performed	$6\sigma_a$	girth weld HAZ	circumferential	0.50 t	30
<b>Y11</b>	performed	$6\sigma_a$	through girth weld	axial	0.67 t	40
<b>Y12</b>	performed	$8\sigma_a$	girth weld HAZ	circumferential	0.50 t	40

\* If fatigue was applied, the number of cycles was 100,000 cycles.

## 8. FULL-SCALE INVESTIGATIONS PROCESS

Our samples (pipeline sections) had the following tests in order:

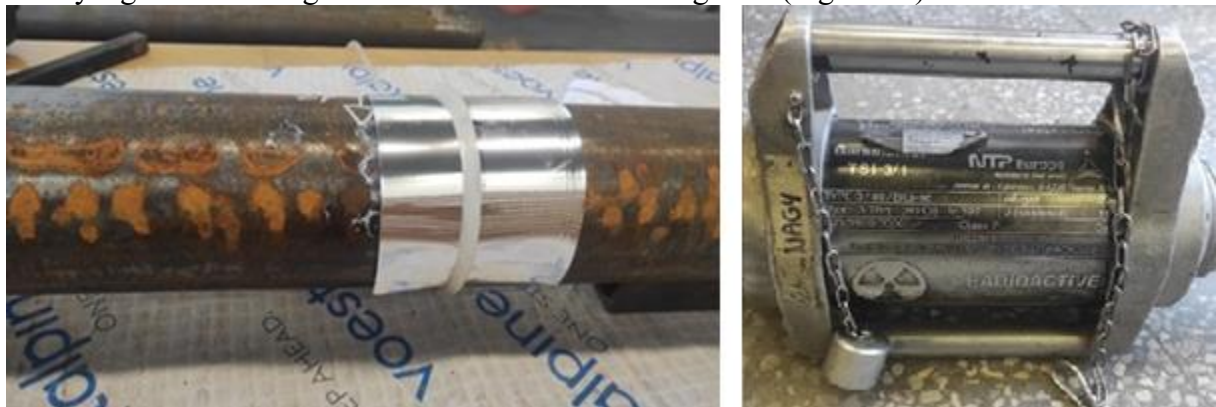
- visual, liquid penetrant, and radiographic investigations (VT, PT, and RT, respectively);
- radiographic investigation (RT);
- fatigue test (100,000 cycles);
- radiographic investigation (RT)
- pressure test (6 hours);
- burst test.

### 8.1. Visual, liquid penetrant, and radiographic investigations

The tested girth welds were made by manual metal arc welding and were inspected by visual, liquid penetrant, and radiographic tests (VT, PT, and RT, respectively). Only girth welds that have been produced to an acceptable quality level have been tested. This also means that the consistently high quality of the girth welds made it possible to investigate the impact of other influencing factors on the damage characteristics.

### 8.2. Radiographic investigations before and after the fatigue test

After each investigation, a radiographic test was performed to check the girth weld and see if there was any significant change that could affect our investigation (Figure 67).

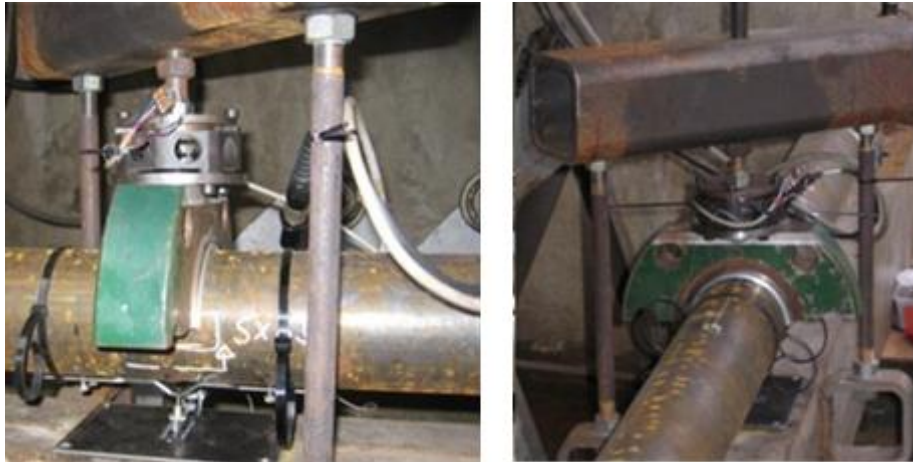


*Figure 67 The preparation for the RT test (left), The device that used to do the RT (right)*

### 8.3. Fatigue test

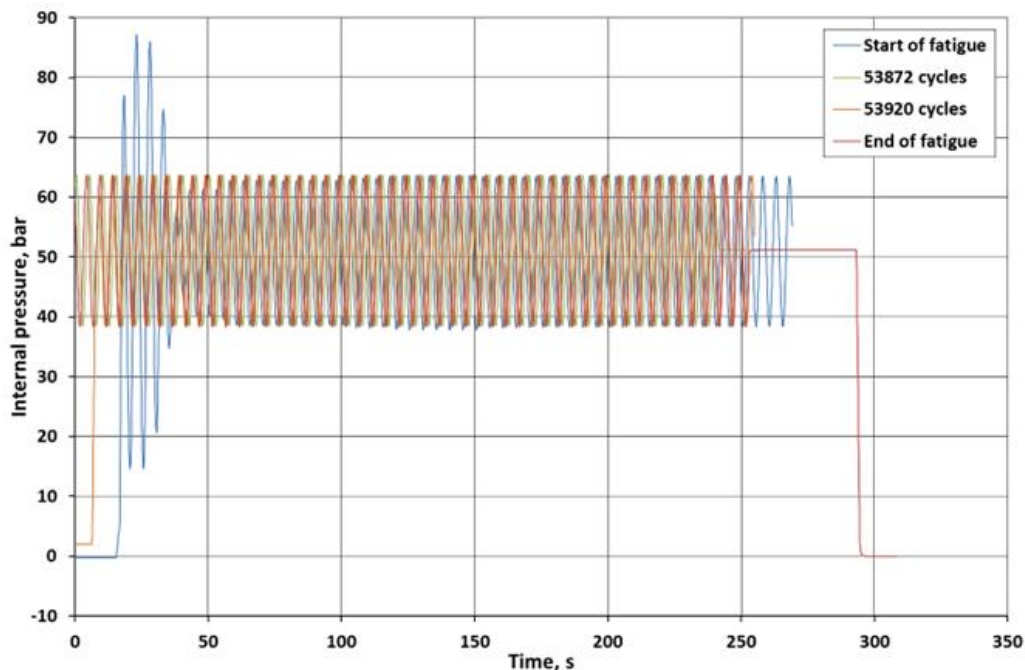
The cycle fatigue test was for 100,000 cycles of internal pressure loading, with or without external bending loading. The cyclic internal pressure varied between 60% and 100% of the operational pressure (64 bar). The external bending loads were applied during the cyclic loading (100,000 cycles) and the burst test. The applied axial stress from superimposed bending was two, four, six and eight times (in relevant figures 2S, 4S, 6S and 8S, respectively) of the axial stress ( $\sigma_a$ ) from

the maximum internal pressure. In the three-point bending arrangement, the tested girth weld was positioned in the middle of a nominal 4 meters long pipeline section; the bending load was set via a load cell and checked by means of a deflection meter [108], [109] (Figure 68). During the fatigue tests 0.2 Hz testing frequency was applied; in addition, during the fatigue and the burst tests water was used as testing media. During the long test period, as the test pit is located outdoors, the ambient temperature changed between 15 °C and 30 °C. This variation of the outside temperature had no significant effect on the execution of the tests or the mode of the fracture behavior of the pipeline sections.



*Figure 68 Load cell and deflection meter for the external bending(left), Transfer of external load for the external bending (right)*

The time required to complete 100,000 fatigue cycles was nearly 6 full days (nearly 139 hours) of uninterrupted testing. By looking at Figure 69 and Figure 70, it can be stated that the variation of the internal pressure was stable throughout the whole process, except for the initial and final transients.



*Figure 69 Internal pressure vs. time functions recorded during the fatigue test of pipeline section with minimum superposed external bending load (Y4)*

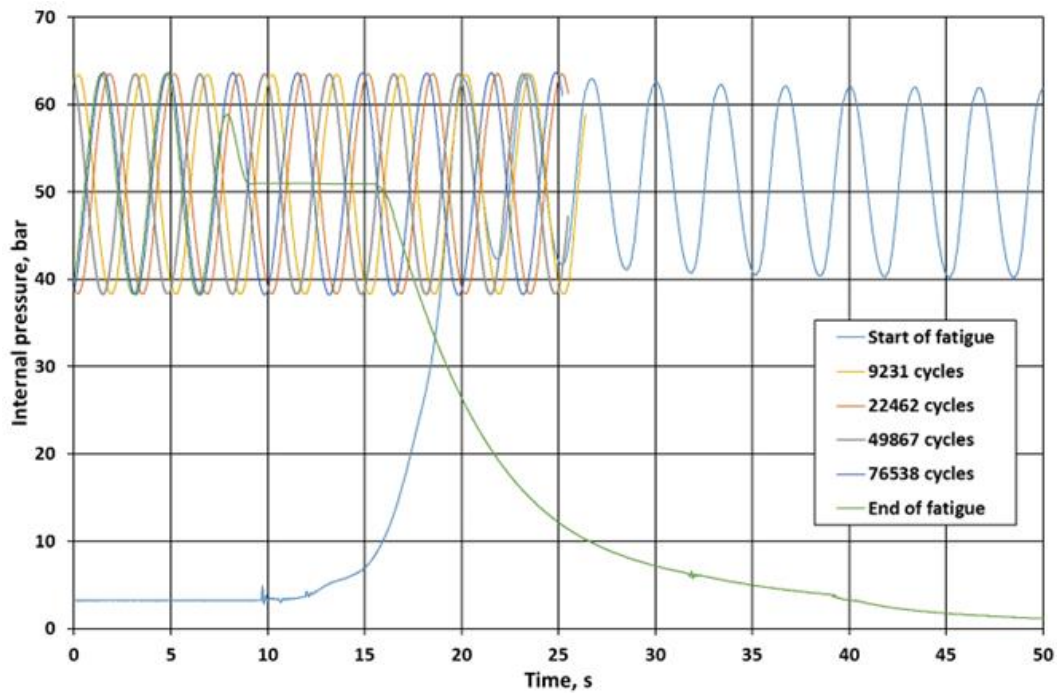


Figure 70 Internal pressure vs. time functions recorded during the fatigue test of pipeline section with maximum superposed external bending load (Y12)

The deflection value and its variation were continuously monitored. These values were recorded every 5,000-8,000 cycles, with a time interval of 50-60 cycles (250-300 s).

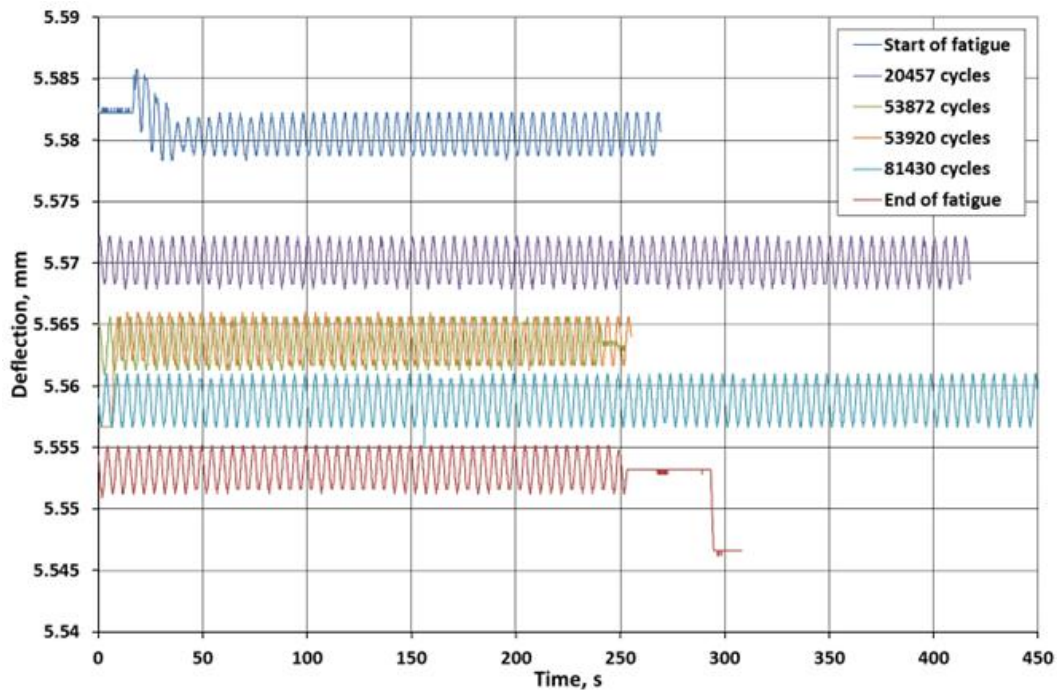


Figure 71 Deflection vs. time functions recorded during the fatigue test of pipeline section with minimum ( $2 \sigma_a$ ) superposed external bending load (Y4)

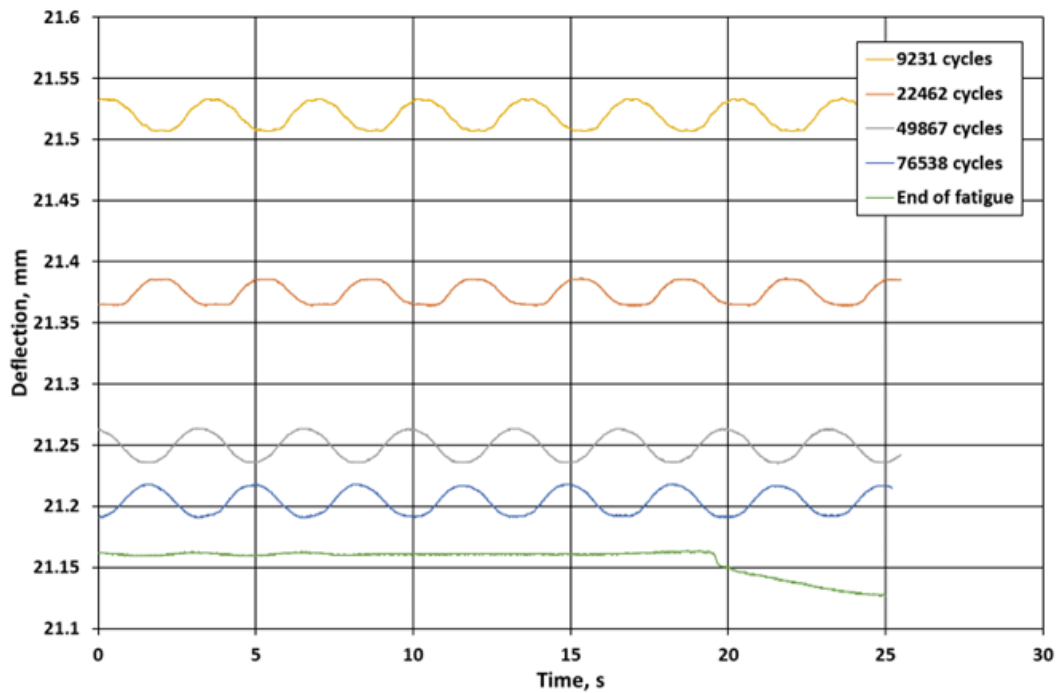


Figure 72 Deflection vs. time functions recorded during the fatigue test of pipeline section with maximum ( $8 \sigma_a$ ) superposed external bending load (Y12)

The deflection-time plots in Figure 71 and Figure 72 also reflect the change in internal pressure and its stability, and illustrate the magnitude of the deflection and the extent of its change. The two figures also highlight the difference in deflection due to minimum and maximum superposed bending loads.

#### 8.4. Pressure test

Every sample from our twelve pipeline sections was subjected to a pressure test for 1.5 times the operation pressure (95 bar) in a closed system for six hours (Table 12). During this period, the pressure and temperature were recorded almost every hour (Figure 73).

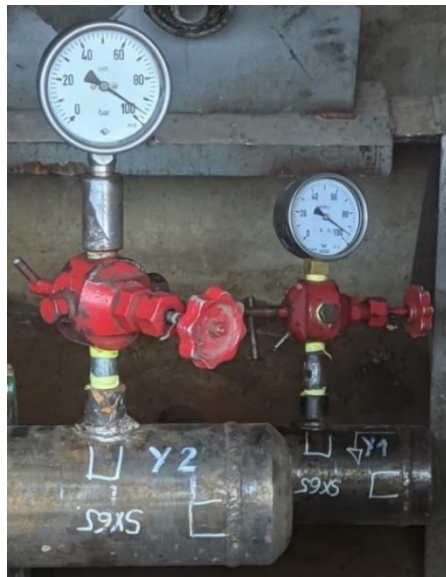


Figure 73 The samples Y1 and Y2 during the pressure test



Table 12 The temperature and the pressure values for the investigated pipeline sections (except Y3) during the 6-hour pressure test

Pipeline section ID	Recorded (Time) and measured (Temperature, Pressure) data	Recorded (Time) and measured (Temperature, Pressure) values						
Y1	Time	8:15	9:44	10:51	11:56	12:55	13:49	14:50
	Temperature (°C)	19	20.3	21.9	23.3	24.4	25.5	26.2
	Pressure (bar)	95	97.5	97.5	100	>100	>100	>100
Y2	Time	8:15	9:44	10:51	11:56	12:55	13:49	14:50
	Temperature (°C)	19	20.3	21.9	23.3	24.4	25.5	26.2
	Pressure (bar)	94	96	100	>100	>100	>100	>100
Y4	Time	9:20	10:20	11:21	12:20	13:19	14:23	15:18
	Temperature (°C)	13.4	14.3	15.3	16.5	20.3	20.3	19.1
	Pressure (bar)	96	96	97	98	100	97	97
Y5	Time	7:39	8:40	9:37	10:39	11:39	12:36	13:38
	Temperature (°C)	12.6	13	13.3	13.8	17.5	22.6	25.1
	Pressure (bar)	96	89	95.5	95	97.5	>100	>100
Y6	Time	11:25	12:26	13:36	14:56	15:27	16:27	17:31
	Temperature (°C)	8.7	8.6	8.5	7.7	7.1	6	5.7
	Pressure (bar)	96	97	98	97	96.5	97	97
Y7	Time	9:00	10:01	11:05	12:00	12:59	14:00	15:00
	Temperature (°C)	12.6	13	13.8	14.3	14.5	14.5	14.1
	Pressure (bar)	95	94	94	93	96	96	95.5
Y8	Time	11:15	12:15	13:13	14:18	15:15	16:20	17:15
	Temperature (°C)	14.3	14.6	15.1	14.9	14.5	13.9	13.4
	Pressure (bar)	96	96	96	94.5	92.5	95	94
Y9	Time	9:16	10:13	11:22	12:17	13:21	14:16	15:16
	Temperature (°C)	7.4	6.7	6.7	6.5	7	6.8	6.1
	Pressure (bar)	95.8	92	97	96.5	97	96.5	96

Pipeline section ID	Recorded (Time) and measured (Temperature, Pressure) data	Recorded (Time) and measured (Temperature, Pressure) values						
Y10	Time	8:50	9:55	10:48	11:48	12:53	13:57	14:50
	Temperature (°C)	8.6	8.4	8.3	8.4	8.4	8.4	8.1
	Pressure (bar)	95.5	92	90	95.5	95.5	95	94.5
Y11	Time	8:15	9:20	10:08	11:13	12:18	13:13	14:22
	Temperature (°C)	7.9	8	7.9	8.4	9	10.4	10.3
	Pressure (bar)	95.5	95.5	95.2	95.5	95.7	96	96
Y12	Time	9:25	10:32	11:34	12:45	13:34	14:39	15:39
	Temperature (°C)	9.6	9.9	10.5	11.2	11.3	10.6	10.4
	Pressure (bar)	94	94	95.5	96	96	95.5	95.5

Due to the change in temperature during the pressure test, the pressure of some samples was elevated above 100 bar, and the exact temperature could not be measured. Consequently, the use of a manometer with an extended range is suggested for future investigations.



During the pressure test, no pipe sections were damaged, and temperature and pressure values remained within acceptable ranges. All tested pipeline sections withstood the 6-hour-long hydrostatic pressure test without any significant loss of internal pressure. The result indicates that the quality of the pipe sections and the test girth welds was not significantly altered by the strength pressure test phase.

### 8.5. Burst test

After the burst tests were completed (Figure 74), the video camera recordings were reviewed, the picture-frames corresponding to the moment of failure were cut, and the internal pressure vs. burst test time diagrams were plotted from the recorded internal pressure values (Figure 75).



*Figure 74 Y1 pipeline section at the moment of its failures*



*Figure 75 The pressure value during the burst test (example)*

## 9. TESTING RESULTS

Results of the visual testing (VT) and the radiographic testing (RT) repeated after the fatigue tests showed no detectable decisive changes in any of the cases. Table 13 summarizes the results of the radiographic examinations performed by Albera'97 Ltd. before and after the fatigue tests. This means that the fatigue stage did not cause significant changes in the quality of the investigated girth welds.

Figure 76, Figure 77, Figure 78, and Figure 79 illustrates the average deflection vs. fatigue cycle number curves for each pipeline section subjected with minimum, intermediate, maximum and all superimposed bending, respectively. The data are derived from the systematic processing of functions similar to the functions of the diagram. The curves for  $2\sigma_a$ ,  $4\sigma_a$ ,  $6\sigma_a$ , and  $8\sigma_a$  stresses, furthermore for circumferential and axial notches are clearly distinguished in the figure. As the figure illustrates, the magnitude of the stress plays a determining role. It is noteworthy that the curves for each pipeline section show the same trends and their location is fully consistent with our approach.

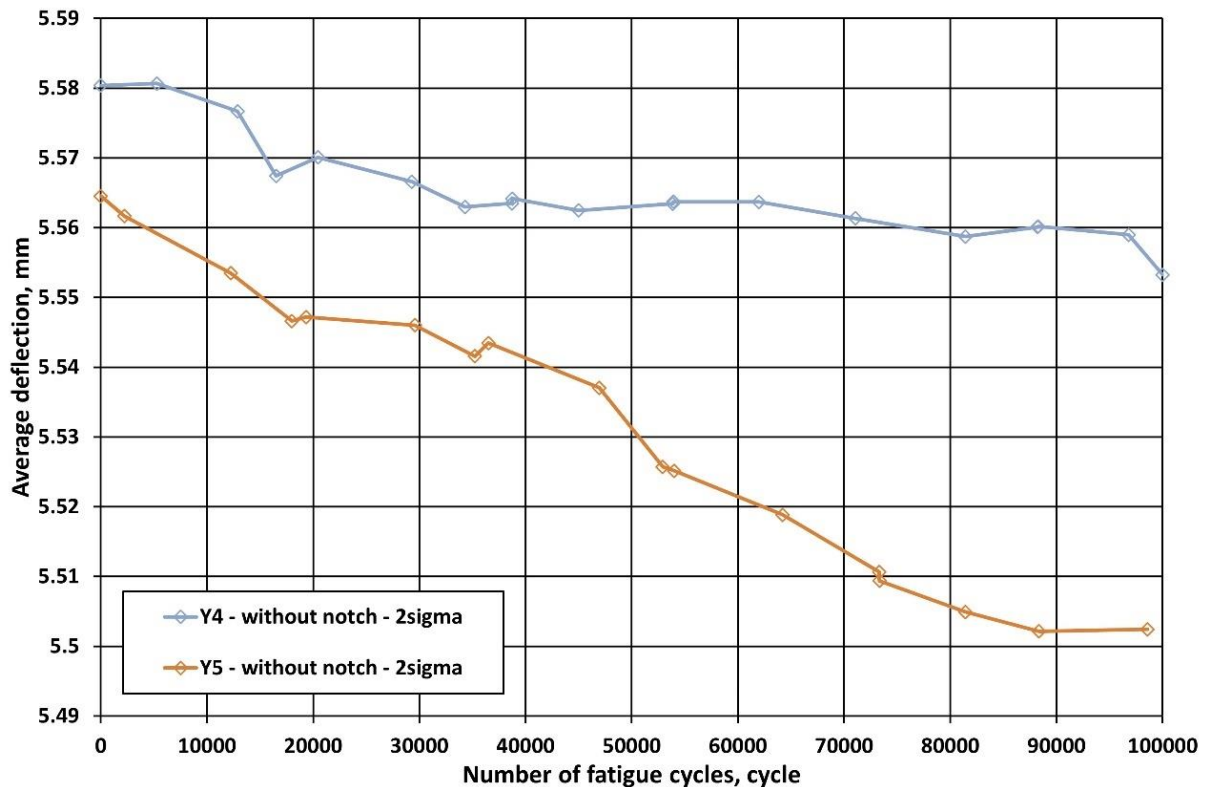


Figure 76 Average deformation (deflection) values and their variation during fatigue tests under minimal external bending load (Y4 and Y5 pipe sections,  $2\sigma_a$ )

Table 13 Results of radiographic testing (RT) performed on the test girth welds by Albera'97 Kft., before and after the fatigue test

Pipeline section ID	Before the fatigue test			After the fatigue test		
	GWS*	T/E	D&C [107]	GWS*	T/E	D&C [107]
<b>Y3</b>	<b>Y3</b>	2022.06.30.	602 – S	<b>N/A</b>	N/A	N/A
<b>Y1</b>	<b>Y1/V13****</b>	2022.06.15.	2015 – S; 602 – S and “Film error”	<b>13*****</b>	2022.07.27.	Nothing
<b>Y2</b>	<b>Y2</b>	2022.06.30.	5013 – S	<b>14</b>	2022.07.27.	Nothing
<b>Y4</b>	<b>Y4</b>	2022.06.30.	602 – S	<b>Y4</b>	2022.10.06.	Nothing and “Contamination in the pipe”
<b>Y5</b>	<b>17</b>	2022.07.27.	2011 – S; 602 – S	<b>Y5</b>	2022.10.06.	2011 – S
<b>Y6</b>	<b>18</b>	2022.07.27.	Nothing	<b>Y6</b>	2022.11.10.	Nothing
<b>Y7***</b>	<b>Y7</b>	2022.10.06.	515 – S	<b>Y7</b>	2022.11.10.	604 – NS
<b>Y8***</b>	<b>Y8</b>	2022.10.06.	2016 – NS	<b>Y8</b>	2022.11.10.	604 – NS
				<b>Y8</b>	2022.11.29.	2015 – NS; 604 – NS and „Grinding traces across the weld”
<b>Y9***</b>	<b>9</b>	2022.11.10.	5012 – S	<b>Y9</b>	2022.11.29.	604 – NS and „Grinding traces near the weld”
<b>Y10***</b>	<b>10*****</b>	2022.11.10.	2015 – S	<b>Y10*****</b>	2022.11.29.	604 – NS and „Grinding traces near the weld”
<b>Y11***</b>	<b>11</b>	2022.11.10.	Nothing	<b>R23</b>	2023.11.07.	602 – S; 604 – S
<b>Y12***</b>	<b>12</b>	2022.11.10.	Nothing	<b>R24</b>	2023.11.07.	602 – S; 604 – S

\* Notation applied by the investigators, which are intentionally disclosed for the identification with official "Radiographic Test Report"-s.

\*\* The radiographic investigations and their assessments are not necessarily carried out by the same persons before and after the fatigue tests.

\*\*\* It was not known to the radiographers that artificial notches were present around the girth welds - in all cases 604 reference numbers (grinding mark, local damage due to grinding) of imperfections were noted, and in some cases the presence of a grinding mark was specifically noted.

\*\*\*\* The RT test report can be seen in appendix 3

\*\*\*\*\* The RT test report can be seen in appendix 4

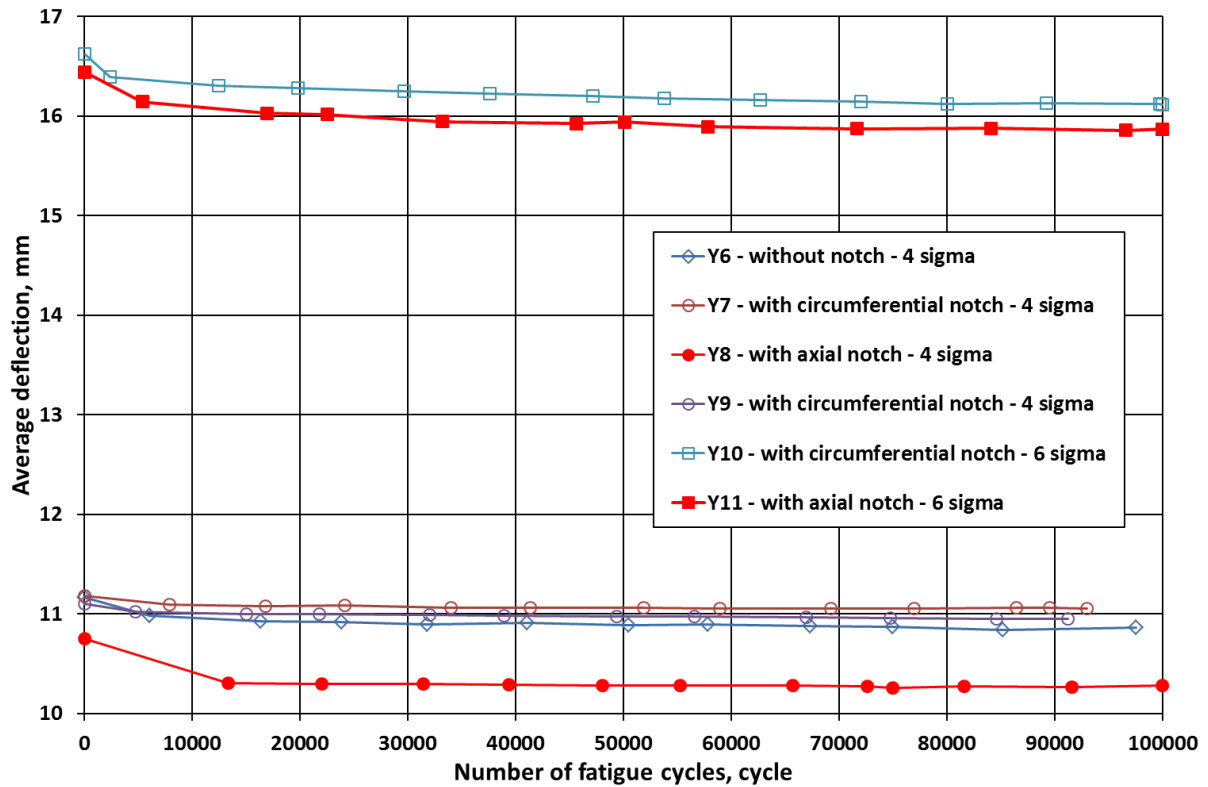


Figure 77 Average deformation (deflection) values and their variation during fatigue tests under intermediate external bending loads (Y6-Y11,  $4\sigma_a$  and  $6\sigma_a$ )

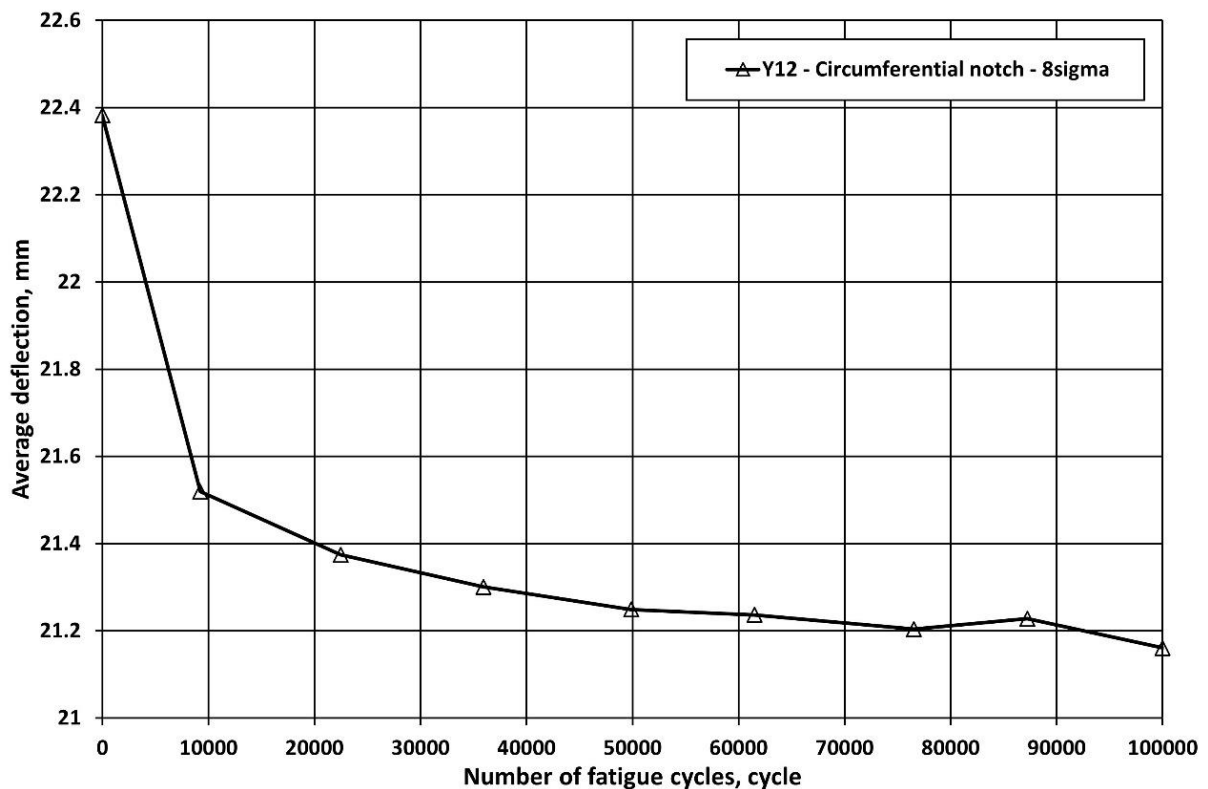


Figure 78 Average deformation (deflection) values and their variation during fatigue tests under maximal external bending load (Y12 pipe section,  $8\sigma_a$ )

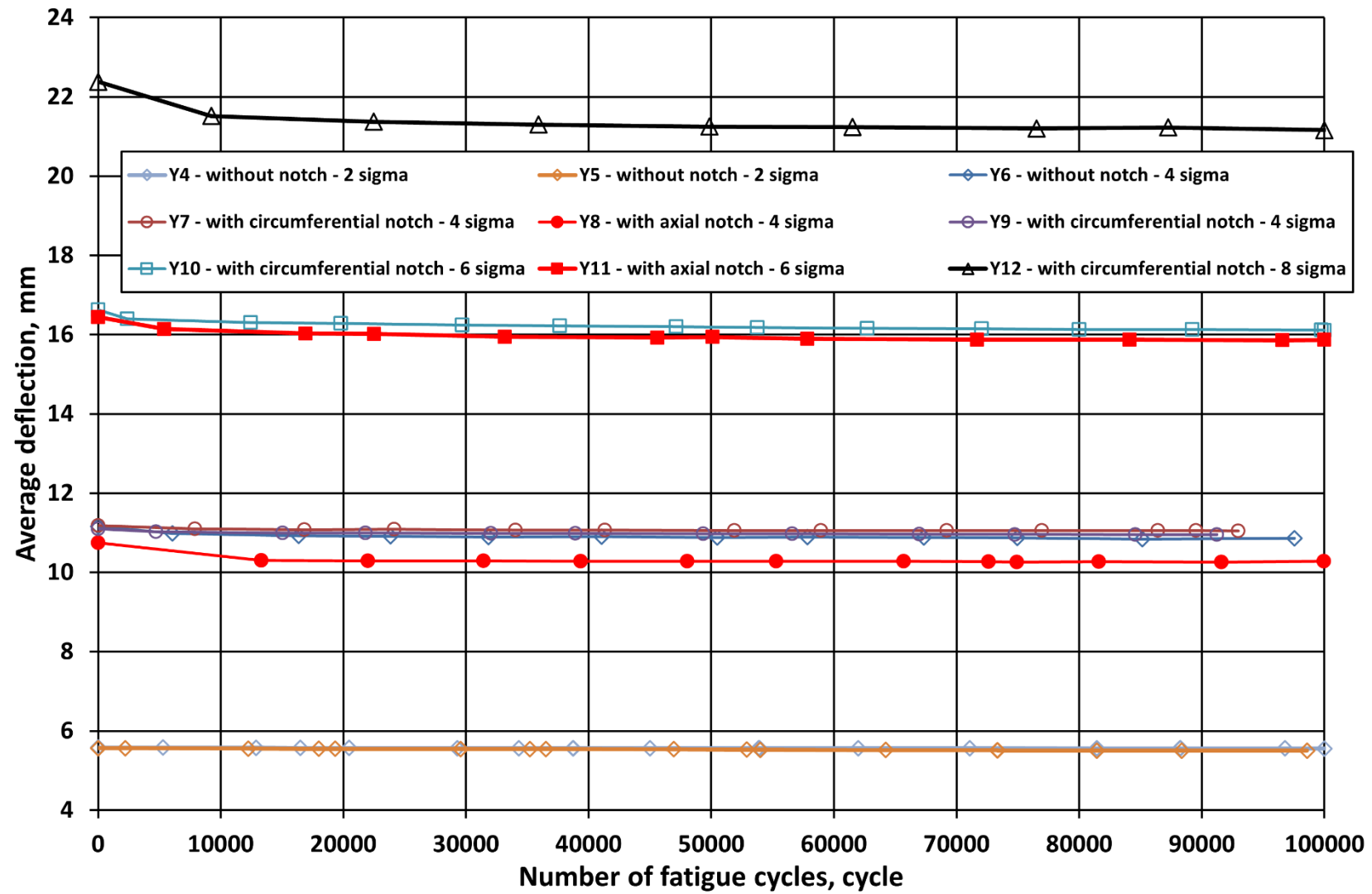


Figure 79 Average deflection values and their changes during the fatigue tests: all pipeline sections

Figure 80 and Figure 81 show the internal pressure vs. burst test time diagrams for the investigated pipeline sections, where the arrows indicate the burst points.

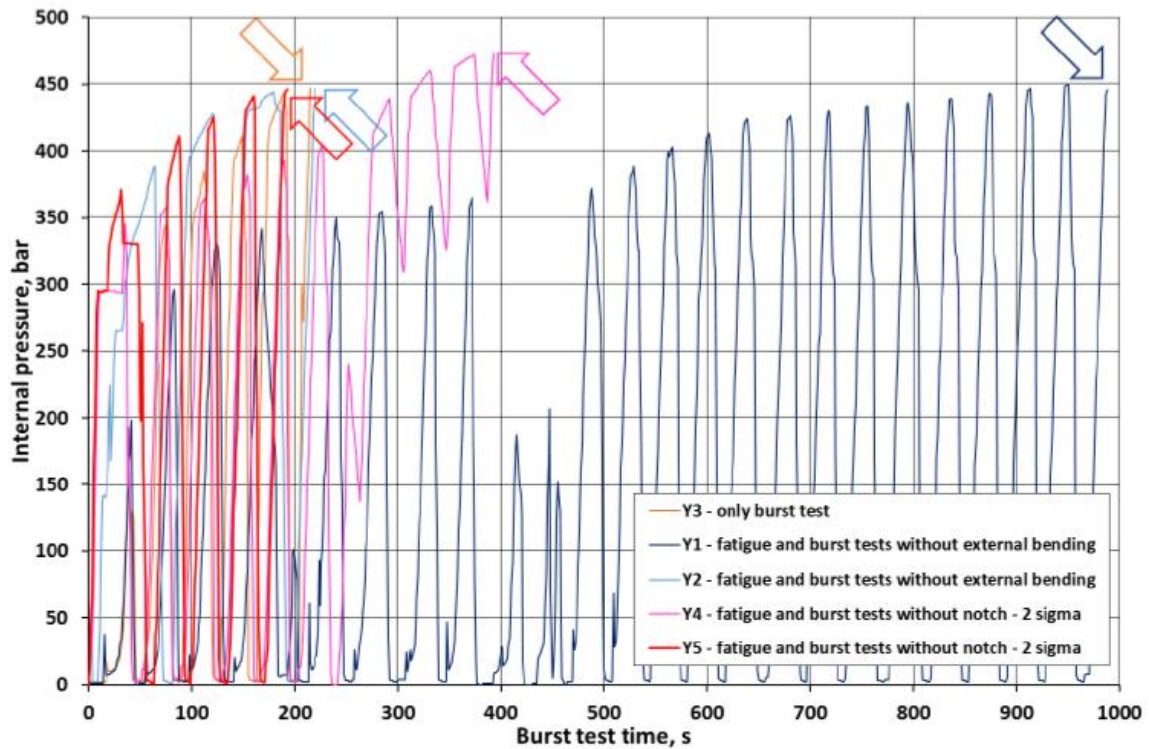


Figure 80 Internal pressure vs. burst test time diagrams of the investigated Y1-Y5 pipeline sections

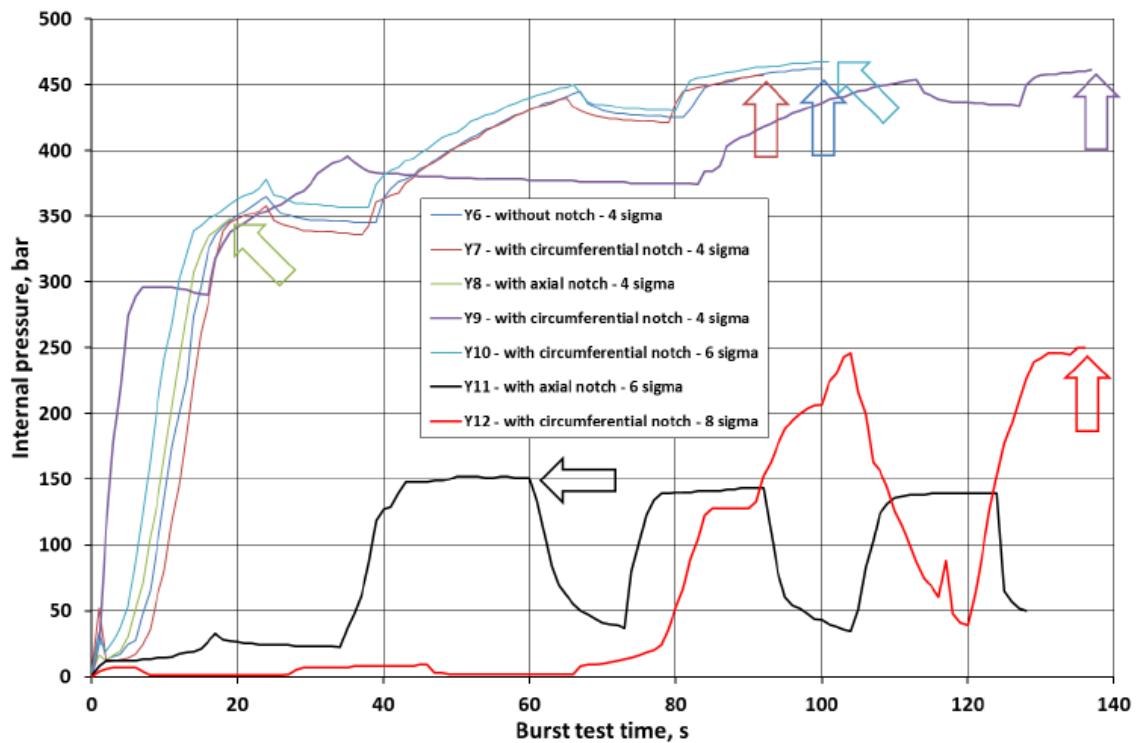


Figure 81 Internal pressure vs. burst test time diagrams of the investigated Y6-Y12 pipeline sections



The main characteristics of the Y1-Y5 and Y6-Y10 diagrams are the same; however different burst test times can be noticed. Partially different behavior was observed for Y11 and Y12 pipeline sections, due to the larger size of the notches and the higher stress ( $\sigma_a$ ) resulting from the higher bending load.

The average internal pressure growth rate values both in the first stage and in the latter stages can be assessed as quasi-static values, no significant dynamic effects were observed. In all cases, we have experienced different numbers of times-like changes on the curves which demonstrate the volume increase of the pipeline sections. The increase in volume is the natural result of elastic-plastic deformation; during these periods, the system draws water from the water supply network. A dimensionless safety factor was interpreted to quantify the behavior of the pipeline sections, with the following equation:

$$\text{Safety factor} = \frac{\text{Burst Pressure}}{\text{Maximum Allowable Operating Pressure}} = \frac{BP}{MAOP} \quad (17)$$

where BP is the measured burst pressure [bar] and MAOP is the Maximum Allowable Operating Pressure [bar].

Table 14 summarizes both the main characteristics and the burst pressure (BP), furthermore the safety factor (SF) values of the investigations, assuming that the value of the MAOP is 64 bar.

Figures following Table 14, in accordance with the sequence applied in Table 13, Table 14, systematically demonstrate the failure characteristics of each pipeline section (Y1-Y12), camera images captured at or very near the moment of failure, and the locations of damage followed by the damage section and the outer diameter of the pipelines after the burst test (Figure 82- Figure ). Images cut from the video recording show clearly and distinctly in which cases the failure occurred on the pipe body and in which cases it occurred in the tested girth weld.

Table 14 The main characteristics and the burst pressure (BP) and the safety factor (SF) values of the investigations

Pipeline section ID	Notch location	Notch direction	Burst pressure(bar)	Failure location	SF ( - )
<b>Y3</b>	N/A	N/A	446	pipe surface	6.97
<b>Y1</b>	N/A	N/A	447	pipe surface	6.98
<b>Y2</b>	N/A	N/A	447	pipe surface	6.98
<b>Y4</b>	N/A	N/A	473	pipe surface	7.39
<b>Y5</b>	N/A	N/A	446	pipe surface	6.97
<b>Y6</b>	N/A	N/A	462	pipe surface	7.22
<b>Y7</b>	girth weld HAZ	circumferential	457	pipe surface	7.14
<b>Y8</b>	through girth weld	axial	348	axial notch through girth weld	5.44
<b>Y9</b>	girth weld HAZ	circumferential	461	pipe surface	7.20
<b>Y10</b>	girth weld HAZ	circumferential	467	pipe surface	7.30
<b>Y11</b>	through girth weld	axial	152	axial notch through girth weld	2.38
<b>Y12</b>	girth weld HAZ	circumferential	250	circumferential notch	3.91



*Figure 82 Moment of failure of the pipeline section Y3 during the burst test: side view (top), longitudinal view (middle), the Y3 pipeline section after the burst test: the damaged section and the tested girth weld (bottom)*



*Figure 83 Moment of failure of the pipeline section Y1 during the burst test: side view (top), longitudinal view (middle), the Y1 pipeline section after the burst test: the damaged section and the tested girth weld (bottom)*





*Figure 84 Moment of failure of the pipeline section Y2 during the burst test: side view (top), longitudinal view (middle), the pipeline section Y2 after the burst test: the pipeline section with the damaged section (and the damaged coupling fitting highlighted with red circle) partially ejected from the test pit (bottom)*



*Figure 85 Moment of failure of the pipeline section Y4 during the burst test: side view (top), longitudinal view (middle), the pipeline section Y4 after the burst test: the damaged section (bottom)*





*Figure 86 Moment of failure of the pipeline section Y5 during the burst test: side view (top), longitudinal view (bottom)*



*Figure 87 Pipeline section Y5 after the burst test: pipe section displaced on the support beam in the test pit (top), damaged section (second), moment of failure of the pipeline section Y6 during the burst test: side view (third), longitudinal view (bottom)*



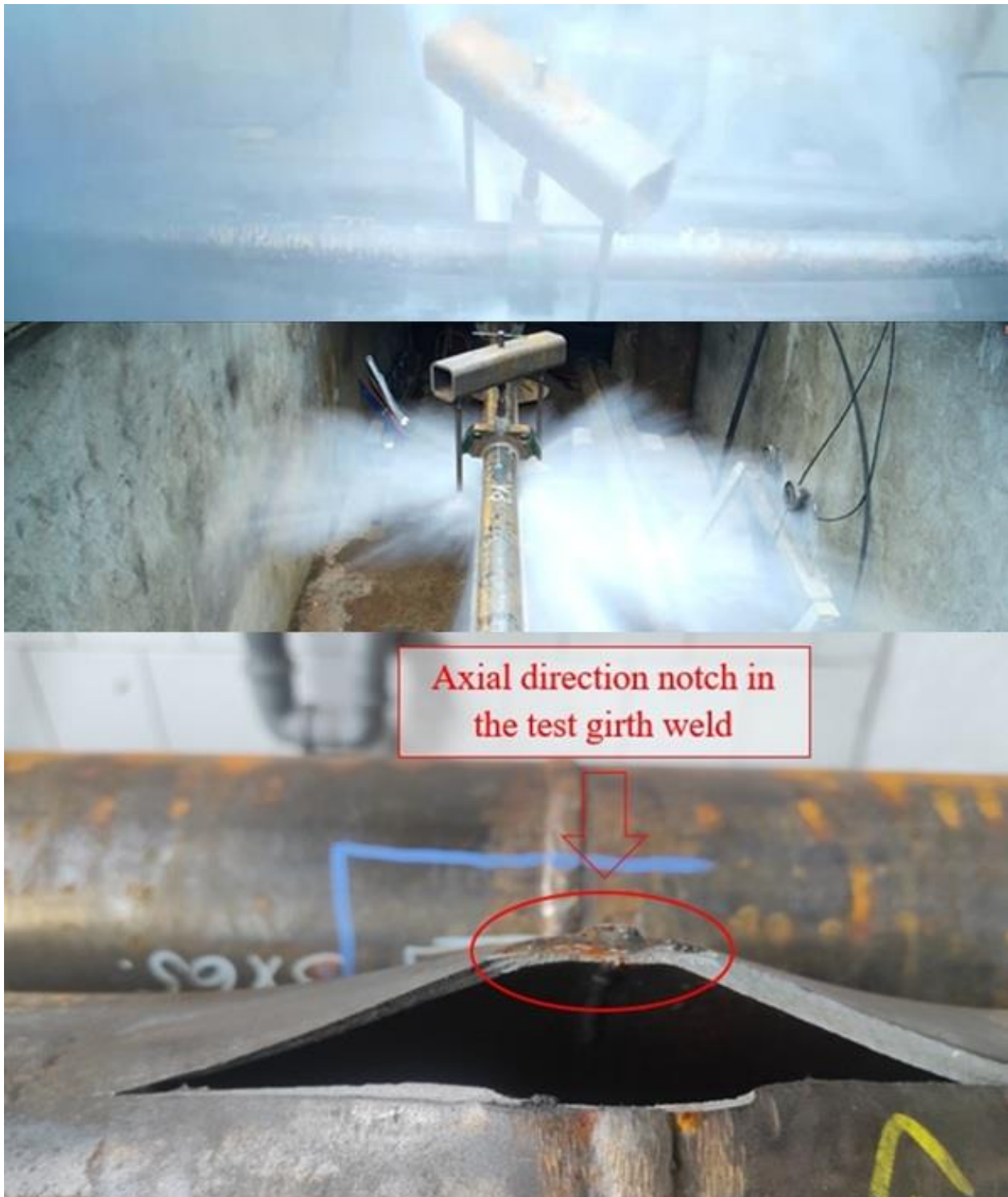


*Figure 88 Pipeline section Y6 after burst test: section of pipe (with the burst support beam and the damaged external load transfer device) in the test pit (top), damaged section (bottom)*

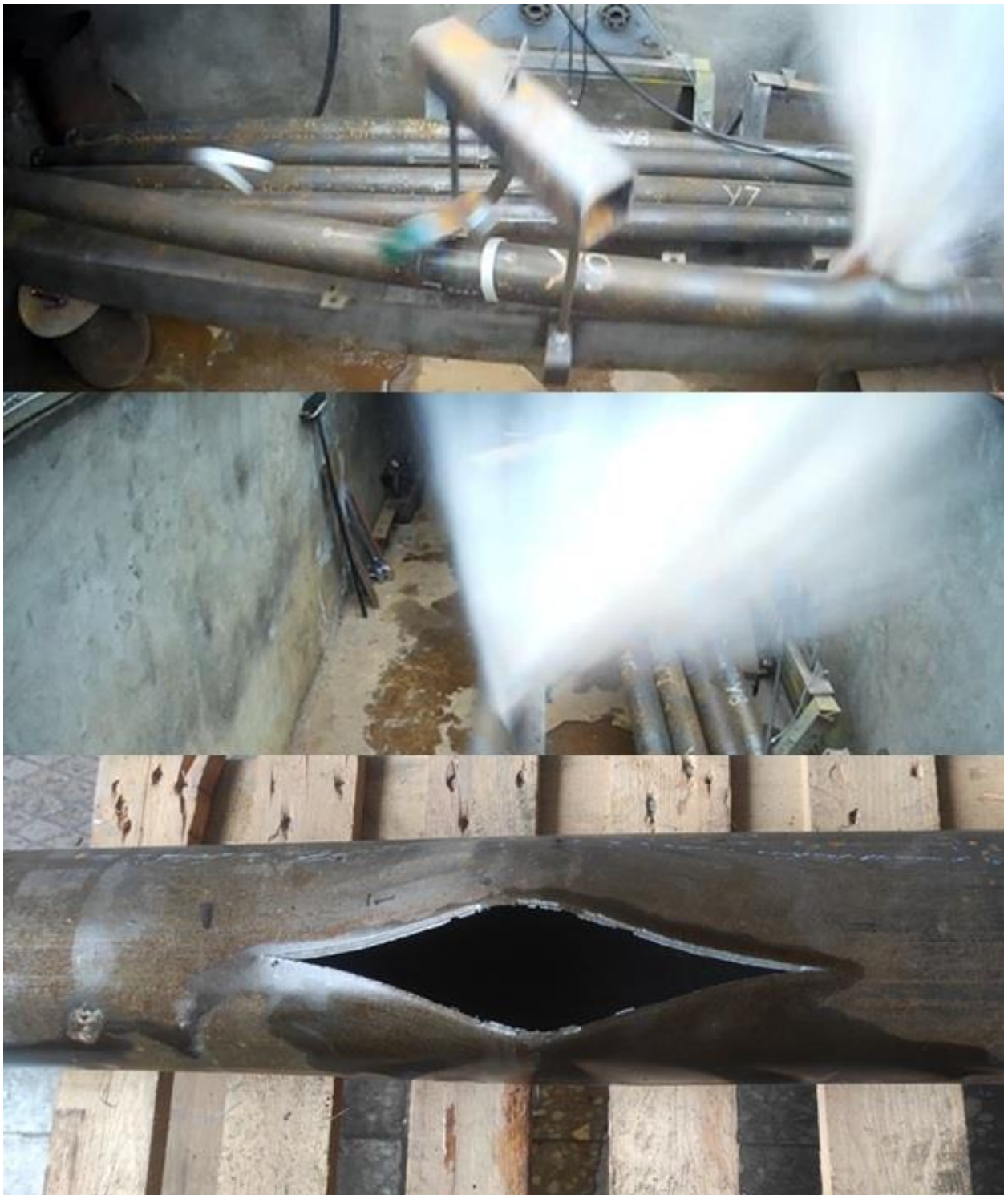


Figure 89 Moment of failure of the pipeline section Y7 during the burst test: side view (top), longitudinal view (second), the pipeline section Y7 after failure: the pipeline section displaced on the supporting beam (and the damaged external load transfer structure) in the test pit (third), the damaged section (bottom)





*Figure 90 Moment of failure of the pipeline section Y8 during the burst test: side view (top), longitudinal view (middle), the pipeline section Y8 after failure: the damaged area with axial notch perpendicular to the girth weld (bottom)*



*Figure 91 Moment of failure of the pipeline section Y9 during the burst test: side view (top), longitudinal view (middle), the pipeline section Y9 after the burst test: the damaged section (bottom)*





*Figure 92 Moment of failure of the pipeline section Y10 during the burst test: side view (top), longitudinal view (middle), the pipeline section Y10 after the burst test: the damaged section (bottom)*



Figure 93 Moment of failure of the Y11 pipeline section during the burst test: side camera image (top), longitudinal camera image (middle), the pipeline section Y11 after the burst test: the damaged section (bottom)





*Figure 94 Moment of failure of the Y12 pipeline section during the burst test: side camera image (top), longitudinal camera image (middle), tested pipe section Y12 after the burst test: the damaged section (bottom)*

Figure 92 shows the characteristic shape of the damaged area of Y1-Y10 pipeline sections; furthermore Table 14 summarizes the measured geometrical data on these areas.

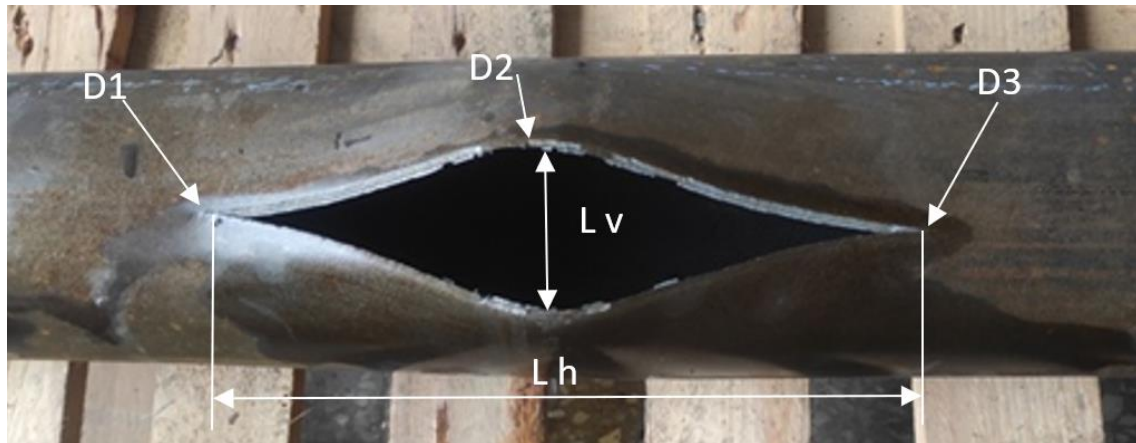


Figure 95 The damage section

Table 15 The damage section measurements

Pipeline ID	Lv (mm)	Lh (mm)	D1 (mm)	D2 (mm)	D3 (mm)
Y1	56	261	126	129	127
Y2	41	234	125	127	124
Y3	64.5	243	124	131	124
Y4	50	240	124	129.5	122
Y5	60	245	123	133	125
Y6	70	255	123	145	122
Y7	61	234	118	151	121
Y8	39	174	115	137	116
Y9	55	254	118	144	117
Y10	61	269	121	151	121

Based on the results of the burst test, it was found that:

- The failure of the investigated pipeline sections without artificial notches (Y1-Y6 pipeline sections) occurred similarly to Figure 82- Figure 88, but in none of the cases in a girth weld, and the burst pressures were significantly higher than the operating pressure.
- The failure of the investigated (in the girth weld HAZ) circumferentially notched pipeline sections Y7 (Figure 89), Y9 (Figure 91), Y10 (Figure 92) and Y12 (Figure 94) pipeline sections with one exception (Y12) occurred similarly too, in all cases in the pipe body, regardless of the notch depth and the magnitude of additional stress from bending load. The failure of the exceptional pipeline section (Y12) occurred in the notch at a significantly lower pressure than in other circumferentially notched cases. Furthermore, the burst pressures were significantly higher than the operating pressure.
- Failure of the pipeline sections containing axial notch Y8 (Figure 90) and Y11 (Figure 93) pipeline sections occurred in the notch and at significantly lower pressure than the other notch-free and notched pipeline sections.
- The failure sections of all the pipelines except Y11, Y12 are measured, in addition to the outer diameter of the pipeline in the middle and at the sides of the failure section, after the failure measurements described in Figure 95 and Table 15. Based on those results, we can notice that the failure for all the samples started at one point, which D2 was measured, then extended in both directions, and at the end of the failure section, D1 and D3 were measured.

## 10.THESES

T1. The damage cause distributions of domestic (Hungarian) hydrocarbon transmission pipelines differ from those of foreign pipelines; the differences can be originated in a higher ratio of damage on the girth welds of the domestic system. The statement has been proved by an analysis and a comparison of domestic and international damage statistics. (1) (2) (8) (11)

T2. The own designed and implemented device for transmitting bending load, in cooperation with and forming an integrated system with the pressure intensification unit, is suitable for reliable testing of full-scale pipeline sections without and with girth welds subjected to cyclic internal pressure and superposed external bending. The statement has been confirmed by the investigations carried out and their results. However, the outside diameter of the investigated pipeline sections depends on the structural element (device) designed to transmission the bending load, therefore limited. (1) (3) (5) (15)

T3. The material discontinuities of the girth welds loaded with a number of internal pressure cycles (60% MAOP - 100% MAOP) in the range of high cycle fatigue did not increase under cyclic loading, and new material discontinuities did not develop; furthermore, this was not affected by the superposition of external loads on the cyclic loading. This statement has been confirmed by the results of radiographic examinations carried out before and after the fatigue tests. (1) (2) (3) (4)

T4. In the case of external loads being superposed on cyclic loads, as complex loads, the damage to the girth welds is primarily influenced and determined by the external load and its magnitude. This statement has been verified by the fact that no failure occurred in the girth welds either under fatigue loading or during the pressure test following fatigue loading. (2) (3)

T5. The load bearing capacity and safety of complex loaded girth welds with artificial defects (notches) is determined by the interaction of location, length and depth of the artificial notches. This statement has been confirmed by the results of tests carried out on pipeline sections containing artificial notches. (3) (6) (7)

T6. Girth welds have a (residual) load-bearing capacity, in other words an operating reserve, even in cases where they contain defects not permitted by the specifications. This statement has been confirmed by the results of tests, where, despite the presence of artificial defects not allowed, the failure did not occur in the girth welds but in the pipe body. The statement is valid up to the limit of the investigated defects. (6) (7) (12)

## 11.SUMMARY AND FURTHER PLANS

This study focused on developing the structural integrity of pipelines through a series of full-scale tests, based on the results of the previous research that helped us understand pipeline behavior under operational and extreme conditions. Collaborating with an industrial partner, on service pipeline samples were acquired to perform the research. A special fixing device was designed and built to hold the samples during testing, to make sure of consistent and reliable results. Starting with radiographic testing (RT) to start with a baseline assessment of the samples' structural integrity, ensuring no pre-existing defects. The samples were subjected to a six-hour hydrostatic pressure test, simulating the operational pressures. After the test, the radiographic test confirmed no structural changes, indicating robust performance under sustained pressure. Following that, a cyclic fatigue test (100,000 cycles) was performed between the 60% and the 100% of the actual working pressure values to simulate long-term operational stress. The radiographic tests again showed no signs of deformation or micro-cracking. The final test part involved burst tests to evaluate failure under varied conditions: Simple burst test: Assessing baseline failure pressure. Burst tests with superimposed loads: Applying external forces to simulate geological or mechanical stresses. Notches during the burst test were performed to be conducted on samples with axial and circumferential notches to study crack propagation under stress concentrations. These burst tests, designed to induce failure, provided critical data on pipeline performance under extreme and defect-prone conditions. While the pressure and fatigue tests demonstrated the samples' resilience, the burst tests revealed failure modes dependent on load type and notch orientation, offering insights for pipeline design and safety protocols.

The own-developed test system is suitable for testing full-scale pipeline sections without and with girth welds subjected to cyclic internal pressure and superimposed external bending. The outside diameter of the pipes to be investigated is limited by the structural element (device) designed to transmit the bending load.

The failure of the tested pipeline sections without artificial notches occurred similarly, but in none of the cases in a girth weld, and the failure pressures (burst pressures) were significantly higher than the operating pressure. The failure of the tested circumferentially notched pipeline sections with one exception (Y12 pipeline section) occurred similarly too, in all cases in the pipe surface, regardless of the notch depth and the magnitude of additional stress from bending. The failure of the exceptional pipeline section (Y12) occurred in the notch at a significantly lower pressure than in other similar cases. Furthermore, the failure pressures (burst pressures) were significantly higher than the operating pressure. Failure of the pipeline sections containing axial notch (Y8 and Y11 pipeline sections) occurred in the notch and at significantly lower pressure than the other unnotched and notched pipeline sections.

Both the performed full-scale tests and the determined safety factor values have confirmed the high load-bearing capacity of the girth welds produced to the required quality. The high load-bearing capacity covers both cyclic and complex loads. This also implies that previous damages in the Hungarian gas transporting system have occurred in girth welds of unacceptable quality and/or subjected to significantly higher overloads.



The investigations and their results have demonstrated the importance of the full-scale tests. Moreover, these investigations have confirmed that further full-scale tests should be executed in the near future.

- Pipeline sections containing girth weld should be investigated applying higher axial stresses from the superimposed external bending (e.g. eight times of the axial stress from the maximum internal pressure).
- Similarly necessary to test pipeline sections that contain deeper and/or longer artificial notches on the tensile bending stress side of the girth welds.
- The effect of the temperature, basically the lower temperatures, should also be investigated. The operating pipelines have below-ground sections, where the temperature at the laying depth is 8 °C under the climatic conditions in Hungary.
- In many countries, including Hungary, there are plans to blend hydrogen into the natural gas transmission system[104]. Therefore, the tests should be extended to cover the testing of girth welds exposed to hydrogen.
- The future planned studies and investigations should be carried out by varying the parameters separately in the short term, and jointly in the medium and long term.

## 12.APPLICATION POSSIBILITIES OF THE RESULTS

Based on the experiences acquired from the use of the developed testing system, as well as the tests performed and their results, the potential applications of the research work are as follows.

- The developed testing system is suitable for full-scale testing of cylindrical structural elements (industrial and transporting pipelines, pressure vessels) subjected to complex loading (static or cyclic internal pressure and external bending). During the investigations, geometric constraints of the system must be taken into account.
- The developed testing system enables and offers possibilities for further development and may serve as a basis for the construction of similar systems. Several directions for further development can be projected: the application of non-ambient temperatures, the use of external media different from the environment and internal media different from water, and the application of tensile and/or torsional static preloading.
- The existing results and the results of further similar tests allow operators to establish rankings. On the one hand, allowable discontinuities can be ranked, and on the other hand, potential loads can also be ranked in terms of both hazard and acceptability. These rankings may influence the design and implementation of welding technologies, as well as the planning and execution of non-destructive testing of welded joints. There is no realistic prospect that the extent of testing for girth welds could be reduced below 100%, but a differentiated and optimized application of testing techniques seems achievable.
- The results can provide a basis for a deeper and/or more complex assessment of the integrity of girth welds by evaluating the influencing effects of welding discontinuities and artificial flaws. This may lead to the revision of currently valid prescriptions and the modification of the limit values of the criteria contained therein. The modification of limit values is conceivable in both directions: both tightening and relaxation are possible.
- The experiences acquired from the examination of girth welds may contribute to the modification of intervention strategies, and thereby help in the prevention and reduction of failures.
- The experiences acquired from the examination of girth welds may also support the assessment of the integrity of seam and spiral welds.

## ACKNOWLEDGEMENTS

First and foremost, I would like to express my deepest gratitude to my family (my parents, my brothers and my sister) for their unwavering love, support, and encouragement throughout this long journey. You have been my foundation, and your belief in me has carried me through the toughest moments.

To Flóra, words fall short in expressing how much your presence has meant to me. Your patience, understanding, and endless encouragement have been my anchor through the highs and lows of this PhD. Thank you for standing by my side, believing in me even when I doubted myself, and for being my constant source of strength and motivation. This accomplishment is as much yours as it is mine.

I am also grateful to my second family here in Hungary and to my friends, who have provided warmth, companionship, and a sense of belonging far from home. Your support made this experience richer and more memorable.

I would like to express my sincere appreciation to the University of Miskolc for providing the academic environment and resources necessary for this research. I am also truly thankful for the financial support I received through the scholarship program, which made it possible for me to fully dedicate myself to my studies and achieve this degree.

A very special and heartfelt thank you goes to my supervisor, Dr. János Lukács, for his invaluable guidance, support, and mentorship. His insights and encouragement played a crucial role in shaping both my research and my academic growth.

I would also like to extend my sincere thanks to all the members of our department for their dedication and contributions to this journey. In particular, I am deeply grateful to Dr. Imre Török, whose wisdom and experience were a guiding light throughout my work. My appreciation also goes to Dr. Zsolt Lukács, Dr. Marcell Gáspár, Dr. László Kuzsella, and Dr. Pap Judit for their support, thoughtful feedback, and the many stimulating discussions we shared. Lastly, I would like to thank the often-unsung heroes of our institute Géza Csukás, László Szentpéteri, András Bartók, Ágnes Csurilla Balogh, Sándor Kecskés Kristóf and András Petrovics whose daily efforts behind the scenes ensure that everything runs smoothly. Your work makes a world of difference, and I am truly thankful.

## REFERENCES

- [1] European Committee for Standardization, “EN 1594: Gas supply systems – Pipelines for maximum operating pressure over 16 bar – Functional requirements,” 2009.
- [2] S. Igi, R. Muraoka, and K. Masamura, “Safety and integrity assessment technology for linepipe,” pp. 36–42, Jan. 2013.
- [3] American Petroleum Institute, “API Standard 1104: Welding of pipelines and related facilities,” 2021.
- [4] N. Gy. , H. I. , K. F. R. and K. Lné. K. Zs. Lukács J., “Szemelvények a mérnöki szerkezetek integritása témaköréből,” *Miskolci Egyetem, Miskolc. ISBN 978-963-358-000-4*, 2012.
- [5] Z. Koncsik, “Szerkezetintegritási kutatások az Innovatív Anyagtechnológiák Tudományos Műhelyben,” *Multidiszciplináris tudományok*, vol. 11, no. 2, pp. 372–379, 2021, doi: 10.35925/j.multi.2021.2.49.
- [6] Z. Koncsik, “A szerkezetintegritás helye és szerepe az oktatásban és a kutatásban,” *Multidiszciplináris Tudományok*, vol. 9, no. 4, pp. 63–71, May 2020, doi: 10.35925/j.multi.2019.4.5.
- [7] American Petroleum Institute, “API Recommended Practice 1111: Design, construction, operation, and maintenance of offshore hydrocarbon pipelines (Limit State Design),” 2015.
- [8] The American Society of Mechanical Engineers, “ASME B31.8: Gas transmission and distribution piping systems,” 2022.
- [9] The American Society of Mechanical Engineers, “ASME B31.4: Pipeline transportation systems for liquids and slurries,” 2022.
- [10] State Audit Office of Hungary, “SZTFH 26/2022. (I. 31.): SZTFH regulation on safety requirements for hydrocarbon transmission pipelines and on Safety regulations for hydrocarbon transmission pipelines (in Hungarian),” 2022.
- [11] The American Society of Mechanical Engineers, “ASME B31G: Manual for Determining the Remaining Strength of Corroded Pipelines,” 2023.
- [12] H. S. M. T. Gallon N, “EPRG hydrogen pipelines integrity management and repurposing guideline -White paper,” 2023. Accessed: Mar. 31, 2025. [Online]. Available: [https://www.eprg.net/fileadmin/EPRG\\_Dokumente/EPRG\\_Hydrogen\\_Pipelines\\_Integrity\\_Management\\_and\\_Repurposing\\_Guideline.pdf](https://www.eprg.net/fileadmin/EPRG_Dokumente/EPRG_Hydrogen_Pipelines_Integrity_Management_and_Repurposing_Guideline.pdf)
- [13] The American Society of Mechanical Engineers, “ASME B31.12: Hydrogen piping and pipelines,” 2023.
- [14] P. J. Haagenzen, S. J. Maddox, and K. A. Macdonald, “Guidance for Fatigue Design and Assessment of Pipeline Girth Welds,” in *Volume 3: Materials Technology; Ocean Engineering; Polar and Arctic Sciences and Technology; Workshops*, ASMEDC, Jan. 2003, pp. 377–395. doi: 10.1115/OMAE2003-37496.
- [15] Hungarian Energy And Public Utility Regulatory Authority, “Data Of The Hungarian Natural Gas System,” 2023. Accessed: Jun. 10, 2025. [Online]. Available: [https://fgsz.hu/file/documents/2/2904/mekh\\_statistikai\\_kiadvany\\_foldgaz\\_2023.pdf](https://fgsz.hu/file/documents/2/2904/mekh_statistikai_kiadvany_foldgaz_2023.pdf)

- 
- [16] Mol Group, “<https://molgroup.info/hu/uzleteink/downstream/logisztika>.” Accessed: Mar. 31, 2025. [Online]. Available: <https://molgroup.info/hu/uzleteink/downstream/logisztika>
- [17] L. H. Yan–hua Feng; Qiang Chi; Fan Fei; Xiong-xiong Gao; Wei-wei Li; Xiaofeng Xu; Hong-yuan Chen; Hua Zhang, “Experimental Research on Fatigue Properties of X80 Pipeline Steel for Synthetic Natural Gas Transmission,” *Math Probl Eng*, vol. 2021, no. NA, pp. 1–9, 2021, doi: 10.1155/2021/6631031.
- [18] F. ; S. Oikonomidis Anton; Truman Christopher E, “Prediction of crack propagation and arrest in X100 natural gas transmission pipelines with a strain rate dependent damage model (SRDD). Part 2: Large scale pipe models with gas depressurisation,” *International Journal of Pressure Vessels and Piping*, vol. 122, no. 1, pp. 15–21, 2014, doi: 10.1016/j.ijpvp.2014.07.001.
- [19] P. T. Razi Farid, “A vibration-based strategy for health monitoring of offshore pipelines’ girth-welds,” *Sensors (Basel)*, vol. 14, no. 9, pp. 17174–17191, 2014, doi: 10.3390/s140917174.
- [20] J. A. ; R. Avila Cassius Olívio Figueiredo Terra; Mei Paulo Roberto; Marinho Ricardo Reppold; Paes Marcelo Torres Piza; Ramirez Antonio J., “Fracture toughness assessment at different temperatures and regions within a friction stirred API 5L X80 steel welded plates,” *Eng Fract Mech*, vol. 147, no. NA, pp. 176–186, 2015, doi: 10.1016/j.engfracmech.2015.08.006.
- [21] F. ; S. Oikonomidis Anton; Truman Christopher E, “Prediction of crack propagation and arrest in X100 natural gas transmission pipelines with the strain rate dependent damage model (SRDD). Part 1: A novel specimen for the measurement of high strain rate fracture properties and validation of the SRDD model parameters,” *International Journal of Pressure Vessels and Piping*, vol. 105, no. NA, pp. 60–68, 2013, doi: 10.1016/j.ijpvp.2013.03.003.
- [22] A. R. H. ; S. Midawi C. H. M.; Gerlich Adrian P., “Assessment of yield strength mismatch in X80 pipeline steel welds using instrumented indentation,” *International Journal of Pressure Vessels and Piping*, vol. 168, no. NA, pp. 258–268, 2018, doi: 10.1016/j.ijpvp.2018.09.014.
- [23] American Petroleum Institute, “API SPECIFICATION 5L,” 2012. Accessed: Jun. 10, 2025. [Online]. Available: <https://www.apiwebstore.org/standards/5L?edition=45>
- [24] P. R. Kirkwood, “Welding of HSLA steels—a perspective’,” in *Proc AIME Int Symposium on Welding Metallurgy of Structural Steels, Denver*, 1987, pp. 21–44.
- [25] K. D. Faes Alfred; De Baets Patrick; Afschrift P, “New friction welding process for pipeline girth welds—welding time optimisation,” *The International Journal of Advanced Manufacturing Technology*, vol. 43, no. 9, pp. 982–992, 2008, doi: 10.1007/s00170-008-1775-z.
- [26] G. Nagy, J. Lukács, and I. Török, “Assessment of Methods in Girth Welds of Steel Pipelines,” *Materials Science Forum*, vol. 473–474, pp. 243–248, Jan. 2005, doi: 10.4028/www.scientific.net/MSF.473-474.243.
- [27] L. B. Shron Vladimir; Yagyaev Elmar; Tabolin Illa, “Residual life assessment of welded joints in the girth weld root,” *MATEC Web of Conferences*, vol. 315, no. NA, pp. 12001–NA, 2020, doi: 10.1051/matecconf/202031512001.
- [28] S. T. Xu William R.; Duan D.-M., “ECA of embedded flaws in pipeline girth welds—a review,” *International Journal of Pressure Vessels and Piping*, vol. 172, no. NA, pp. 79–89, 2019, doi: 10.1016/j.ijpvp.2019.03.030.
- [29] M. ; C. Khajedezfouli Naghdali; Torun Ahmet Refah; Yengejeh E. Alipour, “Fracture assessment of pipeline girth weld at low temperature,” *Journal of the Brazilian Society of*

- Mechanical Sciences and Engineering*, vol. 42, no. 12, pp. 1–11, 2020, doi: 10.1007/s40430-020-02696-6.
- [30] H. J. P. Hoh John H. L.; Tsang Kin Shun, “Stress intensity factors for fatigue analysis of weld toe cracks in a girth-welded pipe,” *Int J Fatigue*, vol. 87, no. NA, pp. 279–287, 2016, doi: 10.1016/j.ijfatigue.2016.02.002.
- [31] İ. K. T. Ömürlü Mevlüt; Özdamar Kazım, “Bayesian Analysis of Parametric Survival Models: A Computer Simulation Study based Informative Priors,” *Journal of Statistics and Management Systems*, vol. 18, no. 5, pp. 405–423, 2015, doi: 10.1080/09720510.2014.961763.
- [32] K. Satoh *et al.*, “Japanese studies on structural restraint severity in relation to weld cracking,” *Weld. World*, vol. 15, pp. 155–189, 1977.
- [33] A. D. Batte, P. J. Boothby, and A. B. Rothwell, “Understanding the weldability of niobium-bearing HSLA steels,” in *Proc. Int. Symp. on ‘Niobium’, Orlando, FL, USA*, 2001, pp. 931–958.
- [34] F. Heisterkamp, K. Hulka, and A. D. Batte, “Heat affected zone properties of thick section microalloyed steels—a perspective,” *The Metallurgy, Welding, and Qualification of Microalloyed(HSLA) Steel Weldments*, pp. 659–681, 1990.
- [35] A. B. Rothwell and D. V Dorling, “The toughness properties of girth welds in modern pipeline steels,” in *Proc Int Conf ‘HSLA steels: Technology and Applications’*, ASM, 1984, pp. 943–955.
- [36] L. J. Cuddy, J. S. Lally, and L. F. Porter, “Improvement of toughness in the HAZ of high-heat-input welds in ship steels,” *HSLA Steels, Technology and Applications*, pp. 697–703, 1983.
- [37] C. Shiga, “Effect of steelmaking, alloying and rolling variables on the HAZ structure and properties in microalloyed plate and line pipe,” in *Proc. Int. Conf. on the Metallurgy, Welding and Qualification of Microalloyed Steel Weldments*, 1990.
- [38] M. Gräf, K. Niederhoff, and R. M. Denys, “Properties of HAZ in two-pass submerged arc welded large-diameter pipe,” *Proc. Pipeline Technology*, vol. 2, 2000.
- [39] A. D. Batte and P. R. Kirkwood, “Developments in the weldability and toughness of steels for offshore structures,” *ASM International*, pp. 175–188, 1988.
- [40] S. Aihara and K. Okamoto, “Influence of local brittle zone on HAZ toughness of TMCP steels,” *The Metallurgy, Welding, and Qualification of Microalloyed(HSLA) Steel Weldments*, pp. 402–426, 1990.
- [41] P. Hopkins, “Transmission pipelines: how to improve their integrity and prevent failures,” in *Proceedings of the 2nd International Pipeline Technology Conference, Ostend, Belgium*, 1995, pp. 11–14.
- [42] W. Y. Zheng, “Stress corrosion cracking of oil and gas pipelines in near neutral pH environment: Review of recent research,” *Energy Materials*, vol. 3, no. 4, pp. 220–226, 2008.
- [43] C. R. F. Azevedo, “Failure analysis of a crude oil pipeline,” *Eng Fail Anal*, vol. 14, no. 6, pp. 978–994, 2007.
- [44] Pacific Gas and Electric Company Natural Gas Transmission Pipeline Rupture and Fire, “Pipeline Accident Report,” San Bruno, California, Sep. 2010. Accessed: Jun. 10, 2025. [Online]. Available: <https://www.nts.gov/investigations/accidentreports/reports/par1101.pdf>
- [45] Columbia Gas Transmission Corporation Pipeline Rupture, “Pipeline Accident Report,” Sissonville, West Virginia, Dec. 2012. [Online]. Available: [www.ntis.gov](http://www.ntis.gov)



- [46] Natural Gas Pipeline Rupture and Fire Near Carlsbad, "Pipeline Accident Report," New Mexico, Aug. 2000. Accessed: Jun. 10, 2025. [Online]. Available: <https://www.nts.gov/investigations/AccidentReports/Reports/PAR0301.pdf>
- [47] European Gas Pipeline Incident Data Group (EGIG), "GAS PIPELINE INCIDENTS," Mar. 2018. [Online]. Available: <http://www.EGIG.eu>
- [48] M. R. Acton and P. J. Baldwin, "Ignition probability for high pressure gas transmission pipelines," in *International Pipeline Conference*, 2008, pp. 331–339.
- [49] R. J. Eiber and D. J. Jones, *Topical Report on an Analysis of Reportable Incidents for Natural Gas Transmission and Gathering Lines June 1984 Through 1990*. Battelle, 1992.
- [50] P. Chován and J. Lukács, "Csővezetékintegritás-irányítási rendszer – válasz a földgázszállító rendszer üzemeltetésével kapcsolatos kihívásokra," *Scientia et Securitas*, vol. 4, no. 3, pp. 192–202, Jun. 2024, doi: 10.1556/112.2023.00197.
- [51] R. M. Denys, "Girth-weld defect qualification methods need to be rationalized.," *Pipe Line & Gas Industry*, vol. 82, no. 9, pp. 35–39, 1999.
- [52] G. Nagy, J. Lukács, and I. Török, "Assessment of methods in girth welds of steel pipelines," in *Materials Science Forum*, Trans Tech Publ, 2004, pp. 243–248.
- [53] "pipeline-construction-welding-one-of-the-leading-causes-of-pipeline-failure." Accessed: Jun. 08, 2023. [Online]. Available: <https://sites.google.com/site/metroforensics3/pipeline-construction-welding-one-of-the-leading-causes-of-pipeline-failure>
- [54] K. Y. Lee, "Challenges with Field Girth Welding," 2021. Accessed: Mar. 17, 2021. [Online]. Available: <https://primis.phmsa.dot.gov/rd/mtgs/071812/kenlee.pdf>
- [55] J. Sanborn, "Welding –Quality Concerns & In-Service Welding." Accessed: Mar. 10, 2023. [Online]. Available: [https://www.michigan.gov/documents/mpsc/Welding\\_536247\\_7.pdf](https://www.michigan.gov/documents/mpsc/Welding_536247_7.pdf)
- [56] Bruce Bil, "Improving API 1104 for the Twenty-second Edition API-AGA Joint Committee on Oil and Gas Pipeline Field Welding Practices -Secretary," Austin, Texas, Jan. 2017.
- [57] A. Y. Dakhel and J. Lukács, "How to prevent damages of transporting pipeline girth welds?," *Multidiszciplináris tudományok*, vol. 11, no. 4, pp. 208–217, 2021, doi: 10.35925/j.multi.2021.4.25.
- [58] C. Thaulow, E. Østby, B. Nyhus, Z. L. Zhang, and B. Skallerud, "Constraint correction of high strength steel," *Eng Fract Mech*, vol. 71, no. 16–17, pp. 2417–2433, Nov. 2004, doi: 10.1016/j.engfracmech.2004.01.003.
- [59] Q. Feng, R. Li, B. Nie, S. Liu, L. Zhao, and H. Zhang, "Literature Review: Theory and Application of In-Line Inspection Technologies for Oil and Gas Pipeline Girth Weld Defection," *Sensors*, vol. 17, no. 1, p. 50, Dec. 2016, doi: 10.3390/s17010050.
- [60] "corrosion engineering." Accessed: Aug. 10, 2021. [Online]. Available: <https://www.ameoilgas.com/corrosion-engineering>
- [61] R. A. Francis, "Stress Corrosion Cracking And Hydrogen Cracking: Differences Similarities And Confusion," in *Proceedings of ACA Conference*, 2001, pp. 1–8.
- [62] C. M. Soret Yazid; Gaffard Vincent; Besson Jacques, "Local approach to fracture applied to the analysis of a full size test on a pipe containing a girth weld defect," *Eng Fail Anal*, vol. 82, no. NA, pp. 404–419, 2017, doi: 10.1016/j.engfailanal.2017.07.035.
- [63] A. N. Zareei S. M., "Calculation of stress intensity factors for circumferential semi-elliptical cracks with high aspect ratio in pipes," *International Journal of Pressure Vessels and Piping*, vol. 146, no. NA, pp. 32–38, 2016, doi: 10.1016/j.ijpvp.2016.05.008.
- [64] M. Iannuzzi, "Environmentally assisted cracking (EAC) in oil and gas production," in *Stress Corrosion Cracking*, Elsevier, 2011, pp. 570–607. doi: 10.1533/9780857093769.4.570.

- 
- [65] C. A. Chua, D. N. Alleyne, and M. Calva, "Crack growth monitoring using low-frequency guided waves," *Insight - Non-Destructive Testing and Condition Monitoring*, vol. 59, no. 2, pp. 64–71, Feb. 2017, doi: 10.1784/insi.2017.59.2.64.
- [66] J. Lukács, N. Gy, I. Harmati, F. R. Koritárné, and K. LnéKZs, "Selected chapters from structural integrity of engineering structures," *University of Miskolc, Miskolc (In Hungarian)*, 2012.
- [67] F. Rofooei, H. Hojat Jalali, N. Attari, and M. Alavi, *Full-Scale Laboratory Testing of Buried Pipelines Subjected to Permanent Ground Displacement Caused by Reverse Faulting*. 2012.
- [68] T. S. Weeks, J. D. McColskey, M. D. Richards, Y.-Y. Wang, and M. Quintana, "Curved-Wide Plate Testing of X100 Girth Welds," in *Volume 4: Production Pipelines and Flowlines; Project Management; Facilities Integrity Management; Operations and Maintenance; Pipelining in Northern and Offshore Environments; Strain-Based Design; Standards and Regulations*, American Society of Mechanical Engineers, Sep. 2014. doi: 10.1115/IPC2014-33690.
- [69] D. P. Fairchild, J. M. Crapps, W. Cheng, H. Tang, and S. Shafrova, "Full-Scale Pipe Strain Test Quality and Safety Factor Determination for Strain-Based Engineering Critical Assessment," in *Volume 2: Pipeline Safety Management Systems; Project Management, Design, Construction and Environmental Issues; Strain Based Design; Risk and Reliability; Northern Offshore and Production Pipelines*, American Society of Mechanical Engineers, Sep. 2016. doi: 10.1115/IPC2016-64191.
- [70] D. P. Fairchild, S. Shafrova, H. Tang, J. M. Crapps, and W. Cheng, "Full-Scale Testing for Strain-Based Design Pipelines: Lessons Learned and Recommendations," in *Volume 4: Production Pipelines and Flowlines; Project Management; Facilities Integrity Management; Operations and Maintenance; Pipelining in Northern and Offshore Environments; Strain-Based Design; Standards and Regulations*, American Society of Mechanical Engineers, Sep. 2014. doi: 10.1115/IPC2014-33748.
- [71] G. Demofonti, G. Mannucci, H. G. Hillenbrand, and D. Harris, "Evaluation of the Suitability of X100 Steel Pipes for High Pressure Gas Transportation Pipelines by Full Scale Tests," in *2004 International Pipeline Conference, Volumes 1, 2, and 3*, ASMECD, Jan. 2004, pp. 1685–1692. doi: 10.1115/IPC2004-0145.
- [72] Z. Li, B. Gong, G. Lacidogna, C. Deng, and D. Wang, "Strain-based fracture response of X80 steel pipe welded girth based on constraint-modified J-R curves: from SENT specimen to full-scale pipe," *Eng Fract Mech*, vol. 258, p. 108114, Dec. 2021, doi: 10.1016/j.engfracmech.2021.108114.
- [73] Y.-H. Zhang and S. J. Maddox, "Fatigue Testing of Full Scale Girth Welded Pipes Under Variable Amplitude Loading," *Journal of Offshore Mechanics and Arctic Engineering*, vol. 136, no. 2, May 2014, doi: 10.1115/1.4026025.
- [74] Y. Yang *et al.*, "Full-scale experimental investigation of the fracture behaviours of welding joints of APL X80 wide plate based on DIC technology," *Eng Fail Anal*, vol. 131, p. 105832, Jan. 2022, doi: 10.1016/j.engfailanal.2021.105832.
- [75] N. Elyasi *et al.*, "Prediction of Tensile Strain Capacity for X52 Steel Pipeline Materials Using the Extended Finite Element Method," *Applied Mechanics*, vol. 2, no. 2, pp. 209–225, Apr. 2021, doi: 10.3390/applmech2020013.
- [76] Z. Wei, H. Jin, X. Pei, and L. Wang, "A simplified approach to estimate the fatigue life of full-scale welded cast steel thin-walled tubular structures," *Thin-Walled Structures*, vol. 160, p. 107348, Mar. 2021, doi: 10.1016/j.tws.2020.107348.

- 
- [77] W. B. Xuan *et al.*, “Research on Full-Scale Hydrostatic Burst Testing of Different Pipeline Girth Weld Defects,” *Applied Mechanics and Materials*, vol. 853, pp. 351–355, Sep. 2016, doi: 10.4028/www.scientific.net/AMM.853.351.
- [78] S. Igi, R. Muraoka, and K. Masamura, “Safety and Integrity Assessment Technology for Linepipe,” *JFE*. Retrieved October, vol. 15, no. 2022, pp. 16–18, 2013.
- [79] Stress Engineering Services, “Full-scale testing and in-situ monitoring of pipelines.” Accessed: Sep. 26, 2023. [Online]. Available: <https://www.stress.com/capabilities/pipelines/full-scale-testing-pipelines/>
- [80] B. Bolton, V. Semiga, S. Tikku, A. Dinovitzer, and J. Zhou, “Full Scale Cyclic Fatigue Testing of Dented Pipelines and Development of a Validated Dented Pipe Finite Element Model,” in *2010 8th International Pipeline Conference, Volume 1*, ASMEDE, Jan. 2010, pp. 863–872. doi: 10.1115/IPC2010-31579.
- [81] M. D. Chapetti, J. L. Otegui, C. Manfredi, and C. F. Martins, “Full scale experimental analysis of stress states in sleeve repairs of gas pipelines,” *International Journal of Pressure Vessels and Piping*, vol. 78, no. 5, pp. 379–387, May 2001, doi: 10.1016/S0308-0161(00)00063-6.
- [82] A. Bastola, J. Wang, H. Shitamoto, A. Mirzaee-Sisan, M. Hamada, and N. Hisamune, “Full- and small-scale tests on strain capacity of X80 seamless pipes,” *Procedia Structural Integrity*, vol. 2, pp. 1894–1903, 2016, doi: 10.1016/j.prostr.2016.06.238.
- [83] P. P. Darcis, I. Marines-Garcia, E. A. Ruiz, E. C. Marques, M. Armengol, and H. M. Quintanilla, “Full Scale Fatigue Performance of Pre-Strained SCR Girth Welds: Comparison of Different Reeling Frames,” in *29th International Conference on Ocean, Offshore and Arctic Engineering: Volume 5, Parts A and B*, ASMEDE, Jan. 2010, pp. 1039–1049. doi: 10.1115/OMAE2010-21025.
- [84] L. Di Vito *et al.*, “Ultra Heavy Wall Linepipe X65: Full Scale Severe Straining Sequences of Pipeline Strings,” in *Volume 3: Pipeline and Riser Technology*, American Society of Mechanical Engineers, Jul. 2012, pp. 695–705. doi: 10.1115/OMAE2012-83835.
- [85] P. P. Darcis *et al.*, “Fatigue Performance of SMLS SCR Girth Welds: Comparison of Prefabrication-Type WPS,” in *Volume 3: Pipeline and Riser Technology*, ASMEDE, Jan. 2009, pp. 683–692. doi: 10.1115/OMAE2009-79811.
- [86] T. Bajcar, F. Cimerman, B. Širok, and M. Ameršek, “Impact assessment of traffic-induced vibration on natural gas transmission pipeline,” *J Loss Prev Process Ind*, vol. 25, no. 6, pp. 1055–1068, Nov. 2012, doi: 10.1016/j.jlp.2012.07.021.
- [87] G. Demofonti, G. Mannucci, C. Spinelly, and L. Barsanti, “Large-diameter X 100 gas line pipes: Fracture propagation evaluation by full-scale burst test,” *Pipeline Technol.*, vol. 1, Jan. 2000.
- [88] S. Hertelé, A. Cosham, and P. Roovers, “Structural integrity of corroded girth welds in vintage steel pipelines,” *Eng Struct*, vol. 124, pp. 429–441, Oct. 2016, doi: 10.1016/j.engstruct.2016.06.045.
- [89] S. Kristoffersen, P. J. Haagenen, and G. Rørvik, “Full Scale Fatigue Testing of Fatigue Enhanced Girth Welds in Clad Pipe for SCRs Installed by Reeling,” in *Volume 5: Materials Technology; CFD and VIV*, ASMEDE, Jan. 2008, pp. 169–177. doi: 10.1115/OMAE2008-57309.
- [90] A. M. Horn, I. Lotsberg, and O. Orjaseater, “The Rationale for Update of S-N Curves for Single Sided Girth Welds for Risers and Pipelines in DNV GL RP C-203 Based on Fatigue Performance of More Than 1700 Full Scale Fatigue Test Results,” in *Volume 4: Materials Technology*, American Society of Mechanical Engineers, Jun. 2018. doi: 10.1115/OMAE2018-78408.

- 
- [91] S. Hertelé, W. De Waele, R. Denys, M. Verstraete, and J. Van Wittenberghe, “Parametric finite element model for large scale tension tests on flawed pipeline girth welds,” *Advances in Engineering Software*, vol. 47, no. 1, pp. 24–34, May 2012, doi: 10.1016/j.advengsoft.2011.12.007.
  - [92] J. Lukács, Zs. Koncsik, and P. Chován, “Integrity reconstruction of damaged transporting pipelines applying fiber reinforced polymer composite wraps,” *Procedia Structural Integrity*, vol. 31, pp. 51–57, 2021, doi: 10.1016/j.prostr.2021.03.009.
  - [93] Z. Q. Lei, J. Chen, F. X. Wang, W. B. Xuan, T. Wang, and H. Yang, “Full-scale Burst Test and Finite Element Simulation of 32 Inch Oil Pipe with Girth Weld Defects,” *Procedia Eng*, vol. 130, pp. 911–917, 2015, doi: 10.1016/j.proeng.2015.12.240.
  - [94] S. J. Maddox, J. B. Speck, and G. R. Razmjoo, “An Investigation of the Fatigue Performance of Riser Girth Welds,” *Journal of Offshore Mechanics and Arctic Engineering*, vol. 130, no. 1, Feb. 2008, doi: 10.1115/1.2827956.
  - [95] S. J. Maddox and Y.-H. Zhang, “Comparison of Fatigue of Girth-Welds in Full-Scale Pipes and Small-Scale Strip Specimens,” in *Volume 5: Materials Technology; CFD and VIV*, ASMEDC, Jan. 2008, pp. 75–85. doi: 10.1115/OMAE2008-57103.
  - [96] H. Mahdavi, S. Kenny, R. Phillips, and R. Popescu, “Significance of geotechnical loads on local buckling response of buried pipelines with respect to conventional practice,” *Canadian Geotechnical Journal*, vol. 50, no. 1, pp. 68–80, Jan. 2013, doi: 10.1139/cgj-2011-0423.
  - [97] T. NETTO, A. BOTTO, and M. LOURENCO, “Fatigue performance of pre-strained pipes with girth weld defects: Local deformation mechanisms under bending,” *Int J Fatigue*, vol. 30, no. 6, pp. 1080–1091, Jun. 2008, doi: 10.1016/j.ijfatigue.2007.08.001.
  - [98] H. S. da Costa Mattos, J. M. L. Reis, L. M. Paim, M. L. da Silva, R. Lopes Junior, and V. A. Perrut, “Failure analysis of corroded pipelines reinforced with composite repair systems,” *Eng Fail Anal*, vol. 59, pp. 223–236, Jan. 2016, doi: 10.1016/j.engfailanal.2015.10.007.
  - [99] O. O’rjasaeter, O. J. Hauge, G. Ba’rs, and P. E. Kvaale, “Crack Growth During Full Scale Reeling Simulation of Pipes With Girth Welds,” in *23rd International Conference on Offshore Mechanics and Arctic Engineering, Volume 3*, ASMEDC, Jan. 2004, pp. 193–199. doi: 10.1115/OMAE2004-51365.
  - [100] K. C. Meiwes, S. Höhler, M. Erdelen-Peppler, and H. Brauer, “Full-Scale Reeling Tests of HFI Welded Line Pipe for Offshore Reel-Laying Installation,” in *Volume 4: Production Pipelines and Flowlines; Project Management; Facilities Integrity Management; Operations and Maintenance; Pipelining in Northern and Offshore Environments; Strain-Based Design; Standards and Regulations*, American Society of Mechanical Engineers, Sep. 2014. doi: 10.1115/IPC2014-33163.
  - [101] O. L. O’rjasaeter, H. O. Knagenhjelm, and P. J. Haagenzen, “Scale Effects: Correlation of Fatigue Capacity for Full-Scale Pipes and Samll-Scale Specimens,” in *Volume 5: Materials Technology; CFD and VIV*, ASMEDC, Jan. 2008, pp. 485–496. doi: 10.1115/OMAE2008-57997.
  - [102] “Catastrophic failure during Hydro testing. ” Accessed: Jun. 10, 2025. [Online]. Available: <http://www.wermac.org/misc/pressuretestingfailure4.html>
  - [103] S. H. J. van Es, A. M. Gresnigt, D. Vasilikis, and S. A. Karamanos, “Ultimate bending capacity of spiral-welded steel tubes – Part I: Experiments,” *Thin-Walled Structures*, vol. 102, pp. 286–304, May 2016, doi: 10.1016/j.tws.2015.11.024.
  - [104] Government of Hungary, “Hungary’s National Hydrogen Strategy – Strategy for the introduction of clean hydrogen and hydrogen technologies to the domestic market and for establishing background infrastructure for the hydrogen industry. [Online].,” 2021.

- Accessed: Jun. 10, 2025. [Online]. Available:  
<https://kormany.hu/dokumentumtar/magyarország-nemzeti-hidrogenstrategiaja>
- [105] FGSZ Ltd., “Kolumbán, K.: Welding procedure specification – HTKeletMFR-1/2022 – K+F SIMPLE 5.3 Testing girth welds subjected to excess stress. (In Hungarian)),” 2022.
- [106] Zebisch H-J, *Szilárdságtan röviden és tömören – A statikus igénybevételű szerkezeti elemek szilárdságtana*. Budapest: Műszaki Könyvkiadó, 1979.
- [107] International Organization for Standardization, “ISO 6520-1:2007.”
- [108] A. F. Hobbacher, “Erratum to: Recommendations for Fatigue Design of Welded Joints and Components,” 2017, pp. E1–E1. doi: 10.1007/978-3-319-23757-2\_7.
- [109] K. A. ; M. Macdonald S.J., “New guidance for fatigue design of pipeline girth welds,” *Eng Fail Anal*, vol. 10, no. 2, pp. 177–197, 2003, doi: 10.1016/s1350-6307(02)00051-1.

## LIST OF PUBLICATIONS RELATED TO THE TOPIC OF THE RESEARCH FIELD

### In English:

- (1) J. Lukács and A. Y. Dakhel, "Full-scale Fatigue and Burst Tests on Notched Pipeline Girth Welds, under Complex Loading Conditions," *Acta Polytechnica Hungarica*, vol. 21, no. 5. Obuda University, pp. 53–70, 2024. doi: 10.12700/aph.21.5.2024.5.5.
- (2) Dakhel Ahmad Yasser, Gáti József, Koncsik Zsuzsanna, Lukács János, "Fatigue and burst tests of pipeline girth welds under simple and complex loading conditions", 77th IIW Annual Assembly and International Conference on Welding and Joining IIW (2024) pp. 1-21. Paper: XI-1140-2024 , 21 p.
- (3) A. Y. Dakhel, M. Gáspár, Zs. Koncsik, and J. Lukács, "Fatigue and burst tests of full-scale girth welded pipeline sections for safe operations," *Welding in the World*, vol. 67, no. 5. Springer Science and Business Media LLC, pp. 1193–1208, Feb. 25, 2023. doi: 10.1007/s40194-023-01501-x.
- (4) A. Y. Dakhel and J. Lukács, "Full-Scale Tests of Pipeline Girth Welds Under Complex Cyclic Internal Pressure and Static Bending Loading Conditions," *International Journal of Engineering and Management Sciences*, vol. 8, no. 1. University of Debrecen/ Debreceni Egyetem, pp. 76–82, Apr. 30, 2023. doi: 10.21791/ijems.2023.1.10.
- (5) A. Y. Dakhel and J. Lukács, "Full-scale tests of transporting pipeline sections : A review and consequences to our investigations," *Design of Machines and Structures*, vol. 13, no. 1. Design of Machines and Structures, pp. 24–44, Jun. 15, 2023. doi:10.32972/dms.2023.003.
- (6) Ahmad Yasser Dakhel, János Lukács, "Full Scale Tests on Pipeline Sections with Girth Welds under Complex Loading Conditions", Koncsik, Zsuzsanna; Lukács, János (eds.) *Kutatási eredmények a Miskolci Egyetem Gépészmérnöki és Informatikai Karának Anyagszerkezet-tani és Anyagtechnológiai Intézetében Miskolc, Hungary : Miskolci Egyetem, Gépészmérnöki és Informatikai Kar, Anyagszerkezet-tani és Anyagtechnológiai Intézet (2023) 214 p. pp. 169-184. , 16 p.*
- (7) A. Y. Dakhel, M. Gáspár, Zs. Koncsik, J. Lukács *Fatigue, Burst Tests Among Best Ways Assess Pipeline Welds PIPELINE & GAS JOURNAL 250 : 8 pp. 1-17. , 17 p. (2023)*
- (8) Dakhel Ahmad Yasser, Lukács János, "Failure statistics of transporting pipelines and their consequences", Vadászné Bognár, Gabriella; Piller, Imre (eds.) *Doktoranduszok fóruma: Miskolc, 2020. november 19-20. : Gépészmérnöki- és Informatikai Kar szekciókiadványa Miskolc, Hungary : University of Miskolc (2022) 108 p. pp. 23-28. , 6 p.*
- (9) DAKHEL Ahmad Yasser, LUKÁCS János, "Full-Scale Tests of Pipeline Girth Welds Under Complex Cyclic Internal Pressure and Static Bending Loading Conditions", Homolya, Márton; Mankovits, Tamás (eds.) *8th International Scientific Conference on Advances in Mechanical Engineering (ISCAME 2022) : Conference proceedings (Book of Extended Abstracts) Debrecen, Hungary : DE Műszaki Kar, Gépészmérnöki Tanszék (2022) 114 p. pp. 29-30. , 2 p. Scientific*


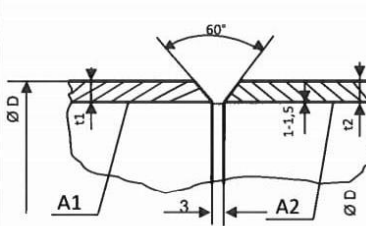
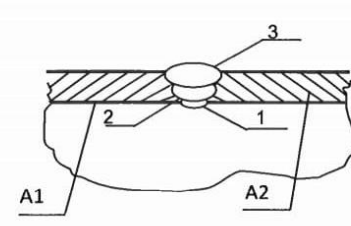



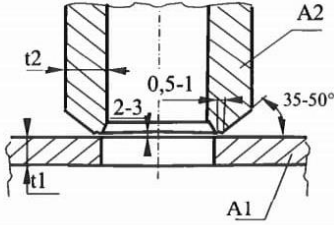
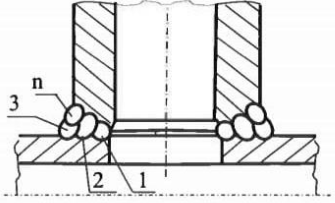
- (10) Dakhel Ahmad Yasser, Gáspár Marcell, Koncsik Zsuzsanna, Lukács János,” Safety of pipeline girth welds based on fatigue and burst tests of full-scale pipeline sections” 75th International Institute of Welding (IIW) Online & Offline Annual Assembly (2022) Paper: IIW DOC XI-1116-2022 , 17 p.
- (11) Dakhel Ahmad Yasser, Lukács János, “Szállító csővezetékek tönkremeneteli módjai és annak következményei - Failure Statistics of Transporting Pipelines and their Consequences” GÉP 72 : 1-2 pp. 15-18. , 4 p. (2021)
- (12) A. Y. Dakhel and J. Lukács, “How to prevent damages of transporting pipeline girth welds?,” Multidiszciplináris tudományok, vol. 11, no. 4. Multidiszciplináris tudományok, pp. 208–217, 2021. doi: 10.35925/j.multi.2021.4.25.

**In Hungarian:**




- (13) Lukács János, Ahmad Yasser Dakhel, “Kísérleti csőszakaszok körvarratainak vizsgálata ciklikus belső nyomás és statikus külső hajlítás együttese esetén”, Koncsik, Zsuzsanna; Lukács, János (eds.) Kutatási eredmények a Miskolci Egyetem Gépészmérnöki és Informatikai Karának Anyagszerkezet-tani és Anyagtechnológiai Intézetében, 2022 Miskolc, Hungary : Miskolci Egyetem, Gépészmérnöki és Informatikai Kar, Anyagszerkezet-tani és Anyagtechnológiai Intézet (2022) 250 p. pp. 157-166. , 10 p.
- (14) J. Kovács, A. Y. Dakhel, and J. Lukács, “A diffúziós hidrogéntartalom hegesztett kötésekre gyakorolt hatása,” Multidiszciplináris tudományok, vol. 11, no. 4. Multidiszciplináris tudományok, pp. 227–240, 2021. doi: 10.35925/j.multi.2021.4.27.
- (15) Lukács János, Ahmad Yasser Dakhel, “Hogyan előzhető meg a csőtávvezetékek körvarratainak káresetei?”, XII. Roncsolásmentes Anyagvizsgáló Konferencia és Kiállítás (RAKK) és 10. Anyagvizsgálat a Gyakorlatban (AGY) Konferencia (2021) Paper: D-4

## Appendix 1


		WPS lap		MB 73.2./07-1						
		Tipus hegesztéstechnológiai utasítás		WPS 01 HT KeletMFR-1/2022						
Tárgy: K+F SIMPLE 5.3 Feszültségnek kitett varratok vizsgálata DN100 varratok [111 Cel PH/PJ]				Lapsz.: 1 Rev: 1						
Rajkszám: UG8112.01.24/95 - 01		Élelkészítés:		Varratfelépítés:						
Anyagminőségek										
A1, A2:										
P355NH										
Anyagcsoport: 1.2 (CR ISO 15608)										
Köpeny/cső átmérő:										
A1, A2: D = Ø114,3 mm										
Köpeny/cső falvastagság:										
t1, t2 = 5,0-5,6 mm										
Élelkészítés: forgácsolás, köszörülés										
WPAR: 1417 ÉMI-TÜV 10.052-V123		Hegesztő minősítés: MSZ EN ISO 9606-1 szerinti.								
Hegesztés technika	Lengetve	<input checked="" type="checkbox"/>	Alátét sáv	<input type="checkbox"/> igen <input checked="" type="checkbox"/> nem	Közberső tisztítás	<input checked="" type="checkbox"/> igen <input type="checkbox"/> nem	Egy oldali varrat	<input checked="" type="checkbox"/> igen <input type="checkbox"/> nem	Gyök kimunkálás	<input type="checkbox"/> igen <input checked="" type="checkbox"/> nem
	Húzza	<input type="checkbox"/>								
Varratrétegek száma		1 (gyök)		2		3				
Hegesztési helyzet		PH		PJ		PJ				
Hegesztő eljárás		111		111		111				
Hozaganyag	típusa	E 38 3 C E6010		E 42 3 Mo C 25 E7010-A1						
	megnevezése	Böhler FOX CEL		Böhler FOX CEL Mo						
	mérete	Ø 3,2		Ø 3,2		Ø 3,2				
Áram	erőssége (A)	45-55		55-70		50-65				
	neme	DC		DC		DC				
	polaritása	egyeses (EN)		fordított (EP)		fordított (EP)				
Feszültség (V)		21,8-22,2		22,2-22,8		22-22,6				
Hegesztési sebesség (cm/min)		7-12		15-20		10-15				
Védőgáz:		(l/min)								
Öblítőgáz:		(l/min)								
Wolfram elektróda:		Tip/Ø [mm]								
Elektróda szárítás		nincs		időtartama:		hőmérséklete:				
Előmelegítés:		módja:		Hőmérséklet:		Sorközi hőmérséklet		Megjegyzés:		
Böhler által ajánlott		Pb láng		min. 50 °C		min. 100 ± 30 °C, max. 200 °C		+5°C alatti környezeti hőmérsékletnél, külön előírás hiányában, kötelezően 60-80°C		
Utóhőkezelés		módja:		fűtés		hőntartás		hűtés		
nem szükséges				sebessége:		hőmérséklete:		időtartama:		
Hegesztéskor a heft eltávolítandó! Új sor kezdése előtt a varratágyat tényszerű állapotba fel kell készíteni!		Radiográfiai vizsgálat 100%		MSZ EN 1435 B		IG-RÜ-16 8.2. mell. 3. tábl.				
		Szemrevételezés 100%		MSZ EN ISO 17637		IG-RÜ-16 8.2. mell. 1. tábl.				
		Mágnesezhető poros vizsgálat 100 %								
Készítette:		Kolumbán Krisztián		Ellenőrizte:		Engedélyezte:				
aláírás:		dátum:		aláírás		dátum		aláírás:		dátum:
		2022.03.01								

 <small>A HÍVŐ-ÉRTÉKELŐ TÁRSASÁG</small>		WPS lap		MB 73.2./07-1	
		Tipus hegesztéstechnológiai utasítás		WPS 02 HT KeletMFR-1/2022	
Tárgy: K+F SIMPLE 5.3 Feszültségnek kitett varratok vizsgálata DN15-25 csomk varratok [111 Cel PC]				Lapsz.: 1 Rev: 0	
Rajzsám: UG8112.01.24/95 - 01		Élelkészítés:		Varratfelépítés:	
Anyagminőségek A1: P355NH A2: P355NH					
Anyagcsoport: 1.2 (CR ISO 15608)					
Köpeny/cső átmérő:					
A1= 114,3 mm (alapső)					
A2= Ø34-50 mm					
Köpeny/cső falvastagság:					
t1 =5,6 mm, t2 = 8,5-11 mm					
WPAR: 1417 ÉMI-TÜV 10.052-V123		Hegesztő minősítés: MSZ EN ISO 9606-1 szerinti.			
Hegesztés technika	Lengette (PH) <input type="checkbox"/>	Alátét sáv	Közbenső tisztítás	Egy oldali varrat	Gyök kimunkálás
	Húzza (PC) <input checked="" type="checkbox"/>	igen <input type="checkbox"/> nem <input checked="" type="checkbox"/>	igen <input checked="" type="checkbox"/> nem <input type="checkbox"/>	igen <input checked="" type="checkbox"/> nem <input type="checkbox"/>	igen <input type="checkbox"/> nem <input checked="" type="checkbox"/>
Varratégek száma		1	2	3-n (szükség szerint)	
Hegesztési helyzet		PC	PC	PC	
Hegesztő eljárás		111	111	111	
Hozaganyag	típusa	E 38 3 C E6010	E 42 3 Mo C 25 E7010-A1		
	megnevezése	Böhler FOX CEL	Böhler FOX CEL Mo		
	mérete	Ø 3,2	Ø 3,2	Ø 3,2	
Áram	erőssége (A)	45-55	55-70	50-65	
	neme	DC (=)	DC (=)	DC (=)	
	polaritása	egyenes (EN -)	fordított (EP +)	fordított (EP +)	
Feszültség					
Huzalelőtolás sebessége(m/min)					
Védőgáz:	(l/min)				
Öblítőgáz:	(l/min)				
Wolfram elektróda : Tip/Ø [mm]					
Elektróda szárítás	nincs	időtartama:		hőmérséklete:	
Előmelegítés:	módja:	Hőmérséklet:	Max. közbenső:	Megjegyzés:	
nem szükséges			200 °C	+5°C alatti környezeti hőmérsékletnél, külön előírás hiányában, kötelezően 60-80°C	
Utóhőkezelés	módja:	fűtés sebessége:	hőntartás		hűtés sebessége:
			hőmérséklete:	időtartama:	
Megjegyzés:		Vizsgálati előírások			
Új sor kezdése előtt a varratágyat fémiszta állapotra fel kell köszörűlni! A csomk leélezése az áthatási ív mentén változó, csőtetőnél 50°, cső oldalánál 35°.		Szemrevételezés 100%		MSZ EN ISO 17637	IG-RÜ-16 8.2. mell. 1. tábl.
		Folyadékdiffúziós repedésvizsgálat 100 %		MSZ EN 571-1:2001	MSZ EN ISO 23277 2X átvételi szint.
Készítette:	Kolumbán Krisztián	Ellenőrizte:	Engedélyezte:		
aláírás:	dátum:	aláírás	dátum	aláírás:	dátum:
	2022.03.01				

## Appendix 2

RADIOGRÁFIAI VIZSGÁLATI JEGYZŐKÖNYV / RADIOGRAPHIC TEST REPORT														
HEGESZTETT KÖTÉS FILMES VIZSGÁLATI JEGYZŐKÖNYV / RADIOGRAPHIC EXAMINATION REPORT WITH FILM														
 <b>GAMMA-CONTROLL</b> ANYAGVIZSGÁLÓ ÉS MINŐSÉGELENŐRZŐ KFT. 6750 Algyő, külterület 01884/14. hrsz. Tel/Fax.: +36 62/517-400 / 61344 <a href="http://www.gamma-controll.hu">www.gamma-controll.hu</a> A NAH által NAH-1-1140/2018 számon akkreditált vizsgálólaboratórium.		Munkaszám: Job No.: -	Jegyzőkönyv szám: Report No.: 011/FGSZ/HSZ/22/RT											
		Megrendelő: Client: FGSZ Földgázszállító Zrt.	Rendelési szám: Order No.: 6400088044											
		Vizsgált objektum: Project: DN100-as varratok												
		Vizsgálat tárgya: Object: Hegesztési varratok diagnosztikai vizsgálata												
Vizsgálat helye: Place of test: Hajdúszoboszló		Időpontja: Date: 2022.04.12												
Rajzsám: Drawing No.: -		Anyagminőség: Material: P355NH												
Vizsgálati terjedelem: Extent of testing: 100 %		Hőkezelés: Heat treatment condition: -												
Hegesztési eljárás: Welding process: 111		Varrat alak: Shape of the weld: BW												
<b>Vizsgálati adatok (test data)</b>														
Vizsgálati szabvány: Testing standard: MSZ EN ISO 17636-1:2013 B		Képmínőség osztály: Image quality classes: W14		Sugárforrás típusa: Radiation source type: Ir-192										
Átvételi követelmény: Acceptance criteria: IG-RU-16 8.2. számú melléklet 3. táblázat		Képmínőség jelölés: Type of IQI: MSZ EN ISO 19232-1:2013 10 FE EN FES0		Sugárforrás mérete: Source size: 3x1,75 mm		Aktivitás: Activity: 0,82 TBq								
Rádiográfiai módszer: Radiographic technique: izotóp		Film típusa: Screen type: AGFA D5		Pb: 0,027 mm		Csőfeszültség: Tube Voltage: - kV		Csőáram: Tube current: - mA						
Berendezés azonosítója: Identification of equipment: GAMMATAT		Film kidolgozás: Film processing: kézi: Manual gépi: X		Vizsgáló: Tested by: Komáromi Tamás Kocsis István										
Vizsgálati darab jelölése (System of marking): A "0" point and direction point with marker														
<b>Vizsgálati eredmények (Test results)</b>														
Film jelölés Film marking: Weld-No.:	Méret (mm) Size (mm)	Értékelt filmléhszám Rated film length (cm)	Fekete Densité	Képmínőség IQI	Átugázott felvétel vastagság (mm) Penetrated thickness (mm)	Sugárforrás- film távolság (mm) Source-to-film distance (mm)	Vizsgálati elrendezés: Arrangement ecc. To Fig	Megvilágítási idő (min.) Expos. Time (min.)	Értékelt eltérések Differences	Film mérete Film size	Hegesztési eljárás Welding process	Hegesztési áram Welder amp.	Működési eredmény Result	Megjegyzés Note
F13	Ø 114,3 x 5,5	29-0-6	3,0	15	11	130	14	0,4	3012	X	111	SX65	A	-
F13	Ø 114,3 x 5,5	1-16	3,0	15	11	130	14	0,4	3012	X	111	SX65	A	-
F13	Ø 114,3 x 5,5	10-25	3,0	15	11	130	14	0,4	514	X	111	SX65	A	-
F13	Ø 114,3 x 5,5	20-35	3,0	15	11	130	14	0,4	2011,514	X	111	SX65	A	-
F14	Ø 114,3 x 5,5	30-0-7	2,8	15	11	130	14	0,4	507	X	111	SX65	A	-
F14	Ø 114,3 x 5,5	1-16	2,8	15	11	130	14	0,4	-	X	111	SX65	A	-
F14	Ø 114,3 x 5,5	10-25	2,8	15	11	130	14	0,4	504	X	111	SX65	A	-
F14	Ø 114,3 x 5,5	19-34	2,8	15	11	130	14	0,4	504	X	111	SX65	A	-
F15	Ø 114,3 x 5,5	30-0-9	2,9	15	11	130	14	0,4	-	X	111	SX65	A	-
F15	Ø 114,3 x 5,5	2-16	2,9	15	11	130	14	0,4	-	X	111	SX65	A	-
F15	Ø 114,3 x 5,5	9-24	2,9	15	11	130	14	0,4	-	X	111	SX65	A	-
F15	Ø 114,3 x 5,5	20-34	2,9	15	11	130	14	0,4	-	X	111	SX65	A	-
F16	Ø 114,3 x 5,5	29-0-6	2,9	15	11	130	14	0,4	-	X	111	SX65	A	-
F16	Ø 114,3 x 5,5	4-18	2,9	15	11	130	14	0,4	504	X	111	SX65	A	-
F16	Ø 114,3 x 5,5	10-25	2,9	15	11	130	14	0,4	504	X	111	SX65	A	-
F16	Ø 114,3 x 5,5	20-35	2,9	15	11	130	14	0,4	514	X	111	SX65	A	-
Megjegyzés/Note: --														
Ez a jegyzőkönyv részleteiben nem másolható! / Copying details is prohibited!														
Elfogadta (átvett): Accepted by (AI):		Értékeltél: Evaluated by: Tóth Róbert RT30101090104Ú		Jóváhagyó: Approved by: Tóth Róbert Felelős vezető helyettes										
		Aláírása: Signature: 		Aláírása: Signature: 										
		Kelt: Date: 2022.04.13												
GAMMA-CONTROLL KFT. 6750 Algyő, külterület 01884/14. hrsz. Adószám: 11094614-2-06 <a href="http://www.gamma-controll.hu">www.gamma-controll.hu</a>														



RADIOGRÁFIAI VIZSGÁLATI JEGYZŐKÖNYV / RADIOGRAPHIC TEST REPORT												RT		
HEGESZTETT KÖTÉS FILMES VIZSGÁLATI JEGYZŐKÖNYV / RADIOGRAPHIC EXAMINATION REPORT WITH FILM														
 <b>GAMMA-CONTROLL</b> ANYAGVIZSGÁLÓ ÉS MINŐSÉGELENŐRZŐ KFT. 6750 Algyő, külterület 01884/14. hrsz. Tel/Fax.: +36 62/517-400 / 61344 <a href="http://www.gamma-controll.hu">www.gamma-controll.hu</a> A NAH által NAH-1-1140/2018 számon akkreditált vizsgálólaboratórium.				Munkaszám: -		Jegyzőkönyv szám: 013/FGSZ/HSZ/22/RT								
				Megrendelő: FGSZ Földgázszállító Zrt.		Rendelési szám: 6400088044								
				Vizsgált objektum: DN100-as varratok										
				Vizsgálat tárgya: Hegesztési varratok diagnosztikai vizsgálata										
Vizsgálat helye: Hajdúszoboszló		Időpontja: 2022.04.12												
Rajzsám: -		Anyagminőség: P355NH												
Vizsgálati terjedeleme: 100 %		Hőkezelés: -												
Hegesztési eljárás: 111		Varrat alak: BW												
<b>Vizsgálati adatok (test data)</b>														
Vizsgálati szabvány: MSZ EN ISO 17636-1:2013 B				Képmínőség osztály: W14				Sugárforrás típusa: Ir-192						
Átvételi követelmény: IG-RU-16 8.2. számú melléklet 3. táblázat				Képmínőség jelző: MSZ EN ISO 19232-1:2013 10 FE EN FE50				Sugárforrás mérete: 3x1,75 mm Aktivitás: 0,82 TBq						
Radiográfiai módszer: izotóp				Film típusa: AGFA D5 Pb:0,027 mm				Csőfeszültség: - kV Csőáram: - mA						
Berendezés azonosítója: GAMMATAT				Film kidolgozás: kézi gépi: X				Vizsgáló: Komáromi Tamás Kocsis István						
Vizsgálati darab jelölése (System of marking): A "0" point and direction point with marker														
<b>Vizsgálati eredmények (Test results)</b>														
Film jelölés	Méret (mm)	Értékelt filmhossz (cm)	Fekete óra	Képmínőség jelző	Átsugárzott vastagság (mm)	Sugárforrás-film távolság (mm)	Vizsgálati elrendezés	Megvilágítási idő (min.)	Értékelési eltérések	Film oldala	Hegesztési eljárás	Hegesztési jel	Minősítés / Result	Megjegyzés
F21	Ø 114,3 x 5,5	30-0-7	3,1	15	11	130	14	0,4	-	X	111	SX65	A	-
F21	Ø 114,3 x 5,5	1-16	3,1	15	11	130	14	0,4	2011	X	111	SX65	A	-
F21	Ø 114,3 x 5,5	10-25	3,1	15	11	130	14	0,4	-	X	111	SX65	A	-
F21	Ø 114,3 x 5,5	19-34	3,1	15	11	130	14	0,4	504	X	111	SX65	A	-
F22	Ø 114,3 x 5,5	30-0-7	3,0	15	11	130	14	0,4	-	X	111	SX65	A	-
F22	Ø 114,3 x 5,5	1-17	3,0	15	11	130	14	0,4	3012	X	111	SX65	A	-
F22	Ø 114,3 x 5,5	10-25	3,0	15	11	130	14	0,4	3012	X	111	SX65	A	-
F22	Ø 114,3 x 5,5	20-35	3,0	15	11	130	14	0,4	-	X	111	SX65	A	-
F23	Ø 114,3 x 5,5	30-0-9	3,0	15	11	130	14	0,4	-	X	111	SX65	A	-
F23	Ø 114,3 x 5,5	1-17	3,0	15	11	130	14	0,4	514	X	111	SX65	A	-
F23	Ø 114,3 x 5,5	10-25	3,0	15	11	130	14	0,4	-	X	111	SX65	A	-
F23	Ø 114,3 x 5,5	20-34	3,0	15	11	130	14	0,4	504,507	X	111	SX65	A	-
F24	Ø 114,3 x 5,5	30-0-7	2,8	15	11	130	14	0,4	3012,504	X	111	SX65	A	-
F24	Ø 114,3 x 5,5	1-17	2,8	15	11	130	14	0,4	3012	X	111	SX65	A	-
F24	Ø 114,3 x 5,5	11-26	2,8	15	11	130	14	0,4	-	X	111	SX65	A	-
F24	Ø 114,3 x 5,5	20-35	2,8	15	11	130	14	0,4	-	X	111	SX65	A	-
Megjegyzés/Note: --														
Ez a jegyzőkönyv részleteiben nem másolható! / Copying details is prohibited!														
Elfogadta (átvett):				Értékelte: Tóth Róbert RT30101090104Ú				Jóváhagyó: Tóth Róbert Felelős vezető helyettes						
Aláírása:				Aláírása:				Aláírása: GAMMA-CONTROLL KFT. 6750 Algyő, külterület 01884/14. hrsz. Rendelési szám: 6400088044 www.gamma-controll.hu						
Kelt:				Kelt:										
Date:				Date:				2022.04.13						



## Appendix 3

## ALBERA '97

Ipari és Szolgáltató Kft.  
Anyagvizsgáló Laboratórium  
3532 Miskolc, Böngér utca 3/a.  
Tel./fax: +36/ 46/564-144.

## Radiográfiai Vizsgálati Jegyzőkönyv

## Radiographic Test Report

## Protokoll über Radiographieprüfung

A NAH által NAH-1-0740/2017 számon akkreditált vizsgálatlaboratórium.

Jegyzőkönyv száma: 1730/2022. Report No.: Protokoll Nr.:	Vizsgálat ideje: 2022.06.15. Datum: Date:	Vizsgálat helye: Miskolc Place: Prüfört:
Vizsgálat tárgya: Miskolci Egyetemen készített hegesztési varrat vizsgálata Subject to be tested: Prüfobjekt:	Munkaszám: - Job No.: Arbeits Nr.:	
Megrendelő: MISKOLCI EGYETEM, 3515 Customer: Besteller:	Gyártó: - Manufacturer: Hersteller:	

Vizsgálati előírás: MSZ EN ISO 17636-1:2013 Spec. of examination: Prüfanforderung:	Anyagminőség: - Material Quality: Materialgüte:	Vizsgálati eljárás: Izotóp Test procedure: Prüfverfahren:
Értékelési előírás: IG-RÜ-16 3. táblázat Spec. for evaluation: Vorschrift für Beur:	Hegesztő eljárás: - Welding process: Schweißverfahren:	Sugárforrás: Ir-192 Radiation source: Strahlenquelle:
Vizsgálati osztály: B Radiographic class: Prüfklasse:	Varrat alakja: BW Weld form: Nahtform:	Aktivitás/ sf. méret: 1,65 TBq/3x1,5 mm Activity/source size: Aktivität/Maß:
Képmínőség jelző: 10 FE EN "F" Image quality indicator: Bildgüteprüfkörper:	Hőkezelés: - Heat treatment: Wärmebehandlung:	Expozíciós idő: 10" Exposure time: Belichtungszeit:
EN ISO 17636-1 szerinti beállítás: 7.1.8.Szerint Test arrangement acc. to EN ISO 17636-1: Aufnahmeanordnung EN ISO 17636-1:	Film osztály: C4 Film Class: Film Klasse:	Film-fókusz távolság: 12 cm Focus-to-film-distance: Abstand Fokus-Film:
Vizsgálat terjedelme: 100% Scope of testing: Prüfumfang:	Film típus: FOMA R5+Pb Film Type: Filmtyp:	Film kidolgozás: automata Film processing: Filmverarbeitung:

Varrat száma Weld No. Naht Nr.	Hegesztő jele Welder No. Schweisser Nr.	Mérete (mm) Dimensions Abmessungen	Értékelt szakasz (cm) Examination Area Beur. Filmlänge	Feketedés Density Schwarzung	IQI BPK	Eltérés jelölése Defect type Fehler typ	Értékelés Evaluation Beurteilung	Javítandó rész Correction (cm) Ausbesserung (cm)
Y1/V13	-	Ø114,3x5,6	35-0-13	2,5/2,3	14	602; 2015; filmhiba	Megfelel	-
	-	Ø114,3x5,6	9-24	2,5/2,3	14	602	Megfelel	-
	-	Ø114,3x5,6	23-0-2	2,5/2,3	14	-	Megfelel	-

Megjegyzés: Rtg. film a rendelőnek átadva.

Note:

Bemerkung:

Herschman Tamás RT10109190301

Vizsgálatot végezte

Examiner/Prüfer

István Zoltán RT20101020205Ú

Értékelő

Inspector/Inspektor

István Zoltán

Laboratóriumvezető

Head of. lab./Leiter

Miskolc, 2022. 06. 17.

Mellékletek/supplement/anlage: 0 Oldal/Page/Blatt



Oldal/Page/Blatt 1/1

Jkv: 1730/2022.

A vizsgálati eredmények csak a megvizsgált darabokra, illetve a helyekre vonatkoznak!  
The results of testing concern only the tested pieces and the tested areas respectively!  
Die Prüfergebnisse beziehen sich nur auf die Prüflinge bzw. auf die geprüften Stellen!

A jegyzőkönyvet a laboratórium írásbeli engedélye nélkül csak teljes terjedelmében szabad másolni!  
Without written permission from the laboratory the report may be copied only in full!  
Das Protokoll darf ohne schriftliche Genehmigung des Labors nur in vollem Umfang kopiert werden!

**ALBERA '97**

*Ipari és Szolgáltatói Kft.  
Anyagvizsgáló Laboratórium  
3532 Miskolc, Bőngér utca 3/a.  
Tel./fax: +36/ 46/564-144.*

**Radiográfiai Vizsgálati Jegyzőkönyv****Radiographic Test Report****Protokoll über Radiographieprüfung**

A NAH által NAI-1-0740/2022 számon akkreditált vizsgálatlaboratórium

Jegyzőkönyv száma: 3853/2022. Report No.: Protokoll Nr.:	Vizsgálat ideje: 2022.11.10. Datum: Date:	Vizsgálat helye: Miskolc Place: Prüfört:
Vizsgálat tárgya: Miskolci Egyetem készített hegesztési varratok vizsgálata Subject to be tested: Prüfobjekt:	Munkaszám: - Job No.: Arbeits Nr.:	
Megrendelő: MISKOLCI EGYETEM, 3515 Customer: Besteller:	Gyártó: - Manufacturer: Hersteller:	

Vizsgálati előírás: MSZ EN ISO 17636-1:2013 Spec. of examination: Prüfverfahren:	Anyagminőség: - Material Quality: Materialgüte:	Vizsgálati eljárás: Izotóp Test procedure: Prüfverfahren:
Értékelési előírás: IG-RÜ-16 3. táblázat Spec. for evaluation: Vorschrift für Beur.	Hegesztő eljárás: - Welding process: Schweißverfahren:	Sugárforrás: Ir-192 Radiation source: Strahlenquelle:
Vizsgálati osztály: B Radiographic class: Prüfklasse:	Varrat alakja: BW Weld form: Nahtform:	Aktivitás/ sf. méret: 1,02 TBq/ 3,5x1,75 mm Activity/source size: Aktivität/Maß:
Képmínőség jelző: 10 FE EN "F" Image quality indicator: Bildgüteprüfzeichen:	Hőkezelés: - Heat treatment: Wärmebehandlung:	Expozíciós idő: 20" Exposure time: Belichtungszeit:
EN ISO 17636-1 szerinti beállítás: 7.1.8.Szerint Test arrangement acc. to EN ISO 17636-1: Aufnahmeanordnung EN ISO 17636-1:	Film osztály: C4 Film Class: Film Klasse:	Film-fókusz távolság: 12 cm Focus-to-film-distance: Abstand Fokus-Film:
Vizsgálat terjedelme: 100% Scope of testing: Prüfumfang:	Film típus: FUJIFILM IX 80 Film Type: Filmtyp:	Film kidolgozás: automata Film processing: Filmverarbeitung:

Varrat száma Weld No. Naht Nr.	Hegesztő jele Welder No. Schweisser Nr.	Mérete (mm) Dimensions Abmessungen	Értékelt szakasz (cm) Examination Area Beur. Filmlänge	Feketedés Density Schwarzung	IQI BPK	Eltérés jelölése Defect type Fehler typ.	Értékelés Evaluation Beurteilung	Javítandó rész Correction (cm) Ausschesserung (cm)
Y6	-	Ø114,3x5,6	35-0-13	2,8/2,5	14	-	Megfelel	-
	-	Ø114,3x5,6	11-26	2,8/2,5	14	-	Megfelel	-
	-	Ø114,3x5,6	24-0-1	2,8/2,5	14	-	Megfelel	-
Y7	-	Ø114,3x5,6	35-0-13	2,8/2,5	14	-	Megfelel	-
	-	Ø114,3x5,6	11-26	2,8/2,5	14	604	Nem felel meg	-
	-	Ø114,3x5,6	25-0-2	2,8/2,5	14	604	Nem felel meg	-
Y8	-	Ø114,3x5,6	36-0-13	2,8/2,5	14	604	Nem felel meg	-
	-	Ø114,3x5,6	11-26	2,8/2,5	14	-	Megfelel	-
	-	Ø114,3x5,6	24-0-2	2,8/2,5	14	-	Megfelel	-
9	-	Ø114,3x5,6	35-0-12	2,8/2,5	14	5012	Megfelel	-
	-	Ø114,3x5,6	10-26	2,8/2,5	14	-	Megfelel	-
	-	Ø114,3x5,6	24-0-2	2,8/2,5	14	-	Megfelel	-
10	-	Ø114,3x5,6	35-0-13	2,8/2,5	14	2015	Megfelel	-
	-	Ø114,3x5,6	10-25	2,8/2,5	14	-	Megfelel	-
	-	Ø114,3x5,6	24-0-2	2,8/2,5	14	-	Megfelel	-
11	-	Ø114,3x5,6	35-0-13	2,8/2,5	14	-	Megfelel	-
	-	Ø114,3x5,6	10-26	2,8/2,5	14	-	Megfelel	-
	-	Ø114,3x5,6	24-0-2	2,8/2,5	14	-	Megfelel	-
12	-	Ø114,3x5,6	35-0-12	2,8/2,5	14	-	Megfelel	-
	-	Ø114,3x5,6	11-26	2,8/2,5	14	-	Megfelel	-

Oldal/Page/Blatt 1/2

Jkv: 3853/2022.

*A vizsgálati eredmények csak a megvizsgált darabokra, illetve a helyekre vonatkoznak!  
The results of testing concern only the tested pieces and the tested areas respectively!  
Die Prüfergebnisse betreffen sich nur auf die Prüflinge bzw. auf die geprüften Stellen!*

*A jegyzőkönyvet a laboratórium írásbeli engedélye nélkül csak teljes terjedelmében szabad másolni!  
Without written permission from the laboratory the report may be copied only in full!  
Das Protokoll darf ohne schriftliche Genehmigung des Labors nur in vollm Umfang kopiert werden!*

Varrat száma Weld No. Naht Nr.	Hegesztő jele Welder No. Schweisser Nr.	Mérete (mm) Dimensions Abmessungen	Értékelt szakasz (cm) Examination Area Beur. Filmlänge	Feketedés Density Schwarzung	IQI BPK	Eltérés jelölése Defect type Fehler typ.	Értékelés Evaluation Beurteilung	Javítandó rész Correction (cm) Ausschesserung (cm)
12	-	Ø114,3x5,6	25-0-12	2,8/2,5	14	-	Megfelel	-

Megjegyzés: Rtg. film a rendelőnek átadva.

Note:

Bemerkung:

*[Signature]*  
Oláh Szabolcs RT10109202913

Vizsgálatot végezte

Examiner/Prüfer

*[Signature]*  
István Zoltán RT20101020205Ü

Értékelő

Inspector/Inspektor

*[Signature]*  
István Zoltán

Laboratóriumvezető

Head of lab./Leiter

Miskolc, 2022.11.10.

Mellékletek/supplament/anlage: 0 Oldal/Page/Blatt



Oldal/Page/Blatt 2/2

Jkv: 3853/2022.

*A vizsgálati eredmények csak a megvizsgált darabokra, illetve a helyekre vonatkoznak!  
The results of testing concern only the tested pieces and the tested areas respectively!  
Die Prüfergebnisse betreffen sich nur auf die Prüflinge bzw. auf die geprüften Stellen!*

*A jegyzőkönyvet a laboratórium írásbeli engedélye nélkül csak teljes terjedelmében szabad másolni!  
Without written permission from the laboratory the report may be copied only in full!  
Das Protokoll darf ohne schriftliche Genehmigung des Labors nur in vollm Umfang kopiert werden!*

## Appendix 4

ALBERA '97

Ipari és Szolgáltató Kft.  
Anyagvizsgáló Laboratórium  
3532 Miskolc, Böngér utca 3/a.  
Tel./fax: +36/ 46/564-144.

## Radiográfiai Vizsgálati Jegyzőkönyv

## Radiographic Test Report

## Protokoll über Radiographieprüfung

A NAH által NAH-1-0740/2017 számon akkreditált vizsgálatlaboratórium

Jegyzőkönyv száma: 2418/2022. Report No.: Protokoll Nr.:	Vizsgálat ideje: 2022.07.27. Datum: Date:	Vizsgálat helye: Miskolc Place: Prüfört:
Vizsgálat tárgya: Miskolci Egyetemen készített hegesztési varratok vizsgálata Subject to be tested: Prüfobjekt:	Munkaszám: - Job No.: Arbeits Nr.:	Gyártó: - Manufacturer: Hersteller:
Megrendelő: MISKOLCI EGYETEM, 3515 Customer: Besteller:		

Vizsgálati előírás: MSZ EN ISO 17636-1:2013 Spec. of examination: Prüfanforderung:	Anyagaminőség: - Material Quality: Materialgüte:	Vizsgálati eljárás: Izotóp Test procedure: Prüfverfahren:
Értékelési előírás: IG-RÜ-16 3. táblázat Spec. for evaluation: Vorschrift für Beur:	Hegesztő eljárás: - Welding process: Schweißverfahren:	Sugárforrás: Se-75 Radiation source: Strahlenquelle:
Vizsgálati osztály: B Radiographic class: Prüfklasse:	Varrat alakja: BW Weld form: Nahtform:	Aktivitás/ sf. méret: 1,88 TBq/3,5x3,5 mm Activity/source size: Aktivität/Maß:
Képmínőség jelző: 10 FE EN "F" Image quality indicator: Bildgüteprüfkörper:	Hőkezelés: - Heat treatment: Wärmebehandlung:	Expozíciós idő: 17" Exposure time: Belichtungszeit:
EN ISO 17636-1 szerinti beállítás: 7.1.8.Szerint Test arrangement acc. to EN ISO 17636-1: Aufnahmeanordnung EN ISO 17636-1:	Film osztály: C4 Film Class: Film Klasse:	Film-fókusz távolság: 12 cm Focus-to-film-distance: Abstand Fokus-Film:
Vizsgálat terjedelme: 100% Scope of testing: Prüfumfang:	Film típus: FUJIFILM IX 80 Film Type: Filmtyp:	Film kidolgozás: automata Film processing: Filmverarbeitung:


Varrat száma Weld No. Naht Nr.	Hegesztő jele Welder No. Schweisser Nr.	Mérete (mm) Dimensions Abmessungen	Értékelt szakasz (cm) Examination Area Beur. Filmlänge	Feketedés Density Schwarzung	IQI BPK	Eltérés jelölése Defect type Fehler typ.	Értékelés Evaluation Beurteilung	Javítandó rész Correction (cm) Ausbesserung (cm)
13	-	Ø114x5	34-0-12	2,5/2,3	15	-	Megfelel	-
	-	Ø114x5	11-26	2,5/2,3	15	-	Megfelel	-
	-	Ø114x5	24-0-2	2,5/2,3	15	-	Megfelel	-
14	-	Ø114x5	33-0-12	2,5/2,3	15	-	Megfelel	-
	-	Ø114x5	10-25	2,5/2,3	15	-	Megfelel	-
	-	Ø114x5	24-0-2	2,5/2,3	15	-	Megfelel	-
17	-	Ø114x5	35-0-13	2,5/2,3	15	-	Megfelel	-
	-	Ø114x5	11-26	2,5/2,3	15	2011; 602	Megfelel	-
	-	Ø114x5	24-0-2	2,5/2,3	15	-	Megfelel	-
18	-	Ø114x5	35-0-13	2,5/2,3	15	-	Megfelel	-
	-	Ø114x5	11-26	2,5/2,3	15	-	Megfelel	-
	-	Ø114x5	24-0-2	2,5/2,3	15	-	Megfelel	-

Varrat száma Weld No. Naht Nr.	Hegesztő jele Welder No. Schweisser Nr.	Mérete (mm) Dimensions Abmessungen	Értékelt szakasz (cm) Examination Area Beur. Filmlänge	Feketedés Density Schwarzung	IQI BPK	Eltérés jelölése Defect type Fehler typ.	Értékelés Evaluation Beurteilung	Javítandó rész Correction (cm) Ausbesserung (cm)
--------------------------------------	---	--	--	------------------------------------	------------	--	--	--


Megjegyzés: Rtg. film a rendelőnek átadva.

Note:

Bemerkung:

  
Oláh Szabolcs RT10109202913  
Vizsgálatot végezte  
Examiner/Prüfer

  
István Zoltán RT20101020205Ü  
Értékelő  
Inspector/Inspektor

  
István Zoltán  
Laboratóriumvezető  
Head of lab./Leiter

Miskolc, 2022. 07. 28.

Mellékletek/supplement/anlage: 0 Oldal/Page/Blatt





**ALBERA '97**

*Ipari és Szolgáltató Kft.*  
*Anyagvizsgáló Laboratórium*  
 3532 Miskolc, Böngér utca 3/a.  
 Tel./fax: +36/ 46/564-144.

**Radiográfiai Vizsgálati Jegyzőkönyv**  
**Radiographic Test Report**  
**Protokoll über Radiographieprüfung**

A NAH által NAH-1-0740/2022 számon akkreditált vizsgálatlaboratórium.

<b>Jegyzőkönyv száma:</b> 4233/2022. <b>Report No.:</b> <b>Protokoll Nr.:</b>	<b>Vizsgálat ideje:</b> 2022.11.29. <b>Datum:</b> <b>Date:</b>	<b>Vizsgálat helye:</b> Miskolc <b>Place:</b> <b>Prüfört:</b>
<b>Vizsgálat tárgya:</b> Miskolci Egyetemen készített hegesztési varratok <b>Subject to be tested:</b> vizsgálata <b>Prüfobject:</b>	<b>Munkaszám:</b> - <b>Job No.:</b> <b>Arbeits Nr.:</b>	
<b>Megrendelő:</b> MISKOLCI EGYETEM, 3515 <b>Customer:</b> Miskolc Egyetemváros <b>Besteller:</b>	<b>Gyártó:</b> - <b>Manufacturer:</b> <b>Hersteller:</b>	

<b>Vizsgálati előírás:</b> MSZ EN ISO 17636-1:2013 <b>Spec. of examination:</b> <b>Prüfanforderung:</b>	<b>Anyagminőség:</b> - <b>Material Quality:</b> <b>Materialgüte:</b>	<b>Vizsgálati eljárás:</b> Izotóp <b>Test procedure:</b> <b>Prüfverfahren:</b>
<b>Értékelési előírás:</b> IG-RÜ-16 3. táblázat <b>Spec. for evaluation:</b> <b>Vorschrift für Beur:</b>	<b>Hegesztő eljárás:</b> - <b>Welding process:</b> <b>Schweißverfahren:</b>	<b>Sugárforrás:</b> Ir-192 <b>Radiation source:</b> <b>Strahlenquelle:</b>
<b>Vizsgálati osztály:</b> B <b>Radiographic class:</b> <b>Prüfklasse:</b>	<b>Varrat alakja:</b> BW <b>Weld form:</b> <b>Nahtform:</b>	<b>Aktivitás/ sf. méret:</b> 0,85 TBq/ 3,5x1,75 mm <b>Activity/source size:</b> <b>Aktivität/Maß:</b>
<b>Képmínőség jelző:</b> 10 FE EN "F" <b>Image quality indicator:</b> <b>Bildgüteprüfkörper:</b>	<b>Hőkezelés:</b> - <b>Heat treatment:</b> <b>Wärmebehandlung:</b>	<b>Expozíciós idő:</b> 20" <b>Exposure time:</b> <b>Belichtungszeit:</b>
<b>EN ISO 17636-1 szerinti beállítás:</b> 7.1.8.Szerint <b>Test arrangement acc. to EN ISO 17636-1:</b> <b>Aufnahmeanordnung EN ISO 17636-1:</b>	<b>Film osztály:</b> C4 <b>Film Class:</b> <b>Film Klasse:</b>	<b>Film-fókusz távolság:</b> 12 cm <b>Focus-to-film-distance:</b> <b>Abstand Fokus-Film:</b>
<b>Vizsgálati terjedelme:</b> 100% <b>Scope of testing:</b> <b>Prüfumfang:</b>	<b>Film típus:</b> FUJIFILM IX 80 <b>Film Type:</b> <b>Filmtyp:</b>	<b>Film kidolgozás:</b> automata <b>Film processing:</b> <b>Filmverarbeitung:</b>

Varrat száma Weld No. Naht Nr.	Hegesztő jele Welder No. Schweisser Nr.	Mérete (mm) Dimensions Abmessungen	Értékelt szakasz (cm) Examination Area Beur. Filmlänge	Feketedés Density Schwarzung	IQI BPK	Eltérés jelölése Defect type Fehler typ.	Értékelés Evaluation Beurteilung	Javítandó rész Correction (cm) Ausbesserung (cm)
Y8	-	Ø114,3x5,6	35-0-14	2,5/2,3	15	2015	Nem felel meg	12-13
	-	Ø114,3x5,6	10-25	2,5/2,3	15	604	Nem felel meg	15*
	-	Ø114,3x5,6	23-0-1	2,5/2,3	15	-	Megfelel	-
Y9	-	Ø114,3x5,6	35-0-13	2,5/2,2	15	604	Nem felel meg	35-0-3**
	-	Ø114,3x5,6	8-23	2,5/2,2	15	-	Megfelel	-
	-	Ø114,3x5,6	22-35	2,5/2,2	15	-	Megfelel	-
Y10	-	Ø114,3x5,6	35-0-13	2,5/2,2	15	604	Nem felel meg	8-12***
	-	Ø114,3x5,6	13-26	2,5/2,2	15	-	Megfelel	-
	-	Ø114,3x5,6	25-0-3	2,5/2,2	15	-	Megfelel	-

**Megjegyzés:** Rtg. film a rendelőnek átadva. \* A varraton keresztül menő köszörülési nyom. \*\*, \*\*\* A varrat mellett köszörülési nyom.

**Note:**

**Bemerkung:**



Oláh Szabolcs RT10109202913

**Vizsgálatot végezte**

Examiner/Prüfer



István Zoltán RT20101020205Ú

**Értékelő**

Inspector/Inspektor



István Zoltán

**Laboratóriumvezető**

Head of. lab./Leiter

Miskolc, 2022.12.02.

Mellékletek/supplement/anlage: 0 Oldal/Page/Blatt

Oldal/Page/Blatt 1/1

Jkv: 4233/2022.

*A vizsgálati eredmények csak a megvizsgált darabokra, illetve a helyekre vonatkoznak!*  
*The results of testing concern only the tested pieces and the tested areas respectively!*  
*Die Prüfergebnisse beziehen sich nur auf die Prüflinge bzw. auf die geprüften Stellen!*

*A jegyzőkönyvet a laboratórium írásbeli engedélye nélkül csak teljes terjedelmében szabad másolni!*  
*Without written permission from the laboratory the report may be copied only in full!*  
*Das Protokoll darf ohne schriftliche Genehmigung des Labors nur in vollem Umfang kopiert werden!*